NAVAL POSTGRADUATE SCHOOL

MONTEREY, CALIFORNIA

THESIS

EXPERIMENTAL DESIGN OF A UCAV-BASED HIGH-ENERGY LASER WEAPON

by

Antonios Lionis

December 2016

Thesis Advisor:	Keith R. Cohn
Co-Advisor:	Eugene Paulo

Approved for public release. Distribution is unlimited.

THIS PAGE INTENTIONALLY LEFT BLANK

REPORT DOCUMENTATION PAGE

Public reporting burden for this collection of information is estimated to average 1 hour per response, including the time for reviewing instruction, searching existing data sources, gathering and maintaining the data needed, and completing and reviewing the collection of information. Send comments regarding this burden estimate or any other aspect of this collection of information, including suggestions for reducing this burden, to Washington headquarters Services, Directorate for Information Operations and Reports, 1215 Jefferson Davis Highway, Suite 1204, Arlington, VA 22202-4302, and to the Office of Management and Budget, Paperwork Reduction Project (0704-0188) Washington, DC 20503.

1. AGENCY USE ONLY (*Leave blank*)	2. REPORT DATE December 2016	3. REPORT TYPE AND DATES COVERED Master's thesis	
4. TITLE AND SUBTITLE EXPERIMENTAL DESIGN OF A UCAV-BASED HIGH- ENERGY LASER WEAPON		**5. FUNDING NUMBERS**	
6. AUTHOR(S) Antonios Lionis			
7. PERFORMING ORGANIZATION NAME(S) AND ADDRESS(ES) Naval Postgraduate School Monterey, CA 93943-5000		**8. PERFORMING ORGANIZATION REPORT NUMBER**	
9. SPONSORING /MONITORING AGENCY NAME(S) AND ADDRESS(ES) N/A		**10. SPONSORING / MONITORING AGENCY REPORT NUMBER**	

11. SUPPLEMENTARY NOTES The views expressed in this thesis are those of the author and do not reflect the official policy or position of the Department of Defense or the U.S. Government. IRB Protocol number ____N/A____.

12a. DISTRIBUTION / AVAILABILITY STATEMENT Approved for public release. Distribution is unlimited.	12b. DISTRIBUTION CODE

13. ABSTRACT (maximum 200 words)

The deployment of a High Energy Laser (HEL) weapon in an airborne platform is a challenging task due to size, weight, and power (SWaP) constraints. Recent technology innovations, however, promise that such HEL development may be a reality in the near future. This study models an Unmanned Combat Aerial Vehicle (UCAV) armed with a HEL weapon and simulates the laser beam's atmospheric propagation. The Design of Experiments (DOE) methodology is then applied to determine the significance of the UCAV-HEL design parameters and their effect on the lethality of the weapon. The weight and energy requirements of two design alternatives are estimated, and the HEL output power is tabulated in relation to the UCAV endurance. Additional simulation shows the effects that platform jitter and beam quality have on the weapon lethality.

14. SUBJECT TERMS directed energy weapons, high energy lasers, atmospheric propagation, unmanned combat aerial vehicle, system architecture, design of experiments			15. NUMBER OF PAGES 133
			16. PRICE CODE
17. SECURITY CLASSIFICATION OF REPORT Unclassified	**18. SECURITY CLASSIFICATION OF THIS PAGE** Unclassified	**19. SECURITY CLASSIFICATION OF ABSTRACT** Unclassified	**20. LIMITATION OF ABSTRACT** UU

THIS PAGE INTENTIONALLY LEFT BLANK

EXPERIMENTAL DESIGN OF A UCAV-BASED HIGH- ENERGY LASER WEAPON

Antonios Lionis
Lieutenant, Hellenic Navy
B.S., Hellenic Naval Academy, 2006

Submitted in partial fulfillment of the
requirements for the degree of

MASTER OF SCIENCE IN APPLIED PHYSICS

and

MASTER OF SCIENCE IN SYSTEMS ENGINEERING

from the

NAVAL POSTGRADUATE SCHOOL
December 2016

Approved by: Keith R. Cohn
                   Thesis Advisor

                   Eugene Paulo
                   Co-Advisor

                   Kevin Smith
                   Chair, Department of Physics

                   Ronald Giachetti
                   Chair, Department of Systems Engineering

THIS PAGE INTENTIONALLY LEFT BLANK

ABSTRACT

The deployment of a High Energy Laser (HEL) weapon in an airborne platform is a challenging task due to size, weight, and power (SWaP) constraints. Recent technology innovations, however, promise that such HEL development may be a reality in the near future. This study models an Unmanned Combat Aerial Vehicle (UCAV) armed with a HEL weapon and simulates the laser beam's atmospheric propagation. The Design of Experiments (DOE) methodology is then applied to determine the significance of the UCAV-HEL design parameters and their effect on the lethality of the weapon. The weight and energy requirements of two design alternatives are estimated, and the HEL output power is tabulated in relation to the UCAV endurance. Additional simulation shows the effects that platform jitter and beam quality have on the weapon lethality.

THIS PAGE INTENTIONALLY LEFT BLANK

TABLE OF CONTENTS

LIST OF FIGURES

THIS PAGE INTENTIONALLY LEFT BLANK

LIST OF TABLES

THIS PAGE INTENTIONALLY LEFT BLANK

LIST OF ACRONYMS AND ABBREVIATIONS

ABL	Airborne Laser
AEW	Airborne Early Warning
CAS	Close Air Support
CEO	Chief Executive Officer
COIL	Chemical Oxygen Iodine Laser
CONOPS	Concept of Operations
DOD	Department of Defense
DODAF	Department of Defense Architecture Framework
DOE	Design of Experiments
DSB	Defense Science Board
GCS	Ground Control Station
HEL	High Energy Laser
HELLADS	High Energy Liquid Laser Area Defense System
M&S	Modeling and Simulation
MBSE	Model Based Systems Engineering
PIB	Power in Bucket
RSM	Response Surface Methodology
SEAD	Suppression of Enemy Air Defense
SSL	Solid State Laser
SWaP	Size, Weight, and Power
TPM	Technical Performance Measure
UAS	Unmanned Aerial System
UAV	Unmanned Aerial Vehicle
UCAV	Unmanned Combat Aerial Vehicle
USAF	United States Air Force
USMC	United States Marine Corps
USN	United States Navy
USSOCOM	United States Special Operations Command

THIS PAGE INTENTIONALLY LEFT BLANK

EXECUTIVE SUMMARY

The deployment of an airborne platform armed with a High Energy Laser (HEL) weapon has been a major challenge for several decades. Attempts in the past included mounting a HEL weapon in large aircraft like a Boeing 747, mainly for strategic missions like defense against tactical ballistic missiles. Despite being very promising in their initial phases, these trial configurations presented various technical and economic issues that resulted in their cancellation. Recently, the focus has shifted from strategic missions to tactical missions. That means that HEL weapons of lower power and, consequently, decreased size and weight would be sufficient for these missions while also being more suitable for airborne applications. Additionally, the improvements in laser weapon technology in terms of size, weight, and power (SWaP) promise that soon a HEL weapon could be deployable from an unmanned aerial vehicle (UAV).

The purpose of this thesis is to model a UAV-based HEL weapon by applying a model-based system engineering (MBSE) approach and simulate its performance. Two alternative HEL design configurations are selected, and their corresponding weight requirements are estimated. Finally, the endurance of the UAV for these different configurations is calculated.

Utilizing Vitech CORE software, we model the architecture of the UAV-HEL system, starting from the system capabilities required for a Close Air Support (CAS) mission execution along with the operational system requirements. We proceed with the functional and physical architecture, and show the functions that each physical component is to accomplish. Finally, we identify the UAV's endurance and the HEL's lethality as the technical performance measures of the overall system.

The first phase of the simulation experiment is focused on exploring how the different operational tactics and HEL design configurations affect the lethality of the system as measured by the irradiance delivered to the target and the power accumulated in a bucket on the target's surface, with a radius of 5 cm and thickness of 3 mm. The motivation of exploring these parameters at the same time, rather than one factor at a

time, calls for application of the Design of Experiments (DOE), a well-structured mathematical process that allows for the determination of the significance of each factor and potential interactions among them by analyzing the simulation's experiment results. The selected parameters in this simulation are the HEL's power; the beam director size; and the UAV altitude, speed, and direction. Having defined the mission of the UAV, we determine the target damage criteria by calculating the required irradiance and power in bucket (PIB) for different dwell times. Specifically, we find that for an aluminum surface target, an irradiance of $11MJ/m^2$ and PIB of 85 kW for a dwell time of 6 seconds would be sufficient to melt the target.

The simulation results show clearly the importance that the operating altitude of the UAV has on the HEL's lethality. These results show that operating altitude has the greatest effect on both irradiance and PIB. Following altitude in importance is the beam director size and then output power. Speed and direction of UAV show no significant effect. Another important simulation result shows that under certain circumstances a 150 kW HEL deployed by a UAV flying at altitudes higher than 3000 m could have the same performance as a 250 kW HEL operated from lower than 500 m of altitude.

Having determined those two power levels as possible alternatives and measured their performance, we then estimate the corresponding weight and power requirements for each alternative. These estimations, which are based on commercially developed systems and provide a nominal approximation, show that a 150 kW HEL would weigh approximately 1670 kg whereas a 250 kW HEL would weigh 2635 kg. Therefore, both alternatives could be mounted and supported by a UAV of the size and capabilities similar to the Predator B. By consulting a subject matter expert on UAVs, we determine a simple mathematical relation between the endurance of the UAV and its payload weight. Using this relation, we find that the lower power HEL would allow an endurance of around 25.5 hours, whereas the bigger one would allow only for 23 hours, which corresponds to a 10 percent decrease in endurance.

Finally, another set of simulation runs is executed, this time using a Matlab-based code called ANCHOR (developed by the Naval Postgraduate School Directed Energy Group) to evaluate the effects that a non-ideal beam quality and platform jitter would

have on the overall performance of the HEL. The results show that a 150 kW HEL's effective range, measured by the PIB threshold achievement, on an UCAV flying at 300 m could decrease from 4.5 km (M^2=1, Jitter=0μrad) to 3 km (M^2=7, Jitter=6μrad). By contrast, for the 250 kW HEL, the effective range would decrease from 5 km (M^2=1, Jitter=0μrad) to 4 km (M^2=7, Jitter=6μrad). For a UCAV flying at 3000 m, a 150 kW HEL effective range would decrease from 7.5 km (M^2=1, Jitter=0) to 2.5 km (M^2=7, Jitter=6μrad), whereas for a 250KW HEL, its effective range would decrease from 10km (M^2=1, Jitter=0) to 3.5km (M^2=7, Jitter=6μrad). This shows that a higher power HEL can compensate better for the degrading effects of beam quality and platform jitter than the lower power HEL, and can provide overall superior performance.

THIS PAGE INTENTIONALLY LEFT BLANK

ACKNOWLEDGMENTS

Initially, I would like to express my gratitude to the Hellenic Navy, which offered me the opportunity to study at NPS despite going through severe financial issues.

I would like to thank my advisors, Professors Keith Cohn and Eugene Paulo, for their constant and critical support and guidance throughout my thesis research.

I would also like to thank the NPS Directed Energy Group that offered me the opportunity to participate as a speaker to the Advanced High-Power Laser Conference in Colorado Springs, CO, in June 2016.

Special gratitude to Dr. Conor Pogue for his valuable assistance with the WaveTrain simulation experiments.

Finally, all my love to my wife and my three boys, who are the reason and motivation for anything I do and achieve.

THIS PAGE INTENTIONALLY LEFT BLANK

I.   INTRODUCTION

The development of a High-Energy Laser (HEL) weapon has been a major goal for the U.S. Department of Defense (DOD) over the past five decades. As the DOD has spent many years and billions of dollars trying to deploy a laser weapon, the potential advantages of such weapon systems are too promising to ignore. Although many of these laser weapon programs were cancelled due to their technical problems and high cost, other programs exist that have demonstrated their capabilities in the field and are thus being further developed.

Previous HEL weapons programs included integration efforts in all types of platforms (ground, naval, air, and space), and their potential mission capabilities spanned the entire spectrum of operations, both defensive and offensive. Four of these programs attempted to integrate a HEL weapon into an aircraft. Professor Joe Blau, in one of his lectures given at the Naval Postgraduate School, mentioned that the first such program was the U.S. Air Force (USAF) Project Delta in 1973, which developed a CO_2 gas laser. The second was the Airborne Laser Laboratory (USAF) in the 1970s, which used the same laser technology. The third was the Airborne Laser (ABL) in 1996, using a chemical oxygen iodine laser, and the fourth, the Advanced Tactical Laser was a follow-on to the ABL program in 2002, which used the same technology in lower output power. Today, the U.S. Air Force Research Laboratory is still conducting research on mounting a HEL in an aircraft. However, a very special airborne platform could also host and employ a HEL weapon: an unmanned aerial vehicle (UAV). General Atomics Aeronautical Systems, Inc. is currently working on this project, and company executives claim that it could be a reality at some point in 2017 (Defense One 2015).

Many of the developed laser weapons, especially those mounted on ground and naval platforms, have UAVs as one of their primary potential targets, because of the vast expansion of the latter in the battlefield and their constantly increasing capabilities. This thesis examines the opposite scenario. We study a notional UAV-based HEL weapon against ground targets. While the employment of a HEL weapon from a UAV would be

an ambitious project, the combination of the intrinsic advantages of both systems could result in a game-changing weapon system.

A.   BACKGROUND

An unmanned combat aerial vehicle (UCAV) is an armed UAV. Various types of UCAVs already operate all over the globe, and they have proved their capabilities in real-world missions. Until now, they have used only conventional missiles (i.e., HELFIRE), but the rapid growth of laser weapon technology suggests that the day of the first deployable UCAV armed with a HEL weapon is not far away. Figure 1 shows a notional HEL weapon mounted on a Predator C Avenger UCAV (General Atomics Aeronautical Systems Inc. 2016).

A HEL weapon shoots "bullets" traveling at the speed of light, provides a deep magazine, has a very low cost per shot, and is highly accurate. A UCAV, on the other hand, offers increased survivability, low operational cost, and no potential human casualties. Bringing both systems into one would indeed provide an ideal weapon system. Integrating a HEL weapon in a UCAV platform would require a laser of an acceptable size and weight and, at the same time, output power high enough to kill the target. Therefore, the UCAV must have an adequate payload capacity to carry the laser and additionally provide it with sufficient electrical energy. In terms of achieving the mission, the UCAV-based HEL's operational effectiveness is measured by its ability to kill the target. The HEL weapon performance characteristics are ultimately limited by the UCAVs' physical design constraints.
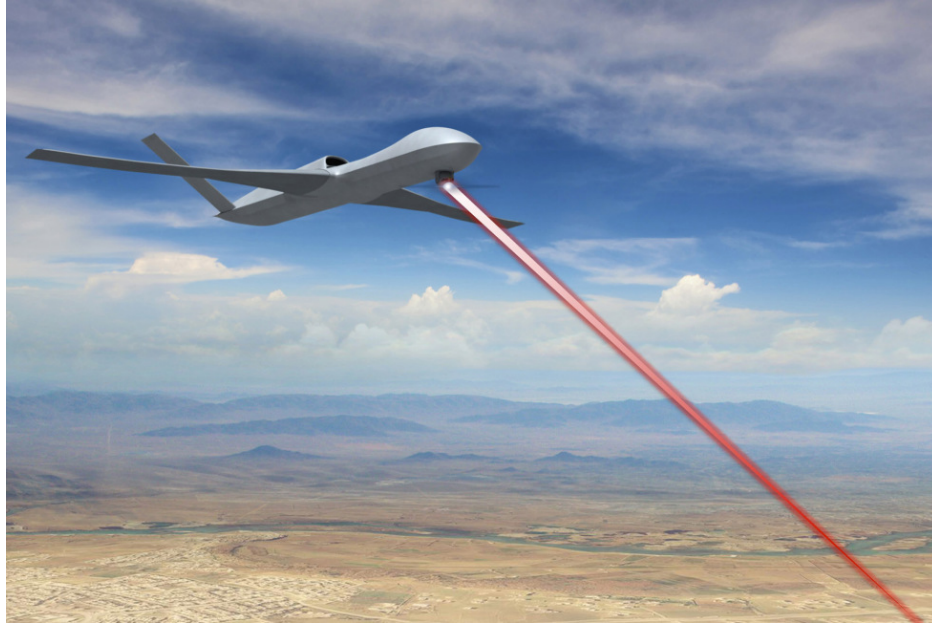
Figure 1. The UCAV-HEL Concept. Source: General Atomics Aeronautical Systems Inc. (2016).

B.   RESEARCH OBJECTIVE

Apart from its design, the UCAV-HEL weapon system's performance is further limited by atmospheric conditions, which vary with position, and engagement tactics. Therefore, modeling and analysis of the laser beam's propagation through the atmosphere for various laser system configurations and UCAV engagement tactics is the primary objective of this study.

Considering the advantages and limitations of HEL weapons and UCAVs for a given mission scenario, the primary question is, "Can we assess the performance of the UCAV with the design of the HEL for a given mission set, using simulation modeling and analysis?" This question can be further decomposed to the following questions: "How would the flight altitude, speed, and direction relate to the HEL's power and beam director size?" and "How would those parameters affect the endurance of the UCAV and the lethality of the HEL?"

Derived from these primary research questions, a few secondary questions also guide this thesis analysis and give more detailed insights. These secondary questions include the following:

- What are the key design parameters that drive the operational performance of the UCAV-HEL?

- What are the key engagement tactics that drive the operational performance of the UCAV-HEL?

- What are the uncontrollable parameters (noise factors) that affect the operational performance of the UCAV-HEL?

C.   SYSTEMS ENGINEERING APPROACH

The theoretical framework of this research follows a typical systems engineering process, with a focus on the conceptual design phase of the system. A systems engineering process always starts with a clear definition of the problem we seek to solve (Blanchard and Fabrycky 2011). Often it is not trivial and requires a lot of effort to come up with a measurable problem statement, which is a good basis for further system development. To achieve that, a systems engineer needs to account for individuals and organizations interested in that system, the so-called stakeholders.

Following the problem definition and identification the systems engineer needs to "identify various system-level design approaches or alternatives, evaluate the feasible approaches to find the most desirable, and recommend a preferred course of action" (Blanchard and Fabrycky 2011, 60). The decisions made in this stage of the system's life cycle will "have a great impact on the ultimate behavioral characteristics and life-cycle cost of the system" (Blanchard and Fabrycky 2011, 61). Figure 2 shows the popular systems engineering "V" model, which provides a view of a system's life cycle development. We could place this study at the very first "block" of the "V" model, "Mission Analysis," also called "Needs Analysis." This phase of a system life cycle explores either the necessity of a current system replacement due to a critical deficiency or an idea triggered by technology advancement, which allows for new more promising applications (Kossiakoff and Sweet 2011). This thesis explores the latter and intends to output an estimate of the system operational effectiveness.
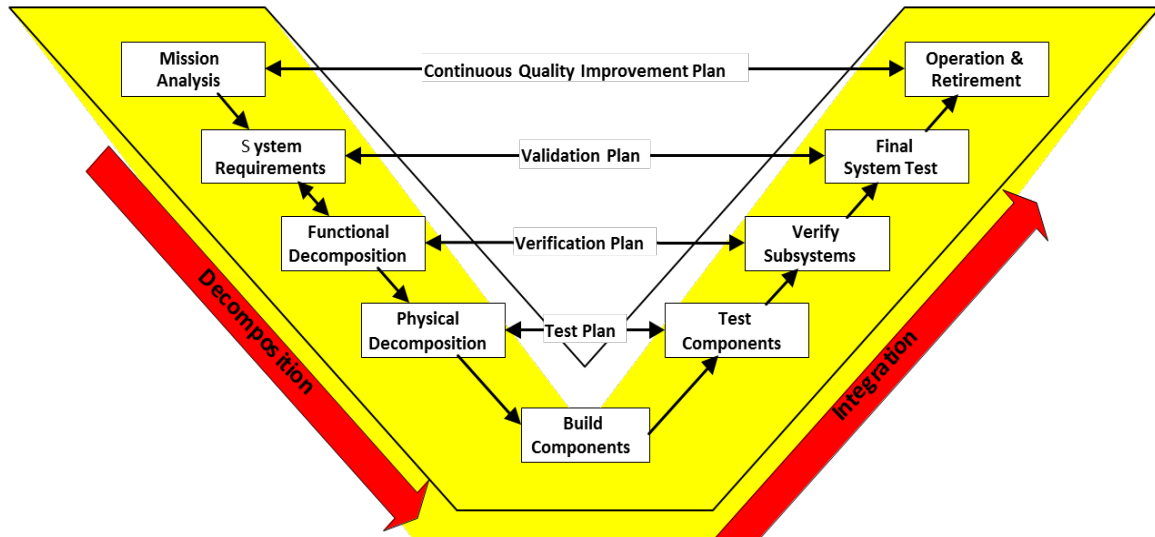
Figure 2. "V" Process Model. Source: Perram et al. (2010).

A very powerful tool that systems engineers have to facilitate the conceptual design of a system is Modeling and Simulation (M&S). Early application of M&S in a system's life cycle ensures valuable information collection for the system before significant resources are committed to its design. Therefore, M&S helps gathering data in the domain of the analyst in a fast and cost-effective manner and permits designers to conduct "what-if" experiments by making selected changes in key parameters (Kossiakoff and Sweet 2011). One of the primary purposes of modeling and simulation is mission and system concept formulation and evaluation. Following a clear and unambiguous definition of the system's mission along with its expected value, "models can be used to explore a trade space by modeling alternative system designs and assessing the critical parameters" on the overall measures of merits (INCOSE 2015, 181). Additionally, the analyst has to determine the perspective within which the system's performance will be modeled and evaluated. Alexander Kossiakoff and William N. Sweet, as shown in Figure 3, define five levels of analysis, constituting what we call the analysis pyramid (Kossiakoff and Sweet 2011). At the base of the pyramid are the foundational physics followed by the system/subsystem level where a single system/ subsystem is studied. Traveling up the pyramid we find multiple systems/single mission level, multiple missions, and finally strategy, where technical details have been

completely abstracted (Kossiakoff and Sweet 2011). The analysis of this research covers the first two levels.
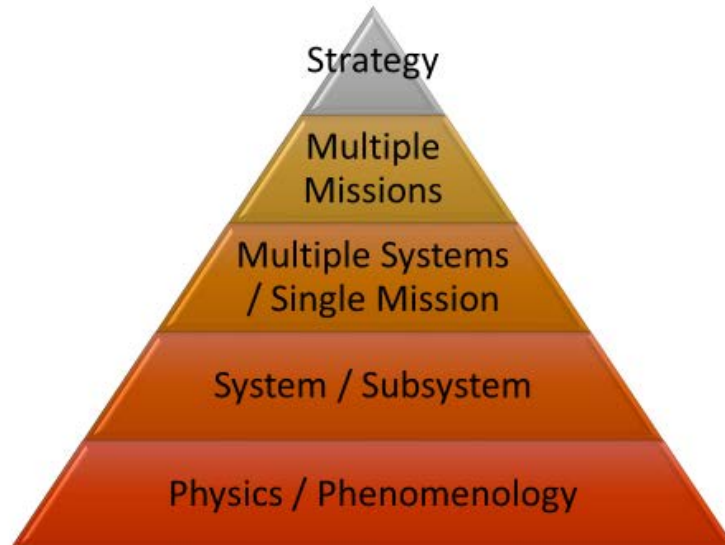
Figure 3. Analysis Pyramid. Source: Kossiakoff and Sweet (2003).

D. METHODOLOGY

The methodology followed in this research is based upon the aforementioned theoretical framework, thus conceptualizing the design of a notional UCAV-based HEL driven by a well-defined need that is followed by the systems architecture model development and a physics-based modeling and simulation analysis. Related research conducted in the past that influenced and guided this study includes Megan M. Melin's research work in modeling and analysis of a notional HEL weapon mounted on a B1-B aircraft in the 2022 timeframe. Melin identified the increased need for Design of Experiments (DOE) while modeling directed energy weapons and the lack of modeling atmospheric variability in HEL weapon system propagation models (Melin 2011). The difference in this study is that it focuses on the role of the tactics followed by the UCAV in relation to the performance of the HEL weapon. Savannah G. Welch investigated the link between a combat system's capability, in particular a shipborne air search radar, and a ship's design (Welch 2011).

This study determines initially the basic design parameters of a UCAV and the laser system's integration considerations. Following that, an atmospheric propagation simulation software tool named WaveTrain is utilized to simulate a UCAV-based HEL weapon in a specified mission scenario for different laser configurations, various atmospheric conditions existing in different locations, and different engagement tactics. The primary engagement tactics we look at are the altitude, the speed, and the direction of the UCAV. The scenario modeled considers a UCAV equipped with an HEL weapon irradiating a ground stationary target in a Close Air Support (CAS) mission. Design of Experiments (DOE) are then applied to the simulation to identify the most significant factors that affect the performance of the integrated system, including two laser weapon design parameters and the three aforementioned operational parameters, and determine the optimum design points. Based on the target's material, the damage criteria are estimated and measured by the required lase time to melt a predetermined volume on the target's surface. Further analysis of those design parameters attempts to shape the trade space among the HEL weapon (lethality) and the UCAVs' (endurance) performance. Figure 4 depicts the overall research methodology.
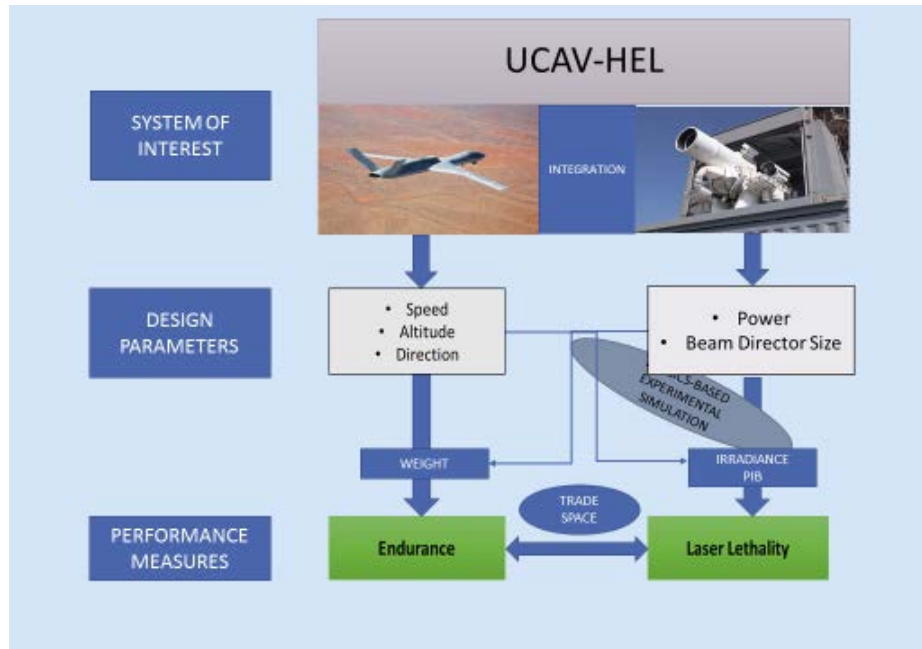
Figure 4. Research Methodology Diagram. Left Photo Source: General Atomics
Aeronautical Systems Inc. (2016). Right Photo Source: Risen (2015).

E. THESIS OUTLINE

The main organization of study is as follows:

Chapter II presents in more detail the two main systems under examination. The fundamentals of laser systems and the basic laser weapon types are presented. Additionally, a brief history, the current status, and the future of UAVs are also presented.

Chapter III presents the physics of the Solid State Lasers (SSL) as the most suitable laser weapon type to mount on a UAV.

Chapter IV presents the atmospheric propagation principles of the laser beam as well as an introduction to laser lethality concept.

Chapter V initially discusses the UCAV design considerations. These are the payload, endurance, radius of action, speed range, and flight altitude. The second part of the chapter discusses the integration considerations of the HEL weapon. Finally, the third

part develops a number of potential concepts of operations (CONOPS) for the UCAV-HEL system.

Chapter VI builds the top-level architecture of the system and identifies the critical technical parameters (TPM) that will be measured and analyzed in the following chapter.

Chapter VII provides an introduction to the experimental methods used in the simulation, followed by the simulation results analysis and trade space exploration of the TPMs.

Chapter VII discusses the conclusions of the research results.

THIS PAGE INTENTIONALLY LEFT BLANK

II.   SYSTEMS OVERVIEW

A.   HIGH ENERGY LASER WEAPON SYSTEMS

The inventor of the concept behind laser operation—stimulated emission of light—was Albert Einstein in 1916. As shown in Figure 5, stimulated emission of an atom occurs when an incident photon causes an atom that was previously sitting on an excited level to decay to a lower energy level, thereby emitting a new photon that has the same energy, phase, and direction as the incident photon. Since they have identical characteristics, coherent photons constructively interfere with each other, resulting in the amplification of the light intensity. A laser (Light Amplification of Stimulated Emission Radiation) is by definition the result of stimulated emission.

$$E_2 - E_1 = \Delta E = h\nu$$
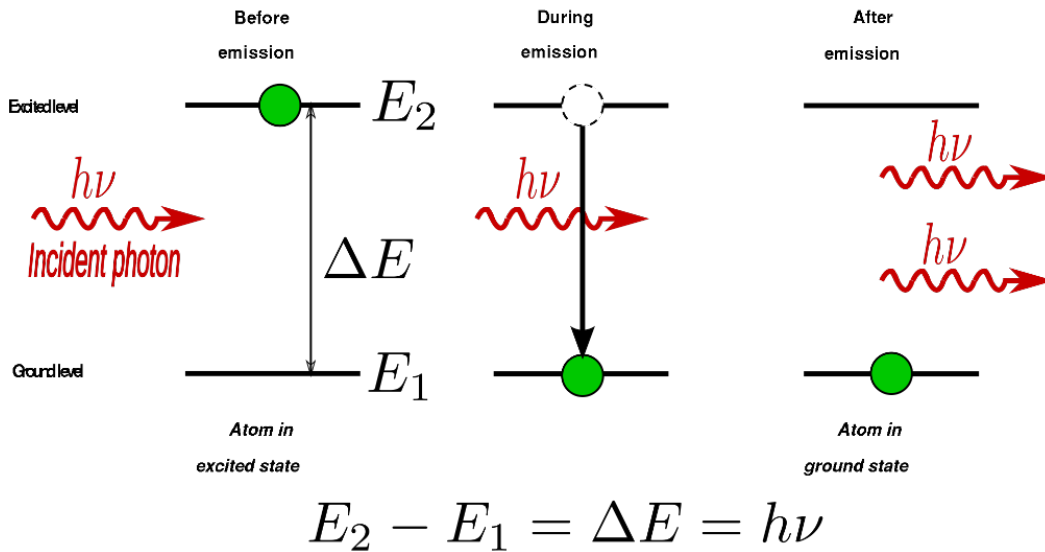
Figure 5. Spontaneous Emission. Source: Blau (2015).

The first attempts at building an actual laser device can be traced back to the 1950s (Perram et al. 2010).

Since then, the military has initiated a huge effort and invested billions of dollars to acquire laser weapon capabilities. The most notable programs include: (1) Project Delta (USAF) in 1973 that developed a CO2 gas laser with a 100 kW output power; (2)

the Airborne Laser Lab (USAF) in the 1970s that used the same laser technology and achieved a 400 kW output power; (3) the Airborne Laser (ABL) in 1996 that used a chemical oxygen iodine laser and reached MW class output power; and (4) the Advanced Tactical Laser, which was a follow-on to the ABL program in 2002 and used the same technology in lower output power (Blau 2015). As one may notice, only airborne laser programs are mentioned here due to the focus of this thesis, but, of course, there are several other developmental programs for ground-based and naval-based laser applications.

HEL weapon systems transmit energy through the atmosphere onto a designated target for a specified time in order to cause damage. The main advantages of HEL weapons are the energy delivery to the target at the speed of light, low marginal cost per shot, deep magazine (for electrically powered lasers), fast engagement times that allow for multiple engagements, ability to counter radically maneuvering air targets, precision engagement and therefore reduced risk of collateral damage, and additional uses other than engaging a target (O'Rourke 2015). Potential limitations of HEL weapon systems include the following: (1) they are suitable for line of sight engagements only; (2) laser beam degradation in power and spot size due to atmospheric effects can reduce their effectiveness; (3) hardened targets will require substantial engagements times; and (4) the risk of collateral damage to friendly aircraft and satellites exists if the laser beam misses the target.

HEL weapon systems have already demonstrated their capabilities against various types of targets in different scenarios. The effectiveness of the weapon is a result of several parameters, including its output power, the range to target, the period of engagement (better known as dwell time), and the environmental conditions. As the HEL weapon systems technology level improves and these weapons become more effective, new potential missions can be achieved and new CONOPS can be visualized.

Table 1 shows different perspectives on approximate laser power levels needed to affect various categories of targets.

Table 1.   Approximate Power Levels to Affect Various Target Types.
Source: O'Rourke (2013).

Source	Beam power measured in kilowatts (kW) or megawatts (MW)				
	~10 kW	Tens of kW	~100 kW	Hundreds of kW	MW
One Navy briefing (2010)	UAVs				
		Small boats			
				Missiles (starting at 500 kW)	
Another Navy briefing (2010)		Short-range operations against UAVs, RAM, MANPADS (50 kW-100kW; low BQ)		Extended-range operations against UAVs, RAM, MANPADS, ASCMs flying a crossing path (>100 kW, BQ of ~2)	Operations against supersonic, highly maneuverable ASCMs, transonic air-to-surface missiles, and ballistic missiles (>1 MW)
Industry briefing (2010)		UAVs and small boats (50 kW)	RAM (100+ kW), subsonic ASCMs (300 kW), manned aircraft (500 kW)		Supersonic ASCMs and ballistic missiles
Defense Science Board (DSB) report (2007)		Surface threats at 1-2 km		Ground-based air and missile defense, and countering rockets, artillery, and mortars, at 5-10 km^a	"Battle group defense" at 5-20 km (1-3 MW)
Northrop Grumman research paper (2005)	Soft UAVs at short range	Aircraft and cruise missiles at short range	Soft UAVs at long range	Aircraft and cruise missiles at long range, and artillery rockets (lower hundreds of kW) Artillery shells and terminal defense against very short range ballistic missiles (higher 100s of kW)	

Several decades ago, when the industry first attempted to build a laser weapon, until today, researchers have investigated many laser production technologies but fewer such technologies have actually been tested out of a laboratory. A common characteristic of all these efforts is to maximize the efficiency of a potential laser weapon in terms of size, weight, power (SWaP), and lethality. In other words, industry has tried to develop smaller weapons with higher capabilities of killing a target. This is easier said than done. Although many of the developed weapons did demonstrate some interesting and evolutionary capabilities, they were not always sufficient to persuade for their further development. The following paragraphs provide a brief overview of three of the major types of laser devices.

1.   Chemical Laser

Chemical lasers are "a class of laser device that transform the energy stored in chemical bonds into a nearly monochromatic beam of coherent electromagnetic radiation of light" (Perram et al. 2010, 123). Two of the more promising types of chemical lasers are deuterium fluoride and chemical oxygen-iodine lasers (COIL). The first one operates in a wavelength of approximately 4 μm. A representative program of this type was the Mid-Infrared Advanced Chemical Laser (MIRACL) in the early 1980s. COILs operate around 1.3 μm; this type was used on the famous but finally canceled (2011) Boeing Airborne Laser program. The advantages of chemical lasers include removal of waste of heat with exhaust, demonstrated ability to achieve high output powers (MW level), relatively mature technology, and good beam quality. The disadvantages of these lasers have mainly to do with their increased size and weight, their limited magazine depth, and the toxicity of the chemical reactants and products.

2.   Free Electron Laser

A free electron laser uses free electrons to create light. The electrons are accelerated to relativistic speeds in a linear accelerator and wiggle in the alternating magnetic field inside the undulator, which causes the electrons to emit light. The energy of spent electrons can be recovered to increase the efficiency of the laser device. The advantages of the free electron laser are its wavelength tunability (extremely important for better atmospheric propagation), its excellent beam quality, and its potential to achieve high output powers (MW level). Their size, price, and relative immaturity, on the other hand, prevent their implementation. Nevertheless, they are still very promising, especially for naval applications, since their size is not suitable for ground-vehicle or aircraft integration. The ability to tune their wavelength makes these lasers fit perfectly in a maritime environment. A free electron schematic is shown in Figure 6.
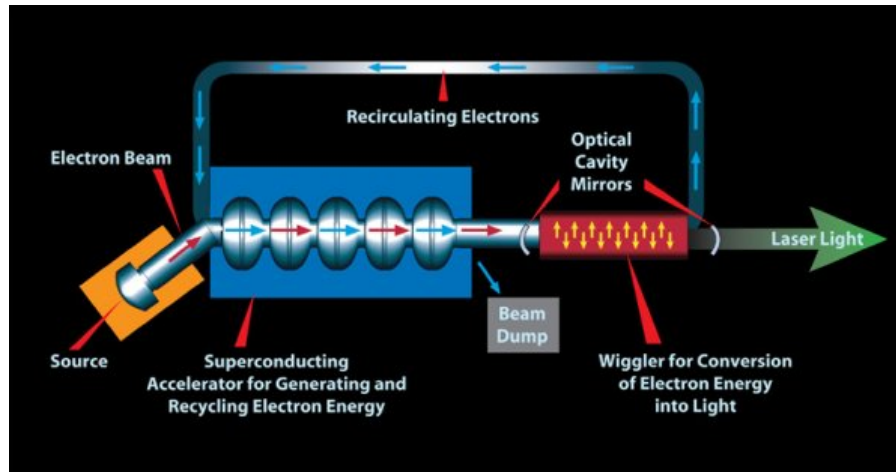
Figure 6. Free Electron Laser Components. Source: Blau (2015).

3.   Solid State Laser

Solid state lasers (SSL) are optically pumped by flash lamps or diodes, and the gain medium is formed with solid rods, slabs, or optical fibers (Perram et al. 2010). They tend to operate at around one micron (1.064 μm), and in contrast with the previously mentioned laser types, they are more compact and lightweight. Additionally, they are relatively efficient. Moreover, they do not need any harmful chemicals or produce ionizing radiation. Nevertheless, due to the low thermal conductivity of their substrates, they require advanced thermal management. Yet even with such management, they are probably not capable of achieving MW-class powers. Military applications therefore require the combination of multiple SSLs in order to achieve sufficient power level; however, achieving good beam quality under that combination is very challenging. The Maritime Laser Demonstrator is a prototype laser weapon that coherently combines seven slab SSLs, each with a power of about 15 kW, to create a beam with a power of about 105 kW (O'Rourke 2013).

B.   UNMANNED AERIAL VEHICLES

A UAV, also called a drone, is an aircraft that does not have a human pilot aboard. The two major categories of UAVs are those that are fully autonomous and those

that are controlled by a human operator in a ground-based control station. In this thesis, we focus on the second type.

1.   UAV History

The roots of the UAV go back to the 1850s when Austria used balloons filled with bombs to attack Venice. In the 20th century, the first drone applications were as targets to be fired upon during training. During World War I the U.S. Navy funded the development of an unmanned aerial torpedo (Barnhart et.al. 2012). After World War II the use of unmanned aircraft changed dramatically from target drone and weapon delivery to reconnaissance and decoy missions (Barnhart et.al. 2012). In the 1960s, the U.S. military began its own classified UAV program in order to protect its pilots from the Soviet surface-to-air missiles by developing UAVs for use as decoys. During the war in Vietnam, the U.S. military confirmed that it had been using UAVs. Specifically, the USAF 100th Strategic Reconnaissance Wing had flown 3,435 UAV missions with 554 UAVs lost to all causes.

In 1973, during the Yom Kippur War, the Israelis, in response to facing heavy casualties, developed the Tadiran Mastiff that featured for the first time in the UAV's history a data-link system as well as cameras to provide real-time video. Consequently, it is considered to have been the first modern battlefield UAV (Tucker 2008).

The interest in UAV grew even greater during the last two decades of the 20th century, when they proved their value in various combat operations such as Desert Storm in 1991, where the first large-scale employment of UAVs occurred (Barnhart et.al. 2012). "Most militaries around the world concluded after the Desert Storm experience that UAS platforms did indeed have a role to play in spotting enemy locations and directing artillery fires" (Barnhart et.al. 2012). However, the September 11, 2001, attacks caused an explosion of the interest in UAVs as reflected in funds allocated to their development in the DOD budget, as shown in Figure 7.
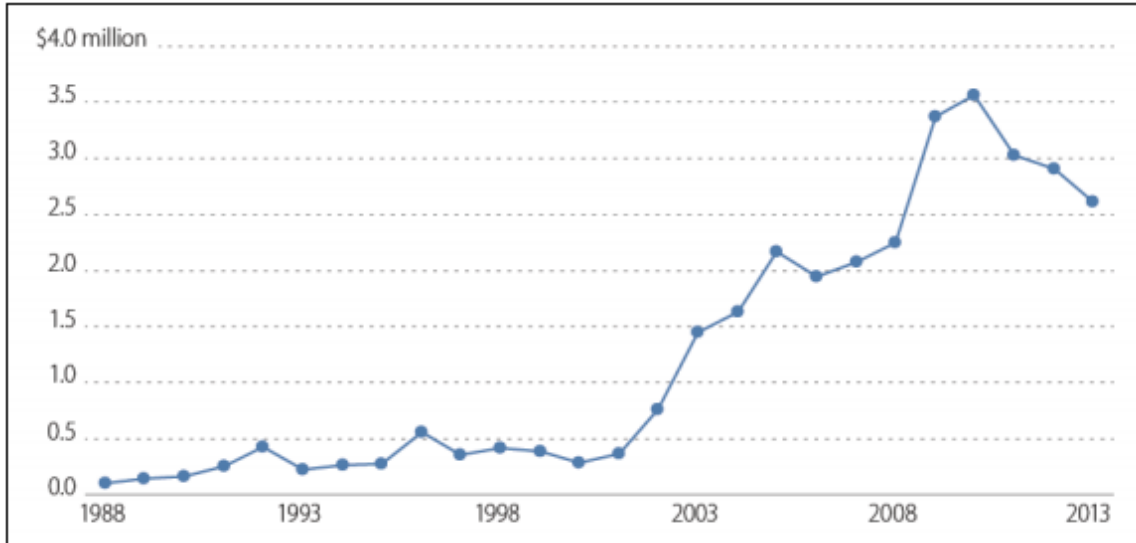
Figure 7. UAS Budgets 1988–2013. Source: Gertler (2013).

2.   Current State

The numbers of UAVs "acquired by military departments have grown and their capabilities have become integral to warfighter operations. The size, sophistication, and cost of the unmanned systems portfolio have grown to rival traditional manned systems" (Department of Defense [DOD] 2013). The UAS Integrated Roadmap also mentions that UAVs have played a major role in combat operations all around the world. Almost 50 countries use a vast array of UAVs that range in size from that of a matchbox to a Boeing 737. These UAVs continue to prove their value while participating in a variety of missions and in many challenging environments. "While UAV technology is continuously evolving, it is essential to map current and projected UAV capabilities in order to have a roadmap of how they will contribute in future operations" (DOD 2013). The U.S. DOD UAV inventory as of July 2013 is shown in Figure 8.
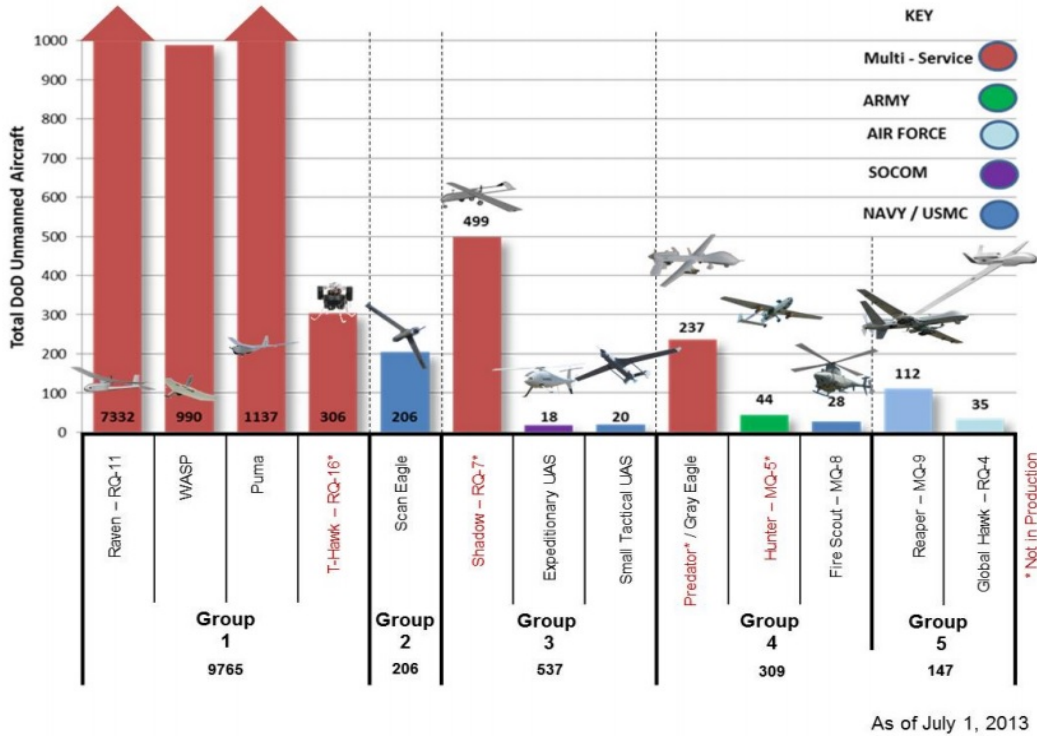
Figure 8. Inventory of DOD UAS. Source: DOD (2013).

As seen in this figure, the UAVs can be classified into five categories based on their size:

1.   Group 5: Very large UAVs (>1320 lbs., Flight Level (FL) > 180), capable of executing penetrating missions. Examples of these large UAVs are the U.S. General Atomics Predator A and Predator B, and the U.S. Northrop Grumman Global Hawk.

2.   Group 4: Large UAVs (>1320 lbs., Flight Level (FL) < 180) capable of executing persistent missions. Examples are the Israeli-U.S. Hunter and the UK Watchkeeper.

3.   Group 3: Medium UAVs (<1320 lbs., FL<180, <250 kts.) capable of executing tactical missions. An example is the U.S. RQ-7 Shadow.

18

4. Group 2: Small UAVs (21–55 lbs., <3500AGL, <250 kts.) capable of executing small tactical missions. An example is the U.S. Navy Scan Eagle.

5. Group 1: Very small UAVs (0–20 lbs., <1200AGL, <100 kts.) capable of executing mini tactical missions. Examples are U.S. Navy/USAF T-Hawk and U.S. Marine Corps/U.S. Special Operations Command Wasp.

An illustrative classification of existing UAVs is shown in Figure 9.
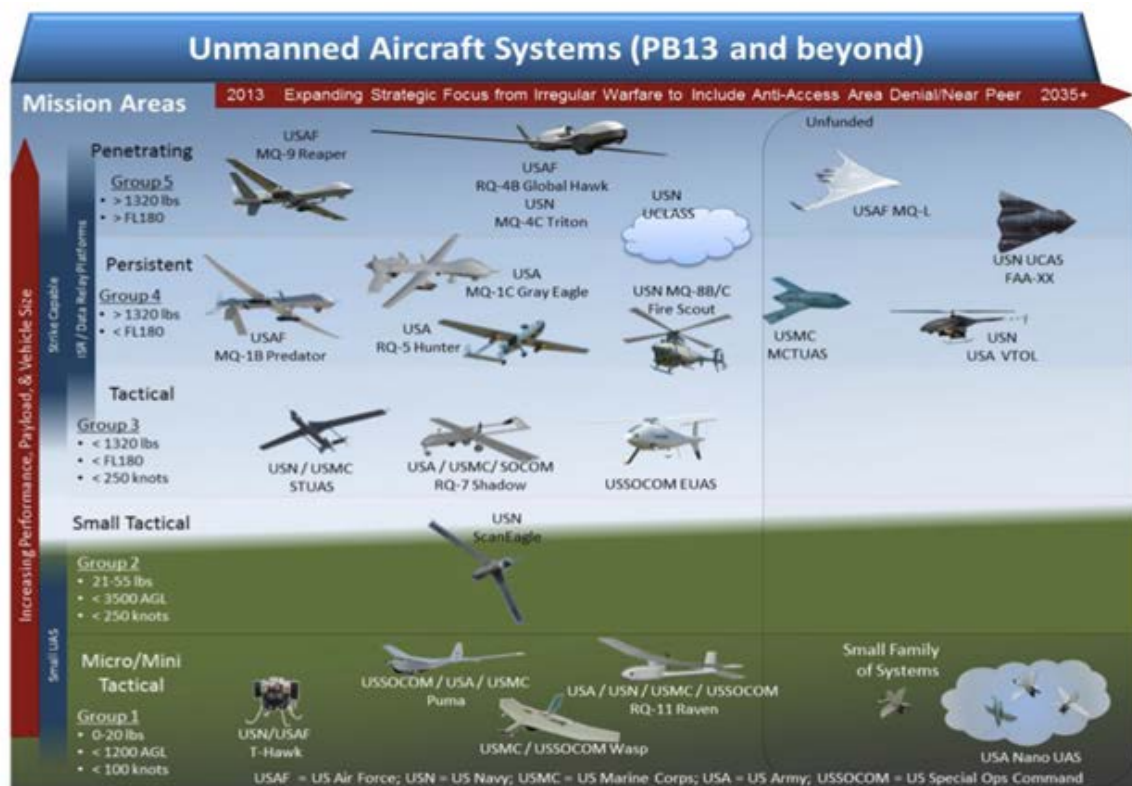
Figure 9. UAV Classification. Source: DOD (2013).

UAVs have several advantages that make them more attractive than manned aircraft in terms of potential applications. UAVs can take on missions that are: (a) *Dangerous*, where the possibility of human losses is high; (b) *Dirty*, a subset of dangerous (i.e., chemical, biological, radiological, or nuclear (CBRN) materials

19

detection); (c) *Dull*, where the repetition of the same task makes the mission boring and may cause fatigue to the crew; (d) *Demanding*, where the performance requirements of the platform are higher than those of manned aircrafts and without the constraints of a human pilot; and (e) *Different*, which cannot be otherwise accomplished by manned aircrafts. However, the UAV's dependence on the global positioning system (GPS) required for navigation, precision targeting, and sensor and antenna pointing, and the UAV's communication requirements remain a constraint. These constraints are a disadvantage of UAVs (Alkire et al. 2010).

3.   Unmanned Combat Aerial Vehicles

"Looking to the future, projected missions' areas for UAVs include air-to-air combat, electronic warfare (EW) and suppression and defeat of enemy air defense" (DOD 2013, 24).

> The six areas of technology key for DOD to enhance capability and reduce cost are interoperability and modularity; communication systems, spectrum, and resilience; security (research and intelligence/technology protection [RITP]); persistent resilience; autonomy and cognitive behavior; and weaponry. (DOD 2013, 28)

Unmanned systems integrated with weapons provide a valuable alternative to manned aircraft in a variety of missions due to their inherent advantages like their wider range of classes and sizes, greater persistence and endurance, and potential to support a larger range of mission sets.

Deploying a UAV armed with a high energy laser weapon, despite being extremely challenging, will eventually offer game-changing capabilities for missions such as Suppressing Enemy Air Defense (SEAD), anti-ship operations, counter-air, CAS, and even some types of non-lethal actions. "The Air Force and Navy have very different missions planned for the UCAV. The Air Force is focused on the SEAD mission, as well as an electronic attack role. The Navy wants a long-dwell air surveillance aircraft that could also perform strike missions" (Bone and Bolkcom 2003).

III.   SOLID-STATE LASER PHYSICS

In contrast to the other two types of laser weapons presented in Chapter II, solid state lasers, due to their intrinsic SWaP features, are the most promising for integration in a UAV. For this reason, a deeper understanding of SSL principles is required.

An SSL consists of a laser pumping source, a gain medium (dopant/substrate), and an optical resonator cavity. The gain medium in these lasers tends to be in the form of slabs, thin discs, or fibers (Perram et al. 2010). The desirable traits of an SSL are the high "wall-plug efficiency," the selection of a gain medium with good thermal conductivity, a substrate that is durable against high power, and a wavelength within the "sweet-spot" of atmospheric transparency.

The gain medium of the SSL has different absorption and emission spectra. Thus, we are interested in pumping light with energies only within the absorption spectrum and that take laser light within the emission spectrum. The laser light that is absorbed travels back and forth within the optical cavity for amplification. The gain coefficient is then defined as (Blau 2015):

$$\frac{dI}{dz} = \gamma I(z) \, ,$$

(1)

where $I(z)$ is the intensity of laser light inside the gain medium. In general, γ is a function of the lasing wavelength and the intensity of the laser light, so it is therefore not a constant. In order to produce lasing light from a solid state laser, we have to achieve population inversion; that is, we must "settle" more atoms on higher (excited) energy levels than those on ground state.

> A two-energy level system would not work for lasing simply because the population inversion could not be maintained. Once the atoms are excited to the higher energy level, the probability of further stimulated emission and absorption are equal, and the condition of saturation occurs, and no population inversion can exist. Therefore, solid-state lasers are either three or four-level systems. (Koechner and Bass 2003)

Accounting for the degree of population inversion and the gain cross section (Blau 2015):

$$\gamma = \Delta N \sigma(f),$$

(2)

where $\sigma(f)$ is the cross section for stimulated emission, which is proportional to the probability of stimulated emission, and ΔN is the population inversion defined as (Blau 2015):

$$\Delta N = \frac{(\#\text{atoms in E3})-(\#\text{atoms in E2})}{\text{per unit volume}},$$

(3)

where E3 and E2 are the excited energy levels within which stimulated emission occurs as shown in Figure 10, which depicts a typical four-level laser energy diagram. Atoms are initially at the level 1 (ground state). Through pumping, we excite atoms to level 4. Afterwards, they rapidly decay to level 3 without radiating light. The decay from that level to level 2 through stimulated emission is the desired lasing transition. Yet not all atoms will decay by stimulated emission. Finally, from level 2, with a fast transition they will return to their starting point (ground state). The rate of change of population in energy level 3 is (Blau 2015):

$$\frac{dN_3}{dt} = N_1 W_p - N_3 W_{st} - N_2 W_{st} - N_3 W_{sp}.$$

(4)

The first term represents the pump rate, the second one the stimulated emission rate, the third one the absorption, and the last one the spontaneous emission rate. N_1, N_2, N_3 and N_4 are the population density of each respective energy level. Since N_3 is much larger than N_2, after the population inversion has occurred, we can ignore the third term of Equation 4.
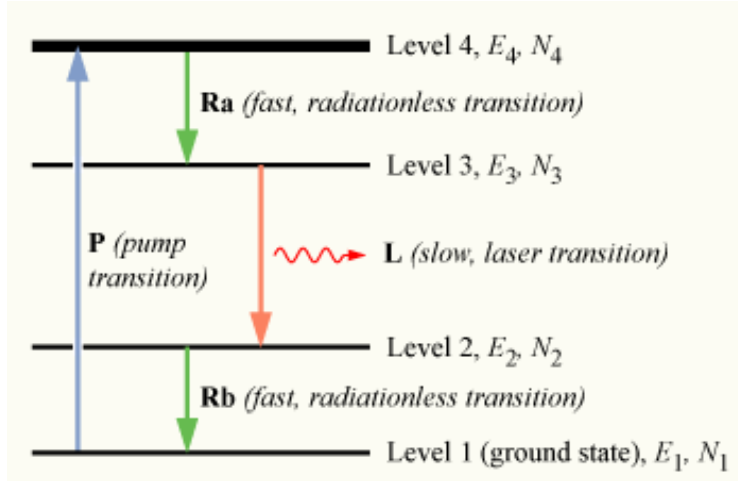
Figure 10. A Four-Level Laser Energy Diagram. Source: Wikipedia (2016).

After pumping for a while, N_3 reaches a steady state

$$\frac{dN_3}{dt}=0 \Rightarrow N_3 \approx \frac{N_1 W_p}{W_{sp}+W_{st}}$$

(5)

where W_{st} represents the probability an atom in E_3 decays to E_2 by stimulated emission and is defined as (Blau 2015):

$$W_{st} = \frac{I\sigma(f)}{hf}$$

(6)

where $h=$ Planck's constant. Rearranging and solving for I we take the *saturation intensity:*

$$I_{sat} \equiv \frac{hfW_{sp}}{\sigma}$$

(7)

where W_p is the probability an atom in E_3 decays to E_2 by spontaneous emission. Saturation intensity is solely a property of the gain medium; note that the gain decreases as laser intensity increases (Blau 2015):

$$\gamma(f) = \frac{N_1 W_p \sigma(f)}{W_{sp}} \left(\frac{1}{1 + \dfrac{I}{I_{sat}}} \right) = \frac{\gamma_0}{1 + \dfrac{I}{I_{sat}}} , \tag{8}$$

where γ_0 is the unsaturated gain coefficient

$$\gamma_o \equiv \frac{N_1 W_p \sigma}{W_{sp}} . \tag{9}$$

Eventually the system will reach a steady state where $dN_3/dt = dI/dt = 0$.

A.   OPTICAL CAVITY

The gain medium inside which the lasing light is generated sits between two optical mirrors, one of which has a reflectivity $R_1 \sim 1$ (nearly total reflection) and the other one is $R_2 < 1$ (partial reflection) with a transmission $T = 1 - R_2$, so that only a very small amount of the lasing light transmits (~ 1 percent). The intensity that finally "leaves" the optical cavity is

$$I_{out} = \frac{1}{2} T I_{ss} , \tag{10}$$

where I_{ss} is the steady state intensity inside the cavity. The higher the reflectivity R_2, the smaller the gain coefficient γ_{th}. This is good because we need smaller gain to reach steady state, but it also increases the circulating power inside the cavity for a given output power. Thus, we have trade-off between transmission T and gain, which motivates for a high gain medium so we can increase T to reduce the circulating power.

The optical resonators are spherical, opposing mirrors with radii r_1 and r_2. There are several different resonator configurations, but the configuration is typically designed to provide a stable cavity. The stability condition is given by (Blau 2015):

$$0 \leq \left(1-\frac{L}{r_1}\right)\left(1-\frac{L}{r_2}\right) \leq 1 \qquad . \tag{11}$$

It is important to note that often in HEL applications we use unstable optical cavity configurations. Typical optical resonator configurations include plane-parallel, concentric, confocal, hemispherical, and concave-convex mirrors. The configuration used for the optical resonator of a SSL determines the effective volume of the optical mode that contributes to the stimulated emission, and it is called mode volume. In general, we need the largest possible mode volume to achieve higher output power while avoiding medium and mirror damage.

B.   WALL-PLUG EFFICIENCY

The ratio of optical power delivered by a laser to the total electric power needed to drive the laser is defined as the wall-plug efficiency of the laser device.

The energy level difference, as shown in Figure 11, determines the quantum defect, which relates the photon energy of the pump source to the photon energy of the laser (Blau 2015):

$$q = hf_p - hf_L = hf_p\left(1-\frac{hf_L}{hf_p}\right), \tag{12}$$

where f_p is the frequency of the pump photon, f_L is the frequency of the lasing photon, and h is Planck's constant. The smaller hf_L is relative to hf_p, the larger the quantum defect, which is an undesirable effect and causes more heat. Note that the ratio hf_L/hf_P sets the maximum possible wall-plug efficiency.

Another component of the wall-plug efficiency is quantum efficiency n_Q, which is defined as the fraction of absorbed pump photons that contribute to the desired lasing transition. For Nd:YAG emitting at 1064 nm that is pumped by a laser diode array at 808 nm, we obtain an n_Q=0.9 (Koechner and Bass 2003).

SSLs are not high-efficient radiation sources with typical wall-plug efficiencies at around 10 percent (Koechner and Bass 2003). That means for a SSL to achieve a 100 kW output power, a total input power of a 1MW is required. However, "further improvements in the efficiency of diode pump sources as a result of refinements in diode structure and processing techniques, coupled with a further optimization of laser materials and designs," could increase the efficiency of SSLs to about 20 or 30 percent (Koechner and Brass 2003, 11).
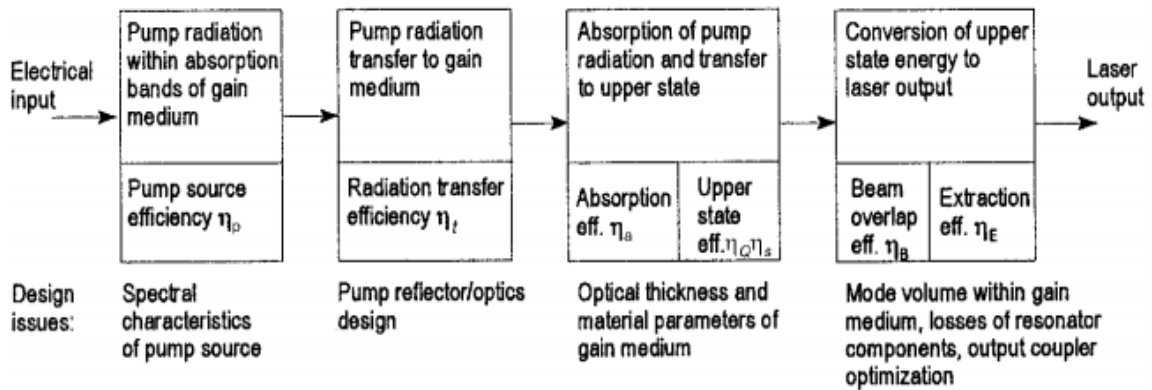
Figure 11. Energy Flow in a Solid-State Laser System.
Source: Koechner and Bass (2003).

C.   PROPERTIES OF SSL MATERIALS

The three principal elements leading to gain in a solid state lasers are: a) the host material, b) the activator/sensitizer, and c) the optical pump source (Koechner and Bass 2003).

Host materials can be divided into two broad groups, crystalline solids and glasses (Koechner and Bass 2003). Crystals have a narrow absorption/gain spectrum, require

specific properties to achieve good beam quality, and have easier thermal management due to their large thermal conductivity. Glasses, on the other hand, have broader absorption/gain spectrum, lower thermal conductivity, and increased size capability for high-energy applications (Koechner and Bass 2003).

Considering the active ions that can serve in SSLs, we can select three as the most popular: neodymium (Nd), ytterbium (Yb) and erbium (Eb). These ions are classified as rare earth ions and "exhibit a wealth of sharp fluorescent transitions representing the whole region of the visible and near-infrared portions of the EM spectrum" (Koechner and Bass 2003, 49). Neodymium-based gain mediums have low pump threshold, lase at around 1060 nm, and have a large gain coefficient. Their quantum defect is quite large. The most popular representative is the Nd:YAG, which has good optical quality and high thermal conductivity (Koechner and Bass 2003). Its absorption spectrum has a peak at 808 nm whereas its emission is at 1064 nm. This is quite a large quantum defect; therefore, it is not applicable especially on high-energy lasers. Ytterbium-based gain mediums have a smaller quantum defect, and they are better candidates for high power applications. Finally, erbium-based gain mediums are promising due to some intrinsic advantages, such as low waste heat production, but their technology maturity is still not sufficient for high power applications.

D. FIBER LASERS

A special type of solid state laser is the fiber laser. A fiber laser holds the same configuration as a solid state laser, but instead of using a rod as its lasing medium, it uses a fiber optic. What makes fiber lasers attractive is that their technology is quite mature and heavily involved in commercial applications. The output power achieved by a single fiber laser module can be as high as 1 kW, so many fiber lasers must be combined to achieve high output powers. Beam combination while simultaneously maintaining good beam quality is an engineering challenge.

As shown in Figure 12, a fiber laser is pumped by an external source (i.e., a diode laser). The doped core or inner cladding has a higher index of refraction than the outer cladding ($n_1 > n_2$), so the incident light will get trapped inside the fiber by total internal

reflection. The maximum allowed angle for total internal reflection is determined by Snell's law and is given by:

$$\sin\left(\theta_{max}\right) = \sqrt{n_1^2 - n_2^2} \equiv NA.$$

(13)

The sine of the maximum angle is a property of the fiber called the numerical aperture. A larger numerical aperture makes light coupling easier inside the fiber whereas a smaller one makes it harder. The interior of the fiber will allow only discrete modes to propagate. To achieve higher beam quality, we need the fiber to support only the lowest level guided mode (i.e., it should be a single mode fiber). To do so, we use a double-cladding structure (Perram et al. 2010). Thus, we have three layers of cladding, the outer, the inner, and the core. The latter one (gain medium) has the highest index of refractivity. That way we achieve a large numerical aperture between the outer and the inner cladding. This makes it is easier to pump into the fiber and support a single guided mode between the core and the inner cladding, which provides better beam quality. Figure 12 shows the structure of a double clad fiber and the two distinct propagating waves.
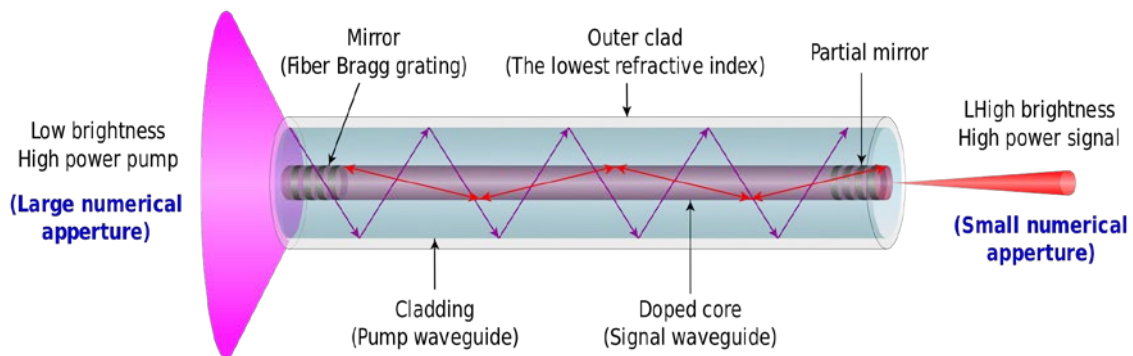
Figure 12. Double Clad Fiber Laser. Source: Blau (2015).

IV. ATMOSPHERIC PROPAGATION AND LETHALITY

In addition to the inherent attributes of a HEL weapon system, its actual effectiveness in terms of its ability to "kill" a target must be estimated. To estimate its lethality, we need to take into account a) the laser beam propagation through the atmosphere and b) the effects of the delivered energy to the target. The former is primarily a factor of the laser's wavelength and the existing atmospheric conditions between the HEL weapon and the target, whereas the latter is a factor of the material of the target.

A. ATMOSPHERIC EXTINCTION

The earth's atmosphere consists of four distinct layers determined by temperature differences at various heights. The two lower layers, the troposphere and the stratosphere, have the most significant effect on a laser weapon system (Perram et al. 2010). For the scope of this thesis, however, the effect of the first layer only is examined. The troposphere, as shown in Figure 13, extends from sea level to an altitude of around 10 km, separated by the tropopause within the stratosphere, and the temperature is indirectly proportional to the altitude.
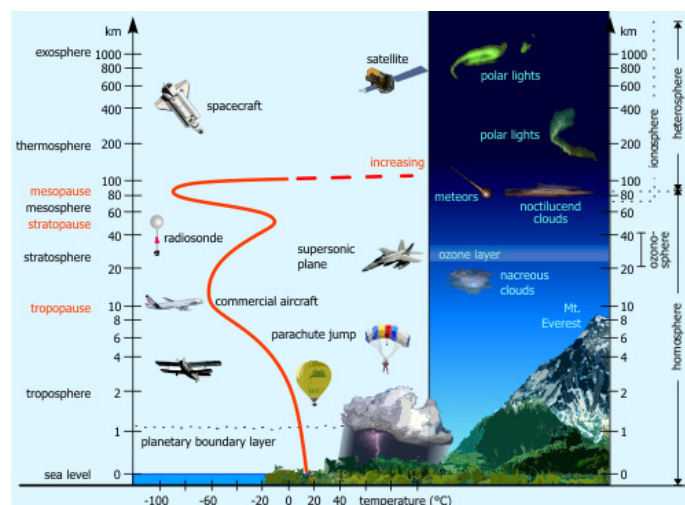
Figure 13. Atmospheric Layers. Source: The Ozone Hole (2016).

The atmosphere is primarily composed of gaseous molecules and aerosols. As the laser beam travels through the atmosphere, these micro particles are responsible for its degradation due to the effects of absorption and scattering. These two effects combined are called the extinction effect. The master equation for the time-averaged irradiance on a target is then given by (Blau 2015):

$$\langle I \rangle \approx \frac{P}{\pi \langle w_{tot} \rangle^2} e^{-\varepsilon l}$$

$$(14)$$

where P is the output power of the laser at beam director, l the distance to the target, ε the total extinction coefficient due to atmospheric absorption and scattering, and $\langle w_{tot} \rangle$ the time-averaged radius of spot on target.

Molecules and aerosols can absorb and scatter incident light. Specifically, molecules can absorb photons at a certain energy and re-emit them at a lower energy. The residual energy related by the molecular after the re-emission results in heating. On the other hand, when light scatters from matter, there is little net absorption of energy, but the light is re-emitted in random directions. This is the scattering effect, which in contrast with absorption that affects the laser beam by converting its electromagnetic energy in heat, directly alters its direction of propagation. These two effects, which combined are known as atmospheric extinction, are described by Beer's Law:

$$P(z) = P_0 e^{-\varepsilon z}$$

$$(15)$$

where P_0 is the output power on the beam director, $P(z)$ the power after a distance z, and ε the extinction coefficient. The extinction coefficient is composed of four parts:

$$\varepsilon = \alpha_m + \alpha_a + \beta_m + \beta_a$$

$$(16)$$

where each a and β is referring to absorption and scattering coefficients, respectively. The subscript m refers to molecular and a to aerosol. Consequently, the larger the extinction coefficient, the greater the attenuation. The illustration in Figure 14 shows the extinction coefficient dependency on the wavelength, where we can identify a few transparencies "windows" that would result in better propagation and therefore more lethal effects to the target. To determine the total extinction, we need to know the extinction coefficients at each point along the beam path. However, these coefficients change with location, altitude, season, and time of day and make their calculation a very difficult task.
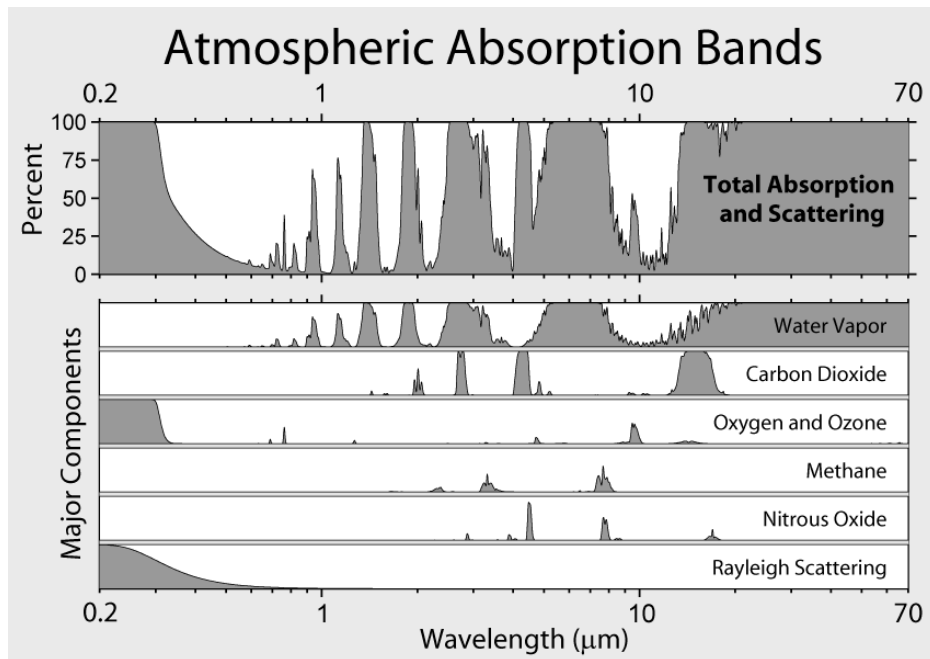
Figure 14. Extinction Coefficient. Source: Blau (2015).

1.   Molecular Effects

The atmosphere is comprised primarily of nitrogen (N_2), oxygen (O_2), water (H_2O), and carbon dioxide (CO_2).

Although the two former atmospheric constituents largely outnumber the latter two, water and carbon dioxide play the most significant role in atmospheric absorption

(Perram et al. 2010). Specifically, water vapor, due to its geometric structure and its multiple vibrational modes, is the greater contributor to atmospheric absorption, and so, the seasonal, time-of-day, horizontal, and vertical variability of atmospheric water vapor will play a critical role in the successful employment of laser weapon systems (Perram et al. 2010). However, the molecular absorption spectrum is very intricate, and the laser spectral width should ideally fit completely within a narrow wavelength window. Figures 15 and 16 shows the typical atmospheric molecular absorption and scattering spectrum, respectively.
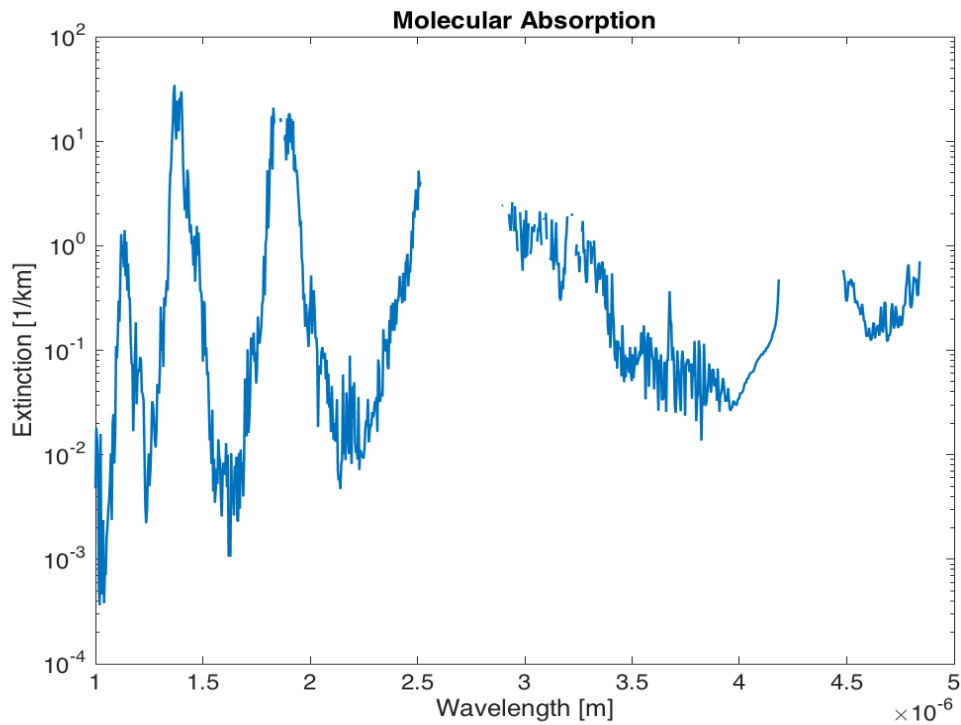
Figure 15. Typical Molecular Absorption Spectrum for the Atmosphere.
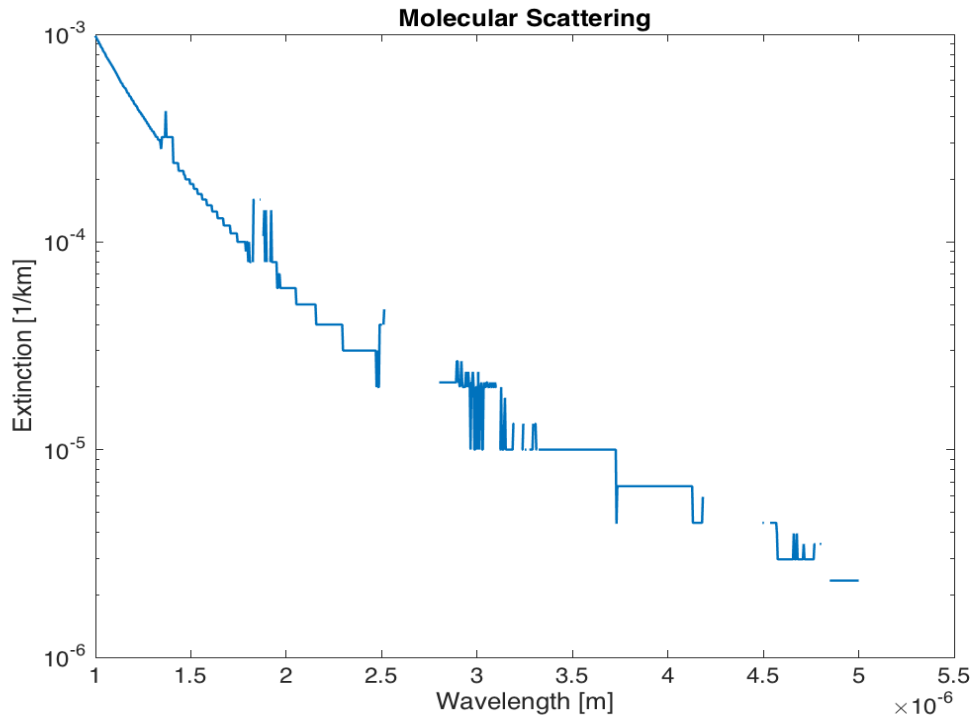
Figure 16. Typical Molecular Scattering Spectrum for the Atmosphere.

2. Aerosol Effects

Aerosol scattering and absorption (Figures 17 and 18) can "play an important role in limiting the laser energy delivered to a remote target" (Sprangle, Penano, and Hafizi 2007, 11). Their value for a maritime environment can be up to 0.2 km^{-1} (Sprangle, Penano and Hafizi 2007). The values of the aerosol coefficients depend on the aerosol size, shape, and refractive index (Fussman 2014). Aerosols have approximately the size of a typical laser wavelength, and aerosol coefficients are strongly dependent on their optical properties, while weakly dependent on the wavelength. In general, aerosol scattering is significantly greater than molecular scattering within the lower atmosphere at a wavelength of 1064 nm (Perram et al. 2010).
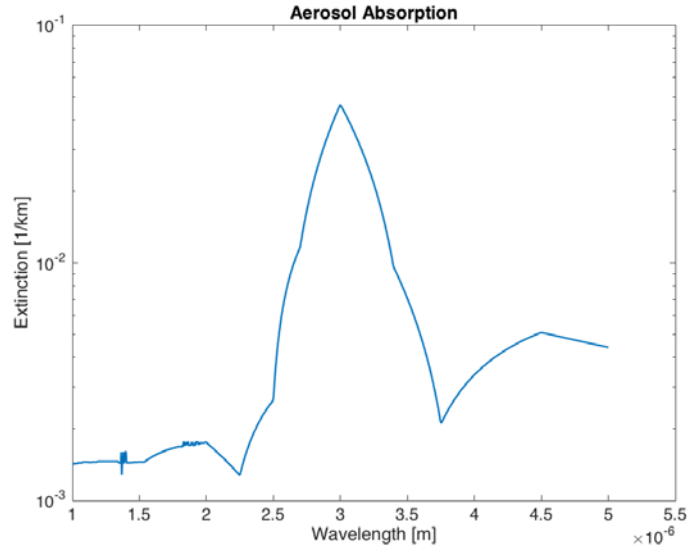
Figure 17. Typical Aerosol Absorption Spectrum for the Atmosphere.
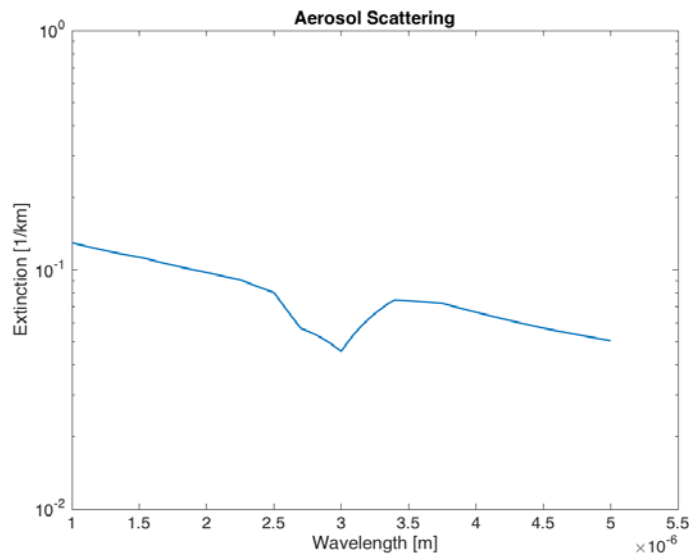
Figure 18. Typical Aerosol Scattering Spectrum for the Atmosphere.

B.   THERMAL BLOOMING

As the laser beam propagates through atmosphere, the index of refraction of the surrounding air mass alters and consequently the beam deviates from its initial direction. This effect is called thermal blooming and, as mentioned, is a direct result of absorption.

The higher the power and focus of the laser beam, the higher the effects of thermal blooming. Assuming constant atmospheric conditions, we can characterize thermal blooming using a so-called dimensionless distortion number (Perram et al. 2010):

$$N_D \approx \frac{-4\sqrt{2}kPn_T\alpha T}{\rho_o C_p D V_{wind}} R$$
(17)

where P is the laser power, k is the wavenumber, $n_T=dn/dT$ the change of index of refraction with temperature, α is the absorption coefficient, T the transmission, D the beam diameter, V_{wind} the effective wind speed perpendicular to the beam, and R the range to the target. Figure 19 shows how significantly the laser's beam shape changes due to thermal blooming as it bends into the wind. Obviously the greater the output power, the range to the target, and the absorption coefficient, the greater the thermal blooming effect. On the other hand, a less focused beam and more effective wind decreases these effects.
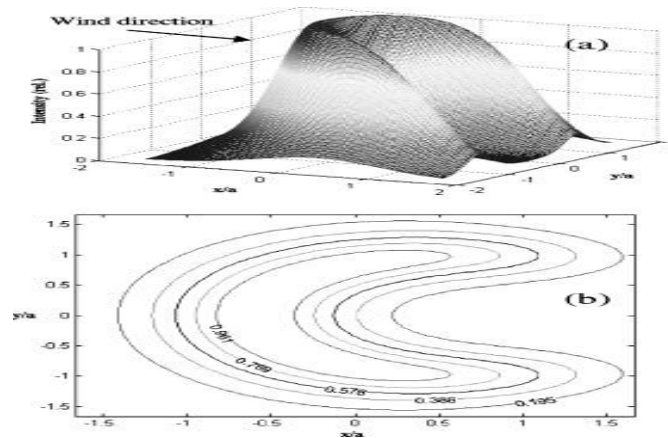
Figure 19. Thermal Blooming Effect on a Laser Beam. Source: Reierson (2011).

C.   TURBULENCE

Another atmospheric phenomenon that can radically affect the laser beam propagation is the atmospheric turbulence. It is almost impossible to predict the turbulence at a specific point in space due to its significantly nonlinear nature; thus,

scientists use a statistical approach to estimate the overall effects of turbulence on a macroscopic scale. A laser beam propagating through atmosphere is affected by turbulence due to vertical temperature and density variations (Figure 20). The temperature and density differences result in changing the air refractive index, and consequently, the propagating beam is distorted due to induced amplitude and phase fluctuations. An empirically captured equation relating temperature to refractive index is (Perram et al. 2010):

$$n(T) - 1 = \left[n(15^o C) - 1 \right] \left[\frac{1.059}{1 + (0.00366^o C^{-1})T} \right].$$

(18)

The major parameters that characterize atmospheric turbulence are the refractive index structure parameter C_n^2, the turbulence inner l_o, and outer L_o scales of turbulence eddies (Abarzhi 2012). The refractive index structure parameter is a measure of turbulence's strength and varies in both time and space. Consequently, it is very difficult to determine its value. However, a large number of measurements around the world and in various altitudes provide a sufficient database to use while experimenting with laser propagation through atmosphere (Perram et al. 2010). Roughly speaking, there are three turbulence regimes: the *strong* ($C_n^2 \geq 10^{-14} m^{-2/3}$), the *moderate* ($10^{-17} \leq C_n^2 (m^{-2/3}) \leq 10^{-14}$), and the *weak* ($C_n^2 \leq 10^{-17} m^{-2/3}$) turbulence regime (Reierson 2011).
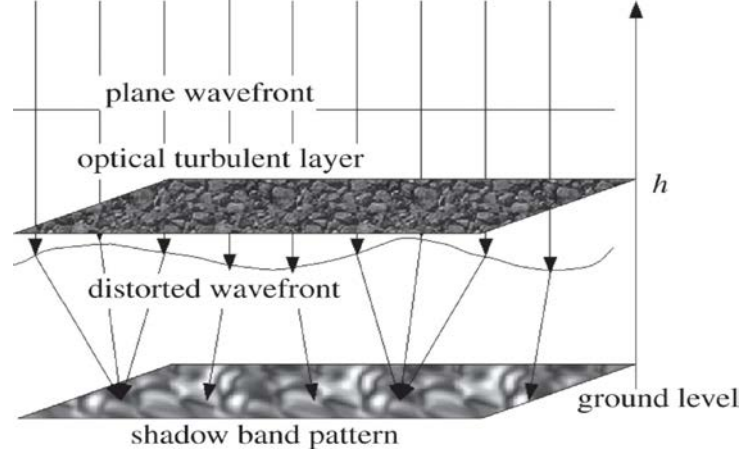
Figure 20. Turbulence Effects on a Plane Wavefront. Source: Sofieva, Dalaudier, and Vernin (2013).

In general, within the turbulence regimes just described C_n^2 demonstrates higher values near sea level. A commonly used parameter that describes the magnitude of the turbulence over a path is the Fried parameter r_o (Perram et al. 2010):

$$r_o = \left[\frac{2.905}{6.88} \left(\frac{2\pi}{\lambda} \right)^2 \int\limits_{path}^{R} C_n^2(h(z))dz \right]^{-3/5}$$

(19)

The Fried parameter is defined as the diameter over which the beam maintains transverse coherence throughout the propagation length (Perram et al. 2010). The lower it is, the higher the magnitude of the turbulence. If r_o is smaller than the beam director size, then turbulence has a significant impact on the beam. For a constant structure, the constant C_n^2 in Equation 19 reduces to:

$$r_o = 0.185 \frac{\lambda^{6/5}}{R^{3/5}(C_n^2)^{3/5}} .$$

(20)

Typical values of the Fried parameter are a few centimeters to a few tens of centimeters.

D. BEAM CONTROL

The primary objective of the HEL weapon's beam control subsystem is to accurately guide the laser beam to the target and maintain a small (focused) spot on the target throughout the engagement. To do this, we must account for the target and platform motion (wander, jitter) and preferably the atmospheric distortions (turbulence, thermal blooming, and extinction).

The beam control subsystem of a HEL includes the beam director, pointing and tracking subsystem, and adaptive optics. The beam director is basically a large telescope that takes a large beam (~1 m) at primary mirror and focuses it to a small spot (~10 cm) at the target. Usually, beam directors add much weight and volume to the entire HEL weapon system as they are large and heavy.

The pointing and tracking subsystems use a sensor and a gyro and feed the beam director to guide the weapon toward the target. The adaptive optics, not included in all HEL weapons, are the primary way to mitigate the effects of turbulence.

E. PERFORMANCE METRICS

The effectiveness of a HEL weapon system depends mainly on the following: 1) output power P, 2) light wavelength λ, 3) the primary mirror's diameter D, and 4) the range to the target R.

Often the goal of a HEL weapon is to focus its delivered laser beam into the smallest spot size possible, which we can estimate using (Perram et al. 2010):

$$w_0 \cong \frac{R\lambda}{\pi(D/2)}.$$

(21)

Gaussian modes characterize the transverse shape of a laser beam. To focus the laser on a small spot, we need output to be in the lowest Gaussian mode; otherwise, the laser spot size increases and thus the beam quality decreases, which is undesirable.

Irradiance is the laser power delivered to the target divided by the beam area ($A = \pi w_0^2$) (Perram et al.2010):

$$I = \frac{P}{A}.$$

(22)

Fluence is the energy delivered to the target; in other words, the irradiance multiplied by the dwell time (Perram et al.2010):

$$F = I\tau_D = \frac{P\tau_D}{A} = \frac{P\tau_D}{\pi w_0^2}.$$

(23)

Finally, a very important performance metric of a HEL is its beam quality, a factor of the spot size to the target, which is affected by several effects like platform jitter, turbulence, thermal blooming, and adaptive optics effectiveness (Perram et al. 2010). The following chapters provide a more detailed analysis of these factors. Table 2 summarizes the key performance metrics of a HEL.

Table 2.   HEL Key Performance Metrics. Source: Perram et al. (2010).

Metric	Variable	Units	Issues
Laser Power	P	kW to MW	Power without beam quality is a poor metric.
Source Brightness	B	MW/μrad^2	Good metric for source, removes engagement.
Delivered Fluence	F	kJ/cm^2	Absolute metric, engagement dependent.
Probability of Kill	P_k	Dimensionless	Compares delivered and required fluence.
Required Dwell Time	τ	s	Good absolute metric for specific mission.
Effective Range	R	km	Good metric for mission comparisons.

F.   DIFFRACTION

The effort to achieve a small-sized laser spot to the target is limited by diffraction and depends on the finite dimensions of the beam director, laser wavelength, and target

range. Under ideal conditions (no atmospheric effects and perfect beam quality) (Perram et al.2010):

$$r_d = R\left(1.22\frac{\lambda}{D}\right),$$
(24)

where R is the range of the target, D is the beam director size, and λ the wavelength. In the case of an ideal Gaussian beam (no absorption, no scattering, no turbulence), the irradiance at the center of the beam waist is given by (Blau 2015):

$$I(r,z) = I_o\left[\frac{w_0}{w(z)}\right]^2 \exp\left(-2\frac{r^2}{w^2(z)}\right),$$
(25)

where $w(z)$ is the radius at which the intensity drops by a factor of $1/e^2$ and w_0 the beam waist (always bigger than $w(z)$ for any z). Figure 21 shows the shape of an ideal Gaussian beam and its corresponding beam waist w_0 at the point of its focus (z=0) where obviously irradiance has its maximum value.
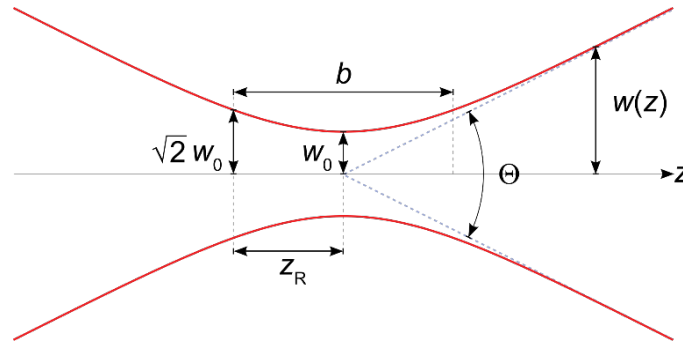
Figure 21. Gaussian Beam Width w(z) as a Function of the Distance z along the Beam. Source: Blau (2015).

The beam waist for an ideal beam is (Blau 2015):

$$w_0 \approx \frac{2\lambda l}{\pi D} ,$$

(26)

where D is the beam director diameter, λ is the wavelength, and l is the distance to the target. Due to the aforementioned atmospheric effects as well as jitter (caused by the platform's vibrations), though, the overall "quality" of the beam is poorer and the effective spot size now defined as:

$$w_0 \approx M^2 \frac{2\lambda l}{\pi D} .$$

(27)

This is similar to Equation 26 but with an additional factor M^2, the so-called beam quality. A perfect Gaussian beam would have a beam quality equal to one corresponding to the best beam quality we could potentially achieve. In reality, though, $M^2 > 1$ and obviously the spot size will increase.

G.   PLATFORM JITTER

Various vibrations of a HEL platform, called platform jitter, are another factor of laser performance degradation. The time-averaged spatial width of spot due to jitter is (Blau 2015):

$$w_j \approx \vartheta_{rms} l ,$$

(28)

where ϑ_{rms} is angular variance due to jitter and l is the distance to the target. For a typical system $\vartheta_{rms} \sim 5 \mu rad$.

H.   LETHALITY

The capability of a high energy laser weapon to cause any kind of damage or performance degradation through the delivery of its laser energy is called *lethality*. Apart from the energy delivered, the material of the target and its resistance to damage affect the lethality of the HEL weapon. Laser interaction with materials involves three basic stages: the absorption of the laser energy, the redistribution of the energy into various

material response modes such as heating and radiation, and the material response effects such as melting rupture and fracture (Perram et al. 2010). Figure 22 presents the thermal soak mechanism of lethality.
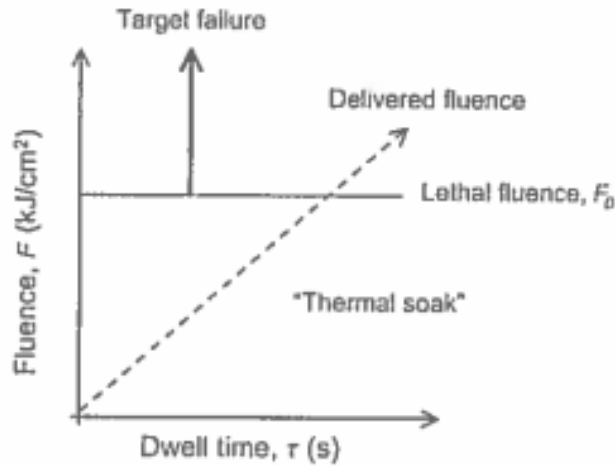
Figure 22. Thermal Soak Mechanism for Lethality. Source: Perram et al. (2010).

In order to melt the target (or, rather, melt the spot on the target where the energy is delivered) we have to account for the required energy needed to reach melting temperature (Blau 2015):

$$Q_1 = c_P m \Delta T ,$$

(29)

where c_P is the specific heat capacity, m is the mass, and ΔT is the temperature change. Once the illuminated spot on the target has reached its melting temperature, we have to account for the energy needed to melt the specific material at the melting point (Blau 2015):

$$Q_2 = m \Delta H ,$$

(30)

where ΔH represents the heat of fusion. Thus, the total energy required to melt the target has to exceed the sum of Q_1 and Q_2. We must also take into consideration the loss mechanisms that remove power from the target area. These are the power radiated away as a blackbody (Blau 2015):

$$P = \varepsilon\sigma A(T_{melt}^4 - T_{environment}^4) ,$$

(31)

where ε is the emissivity, σ the Stefan-Boltzmann constant, A the area being illuminated, T_{melt} the melting temperature, and $T_{environment}$ the environmental temperature. The power conducted to the surrounding volume of the target is (Blau 2015):

$$P_{cond} = kA(T_{melt} - T_{environment})/\Delta x ,$$

(32)

where k is the thermal conductivity and Δx the distance of temperature gradient. As an illustrative example, we can compute the energy needed to melt a 3 mm thick sheet of stainless steel and aluminum in a target area of radius 5 cm. We assume the temperature gradient to be 2 cm, a typical value for metals, and dwell times of a few seconds. The basic properties of stainless steel and aluminum are shown in Table 3.

Table 3.   Stainless Steel and Aluminum Basic Properties

Parameter	Stainless Steel	Aluminum	Units
Density	7.75e3	2.7e3	kg/m3
Specific Heat Capacity	420	897	J/(kg*K)
Melting Temperature	1644	933	K
Heat of Fusion	260	400	KJ/Kg
Emissivity	0.85	0.05	-
Stefan-Boltzmann Constant	5.67e-8	5.67e08	$J/(m^2 *s*K^4)$
Thermal Conductivity	11.2	237	W/(m*K)

Once we have calculated the required energy to melt the target and the total power losses, we can then calculate the required Irradiance as follows (Blau 2015):

$$I = \frac{\left(\left(\dfrac{Q_{melt} + Q_{heat}}{\tau_D}\right) + P_{loss}\right)}{(A*0.2)}$$. (33)

Figures 23 to 26 show the accumulated irradiance and Power in Bucket (PIB) for different dwell times. An additional fractional absorption of 20 percent has been included.

Figure 23. Required Irradiance for a 3-mm Thick Stainless Steel Sheet.
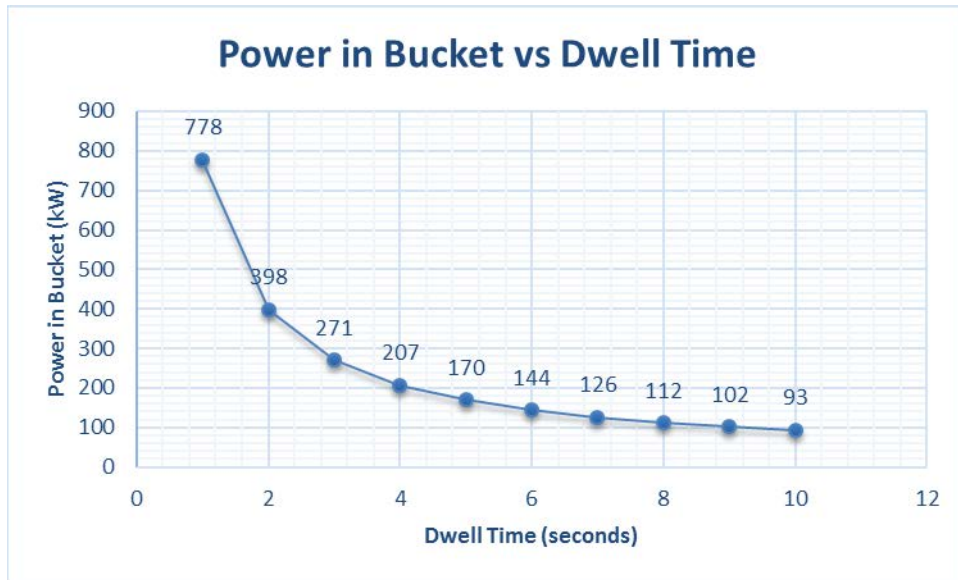
Figure 24. Required Power in Bucket for a 3-mm Thick Stainless Steel Sheet.
Bucket with a Radius of 5 cm.

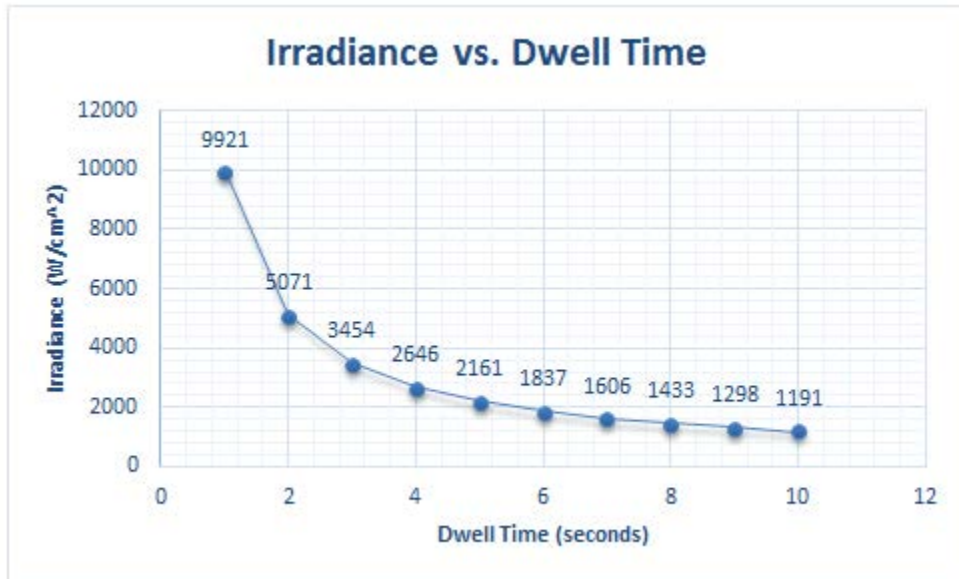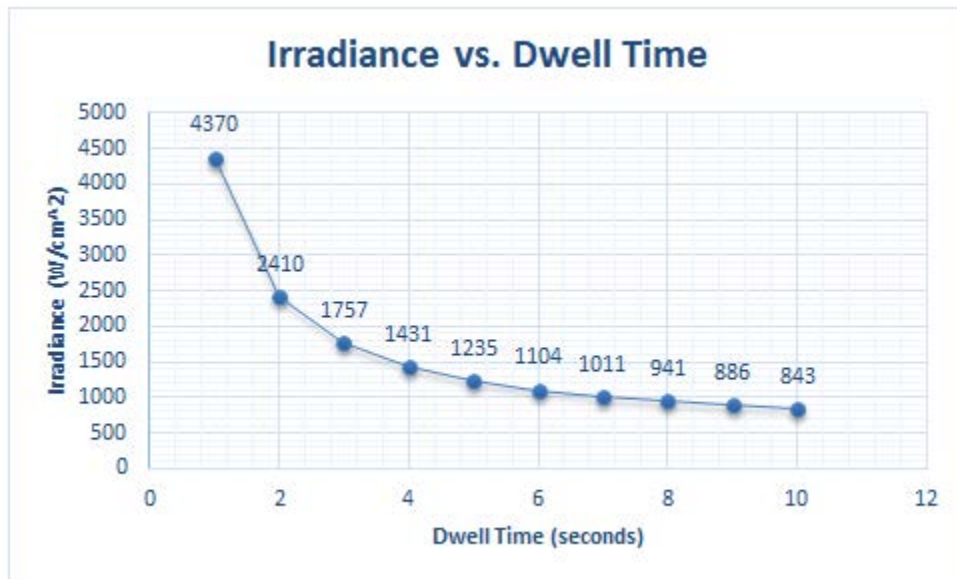Figure 25. Required Irradiance for a 3-mm Thick Aluminum Sheet.
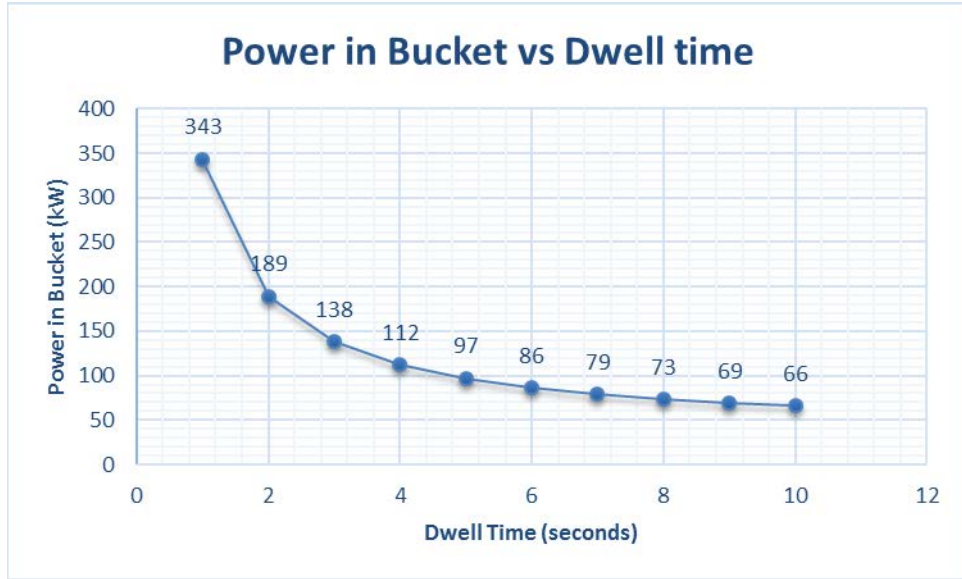
Figure 26. Required Power in Bucket for a 3-mm Thick Aluminum Sheet. Bucket with a Radius of 5 cm.

V.   HEL WEAPON UCAV EMPLOYMENT CONCEPT

Most of the developed UAVs have been designed to carry out missions like reconnaissance and surveillance; therefore, adding weapon capabilities to them and assigning them strike missions is highly constrained by their inherent design characteristics (Gertler 2012). Consequently, a separate class of UAVs is required to be designed and developed that will be able to carry the weaponry load while maintaining increased flight capabilities. "A separate class of UAS is being designed from the ground up to carry out combat missions. Called unmanned combat air vehicles, or UCAVs, these systems feature greater payload, speed, and stealth than current UAS" (Gertler 2012, 4).

A.   DESIGN CONSIDERATIONS

Since UAVs have been available for only a short period of time relative to other military systems, their design and the way they are operated are still evolving. Inevitably, different operational requirements may determine different design characteristics. Ideally, a UAV platform should be adaptable to the many different mission sets of all branches of military service, but cost and mission requirements may make that unreasonable.

In general, a UAS system consists of several subsystems, such as a ground control station, a ground crew including remote pilots and sensor or weapon operators, communication links, and often multiple air vehicles (Gertler 2012). "No one sub-system is more important than another, though some, usually the aircraft, have a greater impact upon the design of the other subsystems in the system than do others" (Austin 2010, 9). Except for the aircraft's design, the design of the rest of the subsystems is out of the scope of this study, and we will assume they are fully compatible with the aircraft and provide the required support for mission execution.

"The type and performance of the air vehicle is principally determined by the needs of the operational mission" (Austin 2010, 10). The UAV's primary task is to carry its mission payload to the area of operations, and to do so, it additionally has to carry other subsystems like the communication links, electrical power generators and of course the fuel load. Reg Austin identifies the most important parameters of the air vehicle to be

the following: a) *Payload*, b) *Endurance*, c) *Radius of Action,* and d) *Speed Range*. In strike missions, all these operational requirements are increased in comparison to normal reconnaissance missions. In addition to these requirements, the *Flight Altitude* is discussed as a very critical operational parameter, especially for a UCAV employing a high energy laser. Finally, another important design parameter is the stealth capabilities of the UCAV.

1. Payload

According to Austin, the payload carried by an aircraft is essential to achieve the mission, but it is not required for the aircraft to fly (Austin 2010). Nevertheless, the size and mass of the payload drives the design requirements of the UAV. Different missions require different capabilities that are mapped into different payload requirements. Typical payload masses range from a fraction of a kilogram up to several thousands of kilograms, and their corresponding volume from cubic centimeters to several cubic meters. The payload also has a significant impact on the endurance, radius of action, and speed, as well as on the maximum altitude at which the UAV will be able to operate. Finally, the dimensions of the payload will affect the stealth capabilities of the UAV and will require additional storage space inside the aircraft body. It is important to note that we do not consider as payload any other subsystems like the communication module, but only the one required for mission execution. The high energy laser weapon is the payload for the UCAV we examine in this thesis. Therefore, the size and volume of the HEL weapon as determined by its output power and other characteristics directly affect the design of the UCAV. There has to be a trade-off between the dimensions of the HEL weapon and its performance with the design of the UCAV. This trade study must be based not only on how each laser parameter affects the mission's success, but also on the corresponding cost.

2. Endurance

The endurance of the UCAV, within its radius of action, is primarily based upon the aerodynamic characteristics of the aircraft. It defines the coverage of the air vehicle, the loiter speed with which the UCAV will patrol within a predefined area, and the operating altitude (Torun 1999). Endurance is also a function of the carried fuel. The

larger the amount of fuel the UCAV can carry, the longer its endurance. However, as we saw previously, the fuel capacity is constrained by the size of the UCAV and indirectly proportional to the payload. The mass of the fuel carried varies from 10 percent of the total system's mass for short-range applications to almost 50 percent for long-range applications, and thus plays a major role in the overall mass of the system (Austin 2010). Usually, systems with high endurance do not have high cruise or dash speed (the speed during the attack) (Torun 1999).

3.   Radius of Action

The radius of action is defined as the maximum range that the UCAV can fly out, execute its mission, and return to its base without refueling. Obviously, the radius of action has to be sufficient to cover the area of interest (Torun 1999). It mainly depends upon the fuel mass carried and how efficiently the fuel is used; generally, it depends on the cruise speed of the UCAV. The radius of action is further limited by the radio-link requirements and the navigation equipment (Austin 2010).

4.   Speed Range

The speed of a UCAV can be categorized by the following: a) cruise speed, the speed that is used while flying to and from the area of interest; b) the maximum speed; and c) the loiter speed, the speed that the UCAV will fly while remaining within the area of interest. As mentioned before, the higher the speed, the shorter the endurance. Consequently, there is a trade-off between the timeliness of the mission, which determines the speed, and the desired endurance. These are typical speed ranges for different roles, as defined by Austin (2010):

- 0–100 knots for a close-range surveillance role;
- 0–150 knots or greater for many off-board naval roles;
- 80–150 knots for long-range surveillance and airborne early warning roles;
- knots–1 mach for future interception / interdiction roles.

5. Operating Altitude

The operating altitude of a UCAV is defined as the altitude at which the payload performance is optimized. As discussed in Chapter IV, the performance of a HEL weapon is degraded by the atmospheric conditions, which can vary with altitude. Consequently, the altitude at which a UCAV will fire the HEL weapon is a critical operational parameter that strongly affects the laser's performance. On one hand, turbulence near the surface might favor a higher operating altitude for best laser performance. On the other hand, strike missions usually require flying in low or very low altitudes in order to increase the survivability of the system by staying invisible to the enemy radars.

Table 4 shows a summary of characteristics for various types of UAVs covering a wide size and capability spectrum.

Table 4.   Characteristics of Selected UAVs. Adapted from Geer and Bolkcom (2005) and Bone and Bolkcom (2003).

Vehicle	Payload Capacity (lbs)	Endurance (hours)	Radius of Action (n.mil.)	Speed (kts)	Altitude (ft)
RQ-4 Global Hawk	3000	28	5400	340	60000
MQ-1B Predator	450	24+	500+	120	25000
MQ-9 Reaper	3750	24	2000	225	50000
RQ-5A Hunter	300	12	144	106	15000
MQ-8 Fire Scout	600	6+	150	117	20000
RQ-7 Shadow	60	6	68	60	15000
MQ-1C Gray Eagle	800	28	1240	60	28000
Scan Eagle	13	20	60	49	19000
UCAS-D	4500	6	2100	High Subsonic	36000
X-45C Phantom Ray	3000	7	1200	450	40000
Avenger	6000	18	-	400+	50000
MQ-5B Hunter II	130	18	144	106	18000

B. HEL WEAPON INTEGRATION CONSIDERATIONS

Meeting all performance requirements for a HEL weapon is not sufficient if it cannot be integrated into the desired platform. A complete electric laser system consists of an electrical power supply, a power management subsystem, cabling, control subsystems, beam transfer optics and mounts, thermal management subsystems, and mechanical mounting structures to hold it all together (Motes & Berdine 2009). As discussed in Chapter I, the integration of a HEL weapon in an airborne platform has already been realized in several programs; yet several factors, both technical and economic, led to their cancellation. The same issues will be faced while integrating a HEL weapon in an unmanned aerial vehicle. SWaP constraints as well as the thermal management are the more critical issues to address.

1. Thermal Management

Thermal management is perhaps one of the most challenging issues one has to deal with when building a high-power laser system. Fiber lasers, perhaps, present fewer thermal management issues "due to their high electrical-to-optical conversion efficiency, tolerance for larger temperature variations and large fiber surface-to-volume ratio" (Motes and Berdine 2009, 286). This large surface-to-volume ratio would allow a fiber laser mounted on a UCAV to be cooled by simply flowing ambient air over the fibers, whereas the diode laser pump would require liquid cooling due to the high concentration of heat (Motes and Berdine 2009). As an example, a fiber laser with a 25 percent electrical-to-optical efficiency that produces 25 kW of optical output power requires 100 kW of input electrical power. Thus, it produces 75 kW of waste heat that must be removed. It could require an additional 25 kW of power to remove the 75 kW of waste heat (Motes and Berdine 2009). Thus, a total of about 125 kW of power will be required to operate the device in this particular example. Obviously, generating such power on a UCAV is difficult. It could therefore be advantageous to use a small generator for power, or to employ batteries to store energy for immediate use, and use a thermal mass to store the heat until it can be more gradually removed. Then the batteries could provide the large output power needed during an engagement, and the smaller generator could

recharge the batteries and operate a cooler to remove the waste heat between shots (Motes and Berdine 2009).

2. Size, Weight, and Power

A second factor (or set of factors) that would constrain the integration of a HEL weapon into a UCAV is its size, weight, and power. Ideally, the size of the HEL system, with the exception of the beam director, should fit inside of the airframe to achieve higher stealth capabilities. The only current laser technology capable of accommodating such a restricted volume is, perhaps, fiber laser technology. "Fiber solid state lasers (SSLs) are widely used in industry—tens of thousands are used by auto and truck manufacturing firms for cutting and welding metals" (O'Rourke 2015, 8). Additionally, industrial lasers have already demonstrated that they are significantly smaller than their bulk solid-state laser equivalents. For example, a typical 4-kW fiber laser has a footprint of 5.4 square feet. Typically, a fiber laser has approximately half the weight of a bulk solid-state laser as a result of its higher efficiency and easier cooling (Motes and Berdine 2009). The UAV must also have the capability to provide the laser system with the required power. By using the configuration mentioned previously, the required battery per-shot energy capacity to fire the laser is (Motes and Berdine 2009):

$$E_L = \frac{1.3 P_L T_L}{\eta_{eo}},$$ (34)

where P_L is the laser output power, η_{eo} is the electrical-to-optical efficiency, and T_L is the desired magazine depth in terms of lase time; this does not include the power for the cooling system. The 1.3 factor in the equation is to account for an additional 30 percent of energy since the batteries are not 100 percent efficient. For example, a 50-kW laser weapon, for a 5-second lase time, with a 25 percent electrical-to-optical efficiency would require approximately 1.3 MJ.

Two types of batteries are available for energy storage: lead acid and lithium-ion batteries. The first one is a mature technology that is already in use on navy ships and has

a 200 MJ/m^3 energy density. The disadvantages of this type are its poor discharge depth (~50 percent), the long recharge time (~few hours), and a short lifetime (~500 recharge cycles). In contrast, the lithium-ion battery is a newer technology with several advantages but also the potential for being a fire hazard. Compared to lead-acid technology, it has higher energy density (~1000 MJ/m^3), better discharge depth (~95 percent), shorter recharge time (~hour), and longer lifetime (~1000 recharge cycles).

C. CONOPS DEVELOPMENT

According to the final report of the Defense Science Board (DSB) Task Force on Directed Energy Weapon Systems and Technology Applications, the advances in electrically based solid-state and fiber laser technology are likely to make useful low-power applications achievable within a few years. Specifically, the task force states:

> Systems with improved efficiency and reasonable beam quality for solid-state and fiber lasers offer the promise of manned and unmanned aircraft applications at power levels of hundreds of kilowatts for self-defense and ground precision ground attack at distances to 10 kilometers with moderate beam control system apertures (5–30 cm). (2007, 11)

A UCAV employing a low to medium power laser weapon seems to be technologically feasible and operationally advantageous. However, as with any other weapon system, it would not provide an operational solution for every mission. The next sections examine the performance capabilities of such a UCAV armed with a laser weapon and provide helpful insight for any potential missions that such a combination could accomplish. Prior to that, a quick overview of applicable missions to a UCAV armed with a HEL is presented.

1. Air-to-Air Missions

Although UAVs primarily are developed to execute Intelligence, Surveillance, Reconnaissance (ISR) missions, UCAVs are being developed with air-to-air weapons that allow them to undertake air superiority missions (Gertler 2015). In fact, an actual air-to-air combat between a Predator drone and an Iraqi fighter aircraft reportedly occurred in 2003, when the former fired a Stinger missile at the latter before the fighter shot it down (Gerlter 2015). However, the existing technology level does not allow for an advanced

air-to-air capability yet "because the situational awareness and reaction time of an offboard pilot is insufficient" against a manned aircraft (Alkire et al. 2010, 44). Therefore, attacking slower airborne targets may be the only viable option for a UCAV. Another potential operational use for a UCAV would be a combined manned-unmanned force; namely, the manned aircraft would lead the unmanned UCAVs and have control over their weapons. Nevertheless, significant challenges would have to be overcome for this to happen; consequently, true air-to-air combat capability seems unattainable in the 2025 timeframe (Alkire et al. 2010).

2. Air-to-Ground Missions

Selected air-to-ground missions, based upon the required power and operational use, would be more applicable for a UCAV armed with a HEL weapon.

*Penetrating Strike***:** Flying deep inside enemy territory that likely will be heavily defended is a high-risk mission. This threat characteristic already makes the UCAV solution an attractive option compared to a manned vehicle since a UCAV has increased range and keeps its pilot far from the hostile environment (Alkire et al. 2010).

Close Air Support (CAS): Close Air Support is currently performed by both manned and unmanned aircraft (Alkire et al. 2010). Key parameters for this type of mission are the range and endurance of the vehicle; consequently, UCAVs are well suited for it. Even better, a UCAV with air refueling capabilities would be able to stay on task for an extended period of time. The combination of these capabilities with the deep magazine capabilities of a HEL weapon would provide an ideal solution for a durable air support platform for ground troops. Additionally, the high accuracy of the laser weapon would allow its use in very close proximity with the friendly forces without risking any friendly losses.

Another very promising use of a UCAV-based HEL weapon, with low to medium power capabilities, would be for non-lethal applications. The DSB's report on Directed Energy Weapons states that low power lasers "can provide the capability to 'dazzle' snipers and the operators of small surface ship threats, as well as blind visible and infrared sensors and night vision systems" (DSB 2007, 11). Therefore, laser weapons

would extend into new mission areas for UCAVs such as homeland security and homeland defense. Border patrolling, maritime security, and counter-terrorism applications would be an ideal fit for a UCAV-based HEL weapon, without the need for high output power and the corresponding demand of weapon size and weight.

THIS PAGE INTENTIONALLY LEFT BLANK

VI.   SYSTEM ARCHITECTURE MODELING

According to Benjamin S. Blanchard and Wolter J. Fabrycky, the conceptual design of a system is "the first and most important phase of the system design and development process" (Blanchard and Fabrycky 2011, 56). The system architecture, as part of the conceptual design process, deals with the top-level system configuration. It is the development and articulation of different perspectives of a system. This chapter is devoted to creating a typical system architecture for a UCAV armed with a HEL weapon, utilizing Vitech's CORE architectural software package. The UCAV system architecture follows the DOD Architectural Framework (DODAF), shown on Figure 27. Not all DODAF schema components are utilized in this project. Those used are indicated with a red arrow and the accompanying number label shows their corresponding sequence.

Figure 27. DODAF Schema. Adapted from Vitech Corporation (2011).

We begin with the required capabilities for the UCAV to accomplish a CAS mission, as described in Chapter V, and the top-level system requirements that implement

these capabilities. Following that, a typical sequence of the operational activities the UCAV would follow for a CAS mission are described and linked to the capabilities that are their basis. The functions that implement the operational activities compose the functional architecture of the UCAV and are then allocated to physical components. The external key interfaces are also described, and finally, the primary technical performance measures (TPMs) are identified. The UCAV system architecture for this study covers only the top-level structure. More detailed modeling of the UCAV is out of the scope of this study and would require extended source availability.

A.   CAPABILITY NEEDS AND SYSTEM REQUIREMENTS

According to the Joint and Naval Capability Terminology List (2007), *Joint Air Operations* is "the ability to employ joint forces to achieve military objectives within and through the air domain. Such operations include those to establish local air superiority, provide missile defense, assault support operations and execute strikes." Tier 2A, among others, includes *Tactical Air Support,* which is further decomposed to *Close Air Support* and *Assault Support*.

Therefore, the specific capability needs for the UCAV-HEL weapon system in order to execute a CAS mission are these:

- High Endurance (Bartley 2002)

- Increased Survivability (Bartley 2002)

- Substantial Firepower Capabilities (Bartley 2002)

- Efficient Command and Control Network (Wilson 2013)

- Improved Targeting Sensors (Bartley 2002)

Derived from those capability needs, we identify the top-level system requirements:

- The UCAV shall have sufficient range and loiter capability to execute the CAS mission.

- The UCAV shall have cruise speed within 80 and 130 kts.

- The UCAV shall have stealth design characteristics.

- The UCAV shall have a reliable flight control system.

- The UCAV shall be able to deploy a HEL weapon.

- The UCAV shall be able to kill a "hard" target at ranges up to 5 km.

- The UCAV shall be able to deliver its weapons accurately to the target.

- The UCAV shall be able to communicate with the rest assets of the communication network.

- The UCAV shall be able to detect the target.

- The UCAV shall be able to engage the target.

Obviously, these requirements would require exhausting analysis during the entire design and development process. However, this would be a good starting point to refine those top-level requirements down to component requirements. Figure 28 collectively shows the top-level capabilities decomposition, starting from the generic capability to execute a CAS mission and going down to the second level of decomposition, as well as the requirements that implement each of these capabilities.
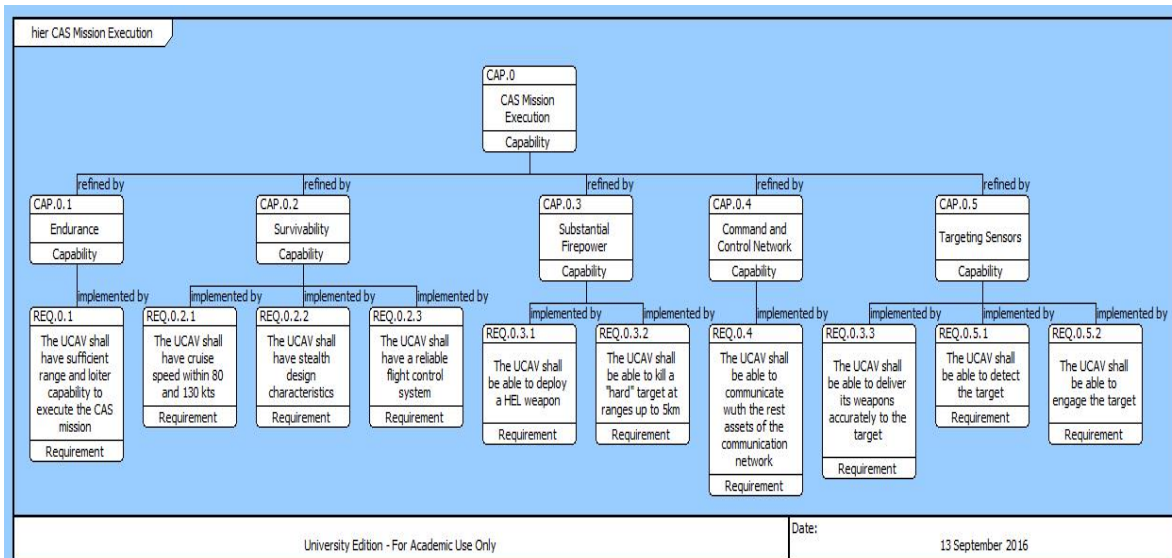

Figure 28. Requirements Traceability.

B.   OPERATIONAL ACTIVITIES

The previously stated capabilities form the basis for the operational activities that constitute the operational viewpoint of the system. The Operational Viewpoint of the

UCAV system describes the tasks followed to execute a typical mission. The Enhanced Functional Flow Block Diagram in Figure 29 shows the sequence of activities followed to *Conduct CAS Mission,* and Table 5 displays the title, number, and description of each operational activity. The green oval boxes in Figure 29 represent *triggers* that control the execution of an operational activity by their presence or absence. A trigger can be energy, material, or information. The grey boxes represent the output (that is, the energy, material, or information) of an operational activity.
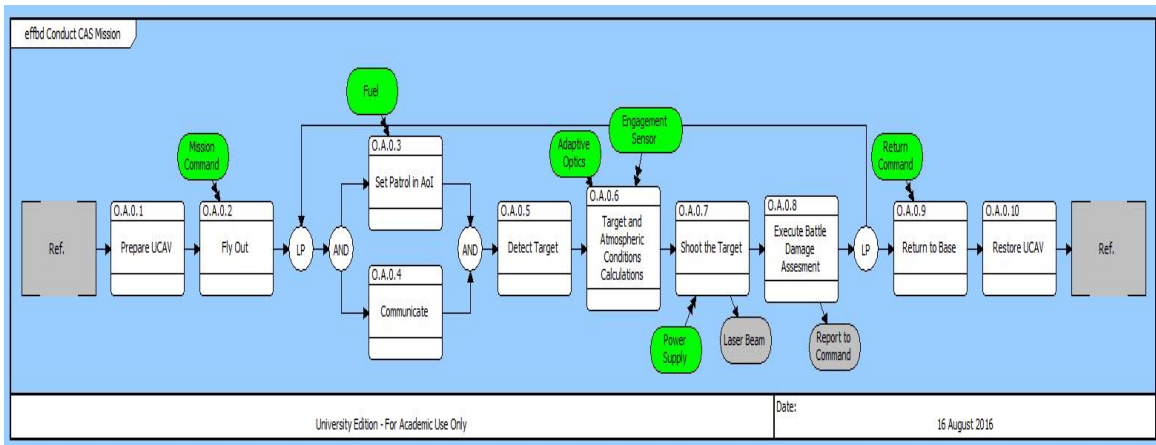

Figure 29. Operational Activities Sequence for "Conduct CAS Mission."

Table 5.   Operational Activities Description.

Number	Title	Description
OA.0.1	Prepare UCAV	Describes all necessary activities (maintenance, logistics, and training) to prepare the UCAV for the mission.
OA.0.2	Fly Out	Describes the movement of the UCAV from its base to the predetermined area and is triggered by the mission commencement command.
OA.0.3	Set Patrol in Area of Interest	Once the UCAV arrives at the Area of Interest it takes the appropriate speed, altitude, and direction to effectively cover the whole area. It is constrained by the available fuel.
OA.0.4	Communicate	The UCAV communicate with the Ground Control Station and other friendly assets.
OA.0.5	Detect Target	The UCAV uses its sensors to detect a target of interest.
OA.0.6	Target and Atmospheric Conditions Calculations	The UCAV uses its sensors to engage the target and measure the atmospheric conditions within its location and the target's location. It is triggered by the adaptive optics subsystem, which compensates for laser beam distortion and the availability of the engagement sensor.
OA.0.7	Shoot the Target	The UCAV fires the laser weapon. It is triggered by the UCAV's power supply availability and outputs the laser beam.
OA.0.8	Execute Battle Damage Assessment	The UCAV determines the lethal effects caused to the target and reports the results to the command.
OA.0.9	Return to Base	The UCAV flies back to its base after it is commanded.
OA.0.10	Restore UCAV	Describes all necessary activities to repair any subsystem failures.

C.   FUNCTIONAL ARCHITECTURE

Operational activities phase is followed by the functional architecture, which more explicitly describes what the system has to do to complete its mission. According to

DODAF schema, the system requirements are the basis of the functions, which implement the operational activities.

In the case of the UCAV-HEL weapon system, the functional hierarchy is presented in Figure 30, to show the top-level functions needed in order to *Utilize UCAV for CAS mission* and are then decomposed to the second level in order to provide greater insight into the functions that the UCAV must accomplish.

Functions are then allocated to physical components. Figures 31 through 38 show the high-level functional allocations to the physical components that will implement them.
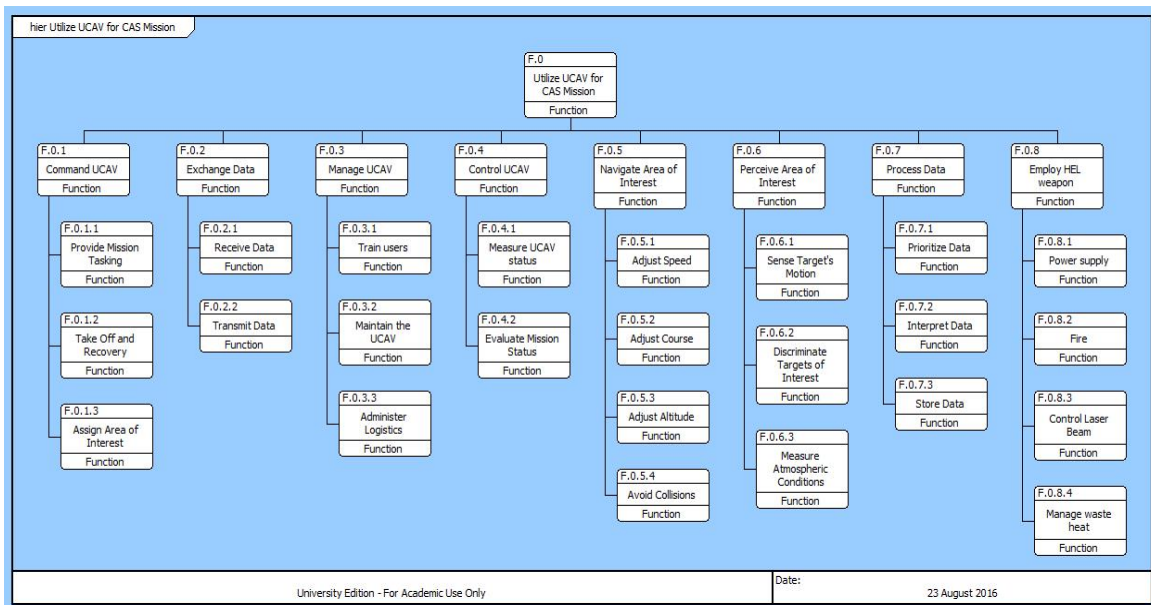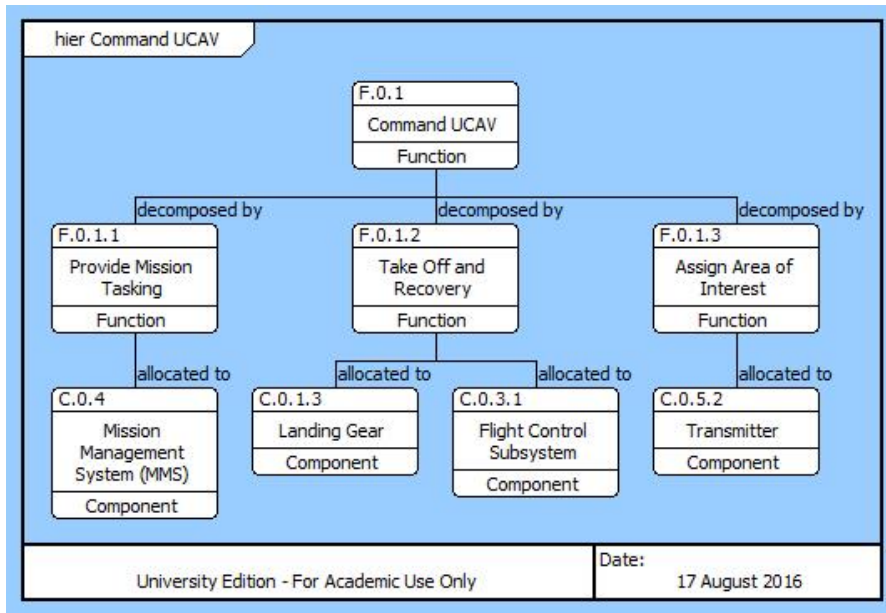

Figure 30. Functional Hierarchy Decomposition.

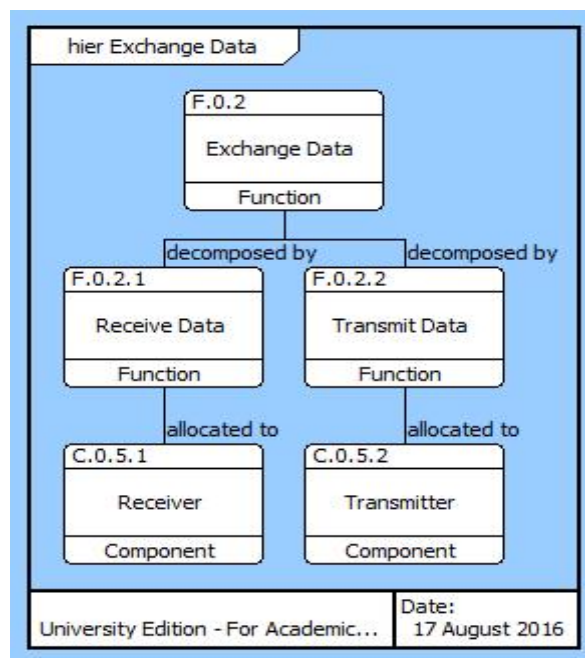Figure 31. Functional Allocations to Physical Components for Function F.0.1.

Figure 32. Functional Allocations to Physical Components for Function F.0.2.

Figure 33. Functional Allocations to Physical Components for Function F.0.3.

Figure 34. Functional Allocations to Physical Components for Function F.0.4.

Figure 35. Functional Allocations to Physical Components for Function F.0.5.
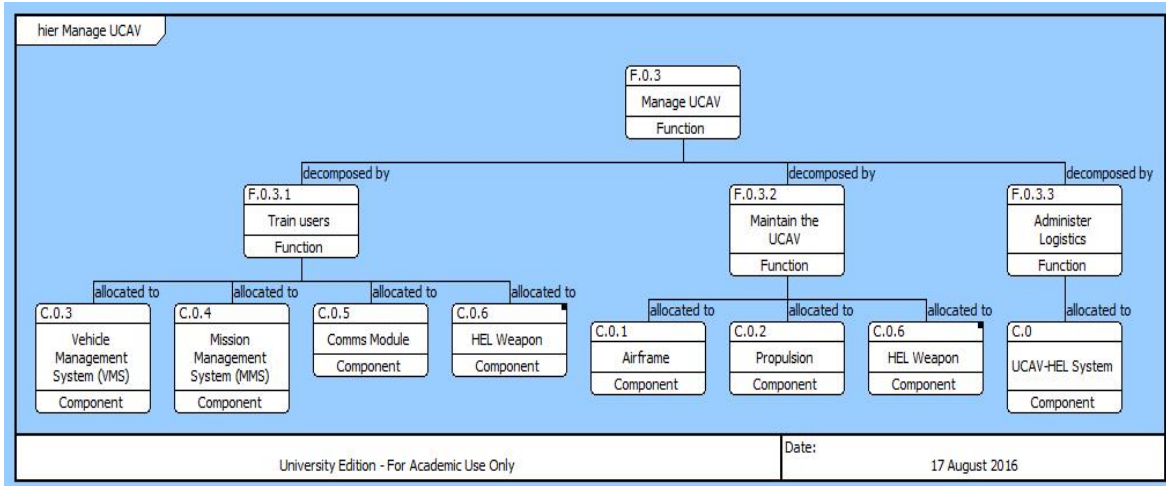

Figure 36. Functional Allocations to Physical Components for Function F.0.6.
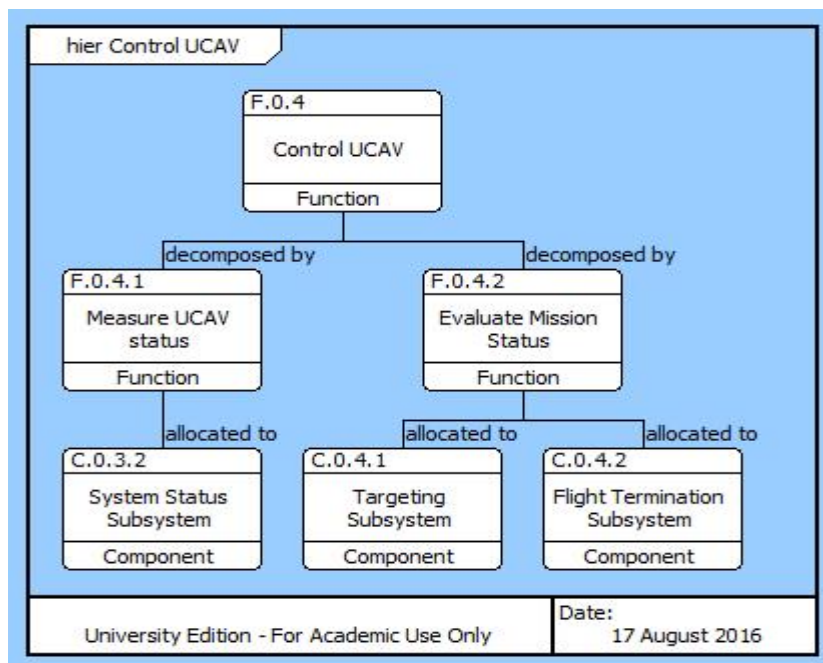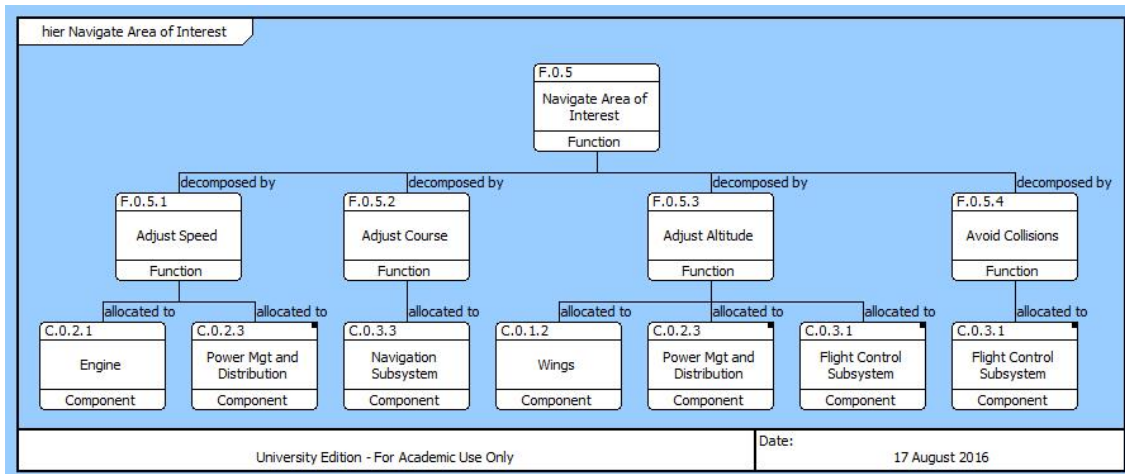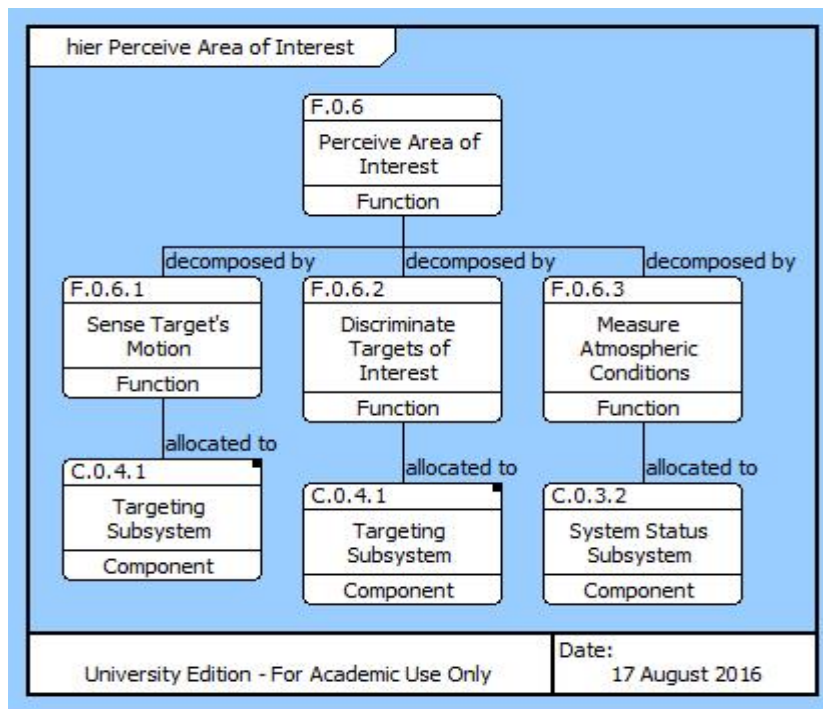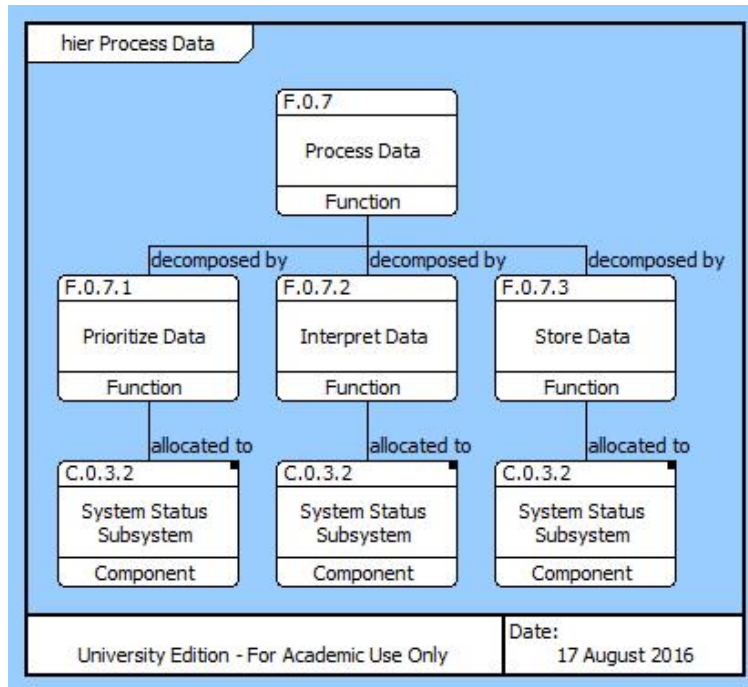
Figure 37. Functional Allocations to Physical Components for Function F.0.7.
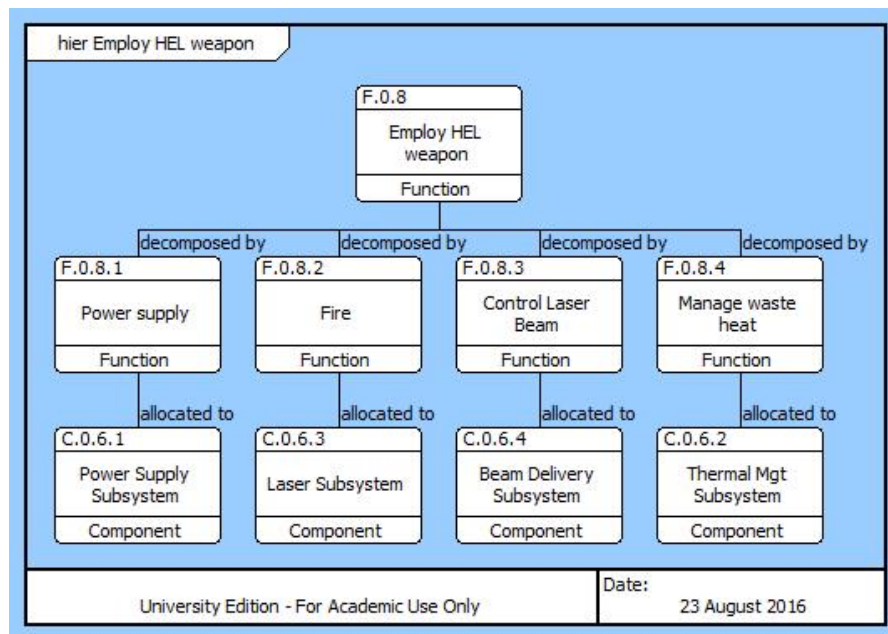
Figure 38. Functional Allocations to Physical Components for Function F.0.8.

D.   PHYSICAL ARCHITECTURE

The physical architecture provides the breakdown of component systems in conjunction with functional architecture. The UCAV system's most critical component is the high energy laser weapon. Yet, looking at the higher level physical architecture of the entire UCAV system, we include not only the HEL weapon subsystem but also all the major subsystems required and related to the functional success of the system.

Figure 39 shows the physical architecture of the system in a hierarchical view.

Figure 39. Physical Architecture Hierarchy.

Table 6 provides the description of the physical components and the corresponding functions that they perform.

Table 6.   Physical Components Description.

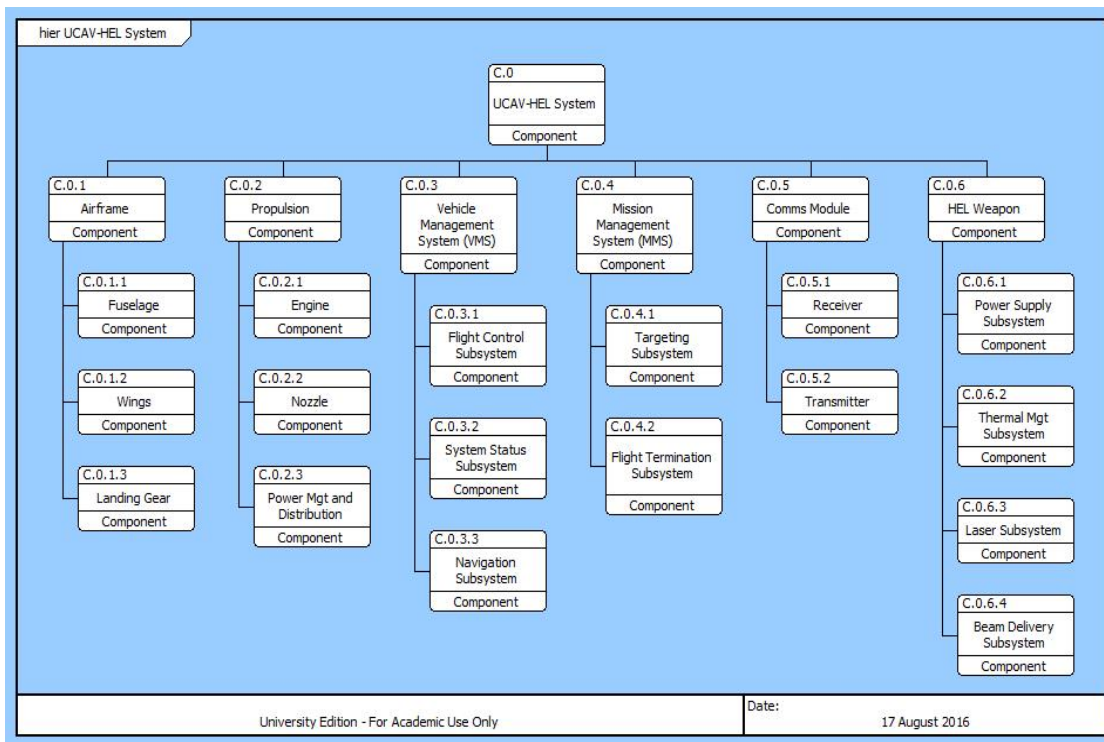| Number	Title	Description
C.0.1	Airframe	The main structure of the UCAV, including the fuselage, the wings, and the landing gear. Performs the "Maintain the UCAV" function.
C.0.1.1	Fuselage	The main body of the UCAV. Performs the "Maintain the UCAV" function.
C.0.1.2	Wings	Support the flying capabilities of the UCAV. Performs the "Adjust Altitude" function.
C.0.1.3	Landing Gear	Performs the "Take Off and Recovery" function.
C.0.2	Propulsion	Supports the endurance capabilities of the UCAV. Performs the "Maintain the UCAV" function.
C.0.2.1	Engine	Generates the required power for the UCAV to fly. Performs the "Adjust Speed" function.
C.0.2.2	Nozzle	Performs the "Maintain the UCAV" function.
C.0.2.3	Power Management and Distribution	Supports the power distribution to UCAV subsystems. Performs the "Adjust Speed" function.
C.0.3	Vehicle Management System (VMS)	Manage and control all UCAV functions. Performs the "Train Users" function.
C.0.3.1	Flight Control Subsystem	Performs the "Flight Control" function.
C.0.3.2	System Status Subsystem	Performs the "Measure Atmospheric Conditions," "Prioritize Data," "Interpret Data," and "Store Data" functions.
C.0.3.3	Navigation Subsystem	Performs the "Adjust Course" function.
C.0.4	Mission Management System (MMS)	Performs the "Provide Mission Tasking" and "Train Users" functions.
C.0.4.1	Targeting Subsystem	Allows for targets' detection and engagement. Performs the "Evaluate Mission Status," "Sense Target's Motion," and "Discriminate Targets of Interest" Functions.
C.0.4.2	Flight Termination Subsystem	Performs the "Evaluate Mission Status" function.
C.0.5	Communications Module	Allows for all types of communications, both Line of Sight and Beyond Line of Sight. Performs the "Train Users" function.
C.0.5.1	Receiver	Allows for receiving data. Performs the "Receive Data" function.
C.0.5.2	Transmitter	Allows for transmitting data. Performs the "Transmit Data" function.
C.0.6	HEL Weapon	Supports the lethal capabilities of the UCAV. Performs the "Maintain UCAV" and "Train Users" functions.
C.0.6.1	Power Supply Subsystem	Provides the required power to the Laser subsystem. Performs the "Power Supply" function.
C.0.6.2	Thermal Management Subsystem	Manages the waste heat of the Laser subsystem. Performs the "Manage Waste Heat" function.
C.0.6.3	Laser Subsystem	Generates the laser beam. Performs the "Fire" function.
C.0.6.4	Beam Delivery Subsystem	Controls the laser beam toward the target. Performs the "Control Laser Beam" function.

E.   INTERFACES

The UCAV-HEL system is a highly complex system that operates by means of interactions, both internal and external. The main interfaces for these interactions reside between subsystems, between human and systems, and between the entire system and external systems (system context).

The system context, as shown in Figure 40, contains the UCAV and the external systems with which the UCAV interacts (that is, the base, environment, target, satellite, operators, Ground Control Station, friendly assets). The most crucial subsystems interface has to do with the target data transfer from the perception subsystem to the laser weapon in order to effectively detect and shoot at a target. Once the sensors detect a target and engage it, immediately the beam control subsystem guides the laser beam from the HEL toward the target. Table 7 provides a detailed description of those interfaces.
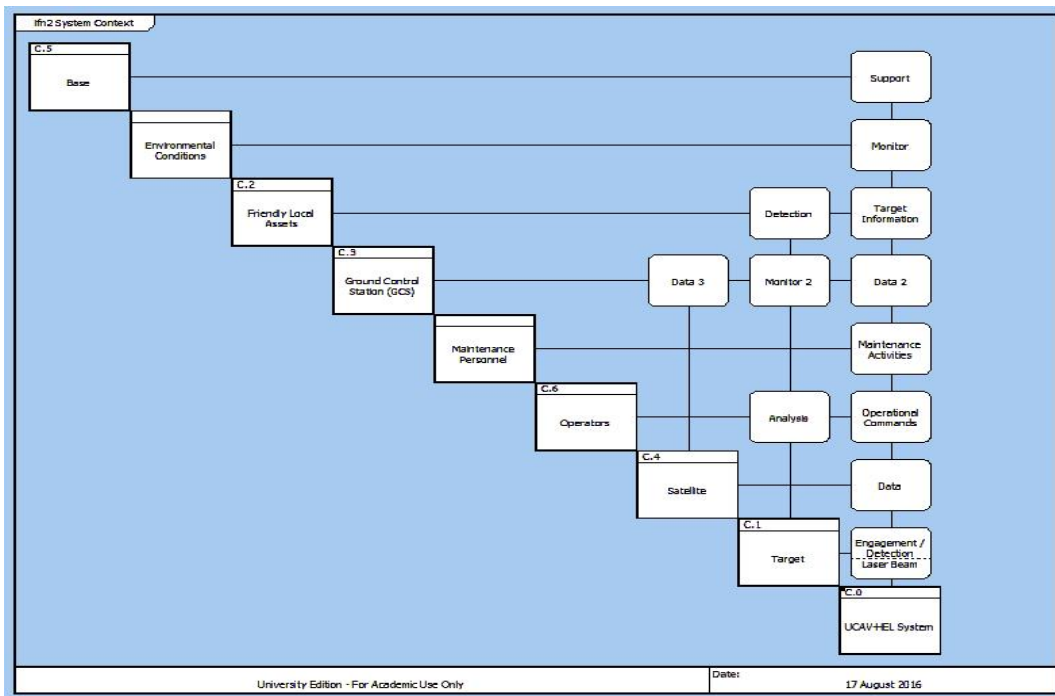

Figure 40. System Context Interface Diagram.

Table 7.   Interface Description.

Interface	Description
UCAV—Target	The UCAV **detects** and **engages** the target**,** and **shoots** the **laser beam** at the target.
UCAV—Satellite	The UCAV receives and transmits **data** from the satellite to communicate.
UCAV—Operators	Operators manage and control the UCAV through **operational commands.**
UCAV—Maintenance Personnel	The maintenance personnel perform the required **maintenance activities** on the UCAV-HEL system.
UCAV—GCS	The UCAV receives and transmits **data** from the Ground Control Station.
UCAV—Friendly Local Assets	UCAV exchanges **target information** with other Friendly Local Assets.
UCAV—Environmental Conditions	The UCAV **monitors** the environmental conditions for efficient HEL weapon utilization.
UCAV—Base	The base where the UCAV is stationed provides **support** to the UCAV.
Target—Operators	The operators execute **analysis** of the target's information.
Target—GCS	The Ground Control Station **monitors** the target.
Target—Friendly Local Assets	The target is **detected** by other local friendly assets.
Satellite—GCS	The Ground Control Station exchanges **data** with the satellite.

F.   TECHNICAL PERFORMANCE MEASURES

The completion of the UCAV system architecture allows for the identification of the TPMs, which are the primary metrics that describe the UCAV's performance. TPMs can be estimated, predicted, or measured quantitatively, and they measure specific characteristics of the system. These characteristics are based upon the design of the system. In this study, we follow the reverse process. We identify the most critical technical characteristics for the UCAV to execute the CAS mission and describe the required trade-offs between them that will drive the design of the UCAV.

The TPMs evolve primarily from the development of the system's operational requirements (Blanchard and Fabrycky 2011). The first step of the system architecture was the capability analysis and the operational requirements derivation from those capabilities. The type of the mission to be executed by the UCAV and the scope of this study lead to the identification of two main TPMs: the endurance of the UCAV and lethality of the HEL. These two measures are assumed to have the greatest impact on the

overall operational effectiveness of the UCAV and are inversely proportional to each other. Table 8 lists the technical performance measures for the UCAV.

Table 8.   UCAV TPMs.

UCAV Technical Performance Measures		
	Operational Requirement	TPM
1	The UCAV shall have sufficient range and loiter capability to execute the CAS mission.	Endurance (hrs)
2	The UCAV shall be able to kill "hard" targets at ranges up to 5 km.	HEL Lethality (W/m^2)

Therefore, the designer has to balance the TPMs effectively. This fact is the primary purpose of the simulation and analysis that follows in the next chapter. Initially the UCAV operational tactics and the HEL design are linked to determine the laser lethality. The same correlations then provide estimates for the UCAV endurance.

THIS PAGE INTENTIONALLY LEFT BLANK

VII. EXPERIMENTAL DESIGN AND SIMULATION

A. DESIGN OF EXPERIMENTS METHODOLOGY

When dealing with highly complex systems, we must consider a large number of design parameters that may play a key role in the performance of the system. Design of Experiments (DOE) is a very useful mathematical process that allows the systems engineer to simultaneously evaluate the effect that each of these design parameters has on the performance and to collect the maximum amount of information possible from a given number of simulation runs.

To explore the effects that the HEL design parameters as well as the UCAVs' operational parameters will have on the overall performance, we utilize DOE; specifically, the response surface methodology (RSM). By including both operational and design parameters in our simulation model, we are then able to determine their interactions. According to Law (2015), the basic terminology used in DOE is the following:

Factors: The input parameters of the simulation.

Response: The output performance measure of the simulation.

Level: The values that a factor can have.

When dealing with a very large number of factors, designers typically follow a two-step approach. The first step, usually a 2^k factorial design, is used to make an initial estimate of the factors that have statistical significance, allowing for exploration of only those in a refined design method such as RSM.

The 2^k full factorial design, where k is the number of the input parameters, is an economical strategy for determining the effects of factors on the response and their interactions with each other (Law 2015). It requires two levels for each parameter that correspond to the maximum and minimum of the range of each parameter. Each of these 2^k possible combinations of the input parameters, called *design points*, will require a simulation run and output a corresponding response value. The whole set of the input

parameter combinations is called the *design matrix*. The two-level full factorial design will be used for initial factor screening and determination of the statistically significant factors that will be further analyzed by the RSM, which utilizes additional design points within the extreme ones to identify potential "curvature" in the factor-response relationships. The number of controllable factors used in this study (five) is low enough to allow skipping the screening phase (2^k factorial design) and to proceed directly to RSM.

Having defined the problem, which is to measure the performance of the UCAV-based HEL weapon and how it is affected by various parameters (design and operational), we then have to select the output measurement of our simulations (i.e., the response). This output must be measurable and give valuable information about the system's performance. The peak irradiance and PIB at the target were determined as the performance measures of the HEL. Specifically, the UCAV-HEL mission was the degradation of a target, estimated to have been achieved by melting a volume of radius 5 cm and thickness 3 mm. In Chapter IV, we calculated the required irradiance and PIB to melt a volume of that size on the surface of an aluminum and stainless steel material. Using Figures 25 and 26 and assuming a 6-second laser dwell time, we see that the required irradiance and PIB are 11 MW/m^2 and 85 kW, respectively, for surfaces made of aluminum.

The next step is to determine the inputs for our simulation. Factors can be classified as either qualitative or quantitative. Quantitative factors are represented by numerical values whereas qualitative factors represent structural assumptions. We can also classify factors to be controllable or uncontrollable, based on whether a human can decide their value or not (Law 2015). During a simulation experiment, we usually focus on factors that are most critical for the system's performance. Each factor has to be constrained within an upper and lower limit, within which several more levels can be added. The overall goal of the experimental simulation is to determine which factors have the greatest effect on the response (Law 2015).

For the air-to-ground laser weapon scenario, there are several factors that can be controlled and used in the experiment. These factors are related to the HEL weapon and

to the operational tactics of the UCAV. Two factors related to HEL's design that are selected as the most critical for its overall performance are: a) output power and b) beam director diameter. Additionally, three factors the operator can control are incorporated in the simulation experiment: a) flight altitude, b) speed, and c) direction of the UCAV with respect to the wind. Atmospheric turbulence, as discussed in Chapter V, is strongly related to the altitude. Thus, by varying the latter we expect different performance for the HEL. Speed and direction relative to the wind are selected because—especially for higher output powers—they are related to the thermal blooming effect, which is another degradation phenomenon for HEL. These factors can also have an important impact on the survivability and the endurance of the UCAV.

Apart from the controllable parameters, other uncontrollable parameters that will strongly affect the accumulated irradiance and PIB of the target are simulated during the experiment. Atmospheric extinction coefficients, turbulence, thermal blooming, and wind are such parameters. For more details on those parameters, refer to Chapter IV.

Figure 42 summarizes the workflow followed in this study as well as the software tool used at each step.

Figure 41. DOE Workflow.

The maximum output power used (250 kW) in these simulations is well beyond what the current technology would allow to be mounted in a platform of the size of a UCAV; however, it was included to determine its potential usefulness. The beam director size range, between 0.2 m and 0.5 m, is a typical range of values used for HEL weapons.

The flight altitude level was selected from 300 m to 4000 m as a nominal altitude range for a UCAV-HEL. Flying at higher altitudes would further decrease the horizontal effective range of the weapon. The speed range, from 80 m/s to 130 m/s, again is a representative speed range for a UCAV such as the General Atomics MQ-9 Reaper. The direction levels, from northern to eastern courses, were selected to examine the wind effect on the HEL performance. The wind direction was set to be from the east. Table 9 summarizes the inputs used for the simulation as well as their corresponding levels.

Table 9.   Simulation Input Parameters with their Corresponding Levels.

Factor	Levels
Power (kW)	50–250
Beam Director Diameter (m)	0.2–0.5
Altitude (m)	300–4000
Speed (m/s)	80–130
Direction (degrees)	0–90

The simulation software utilized to simulate the laser beam propagation through the atmosphere was WaveTain, "a software tool for high fidelity modeling of advanced optical systems such as laser weapons systems," developed by MZA Associates Corporation (Coy 2013). Its stochastic nature allowed for effective statistical analysis; however, it is too slow to allow for multiple replications (a total of 520 runs were executed).

B.   OPERATIONAL CONCEPT

The development of potential CONOPS for the UCAV-based HEL weapon would facilitate the decision making for the system's design. The operational concept can be further decomposed into several scenarios or vignettes.

The developed engagement scenario in this study simulates a UCAV patrolling in a predetermined area and receiving a call for fire upon a ground stationary target with an approximate height of 10 m. The simulation examines the performance of the HEL weapon for different laser design configurations and UCAV tactics while keeping the slant range between the platform and the target constant at 5000 m.

76

C. MODEL ASSUMPTIONS

DOE methodology requires that three assumptions be fulfilled so that the model results are statistically valid. Therefore, before proceeding with the analysis of the simulation results, we have to make sure that all three assumptions are met. According to the statistics guide of the MINITAB software, these assumptions have to do with the residuals (the difference between observed and fitted value) and are the following (Minitab 2016):

1. The errors are normally distributed.

2. Each error is in constant variance with the independent variable (response).

3. Each error is independent of all others.

A good way to determine the fulfillment of these assumptions is graphically by using residual plots. A transformation of the response may then be necessary to fix any problems that arise.

D. SIMULATION RESULTS

The experimented range of the HEL weapon's output power value (50 kW–250 kW) was high enough to cause non-normality issues in the mathematical model we tried to fit to the simulation data. Thus, the simulation was divided into two parts. The first considered the output power from 50 kW–150 kW, and the second one considered output power from 150 kW–250 kW.

1. Peak Irradiance

Figures 42 and 43 show the normal probability and "versus fits" plots for the peak irradiance in the 50 kW–150 kW interval.
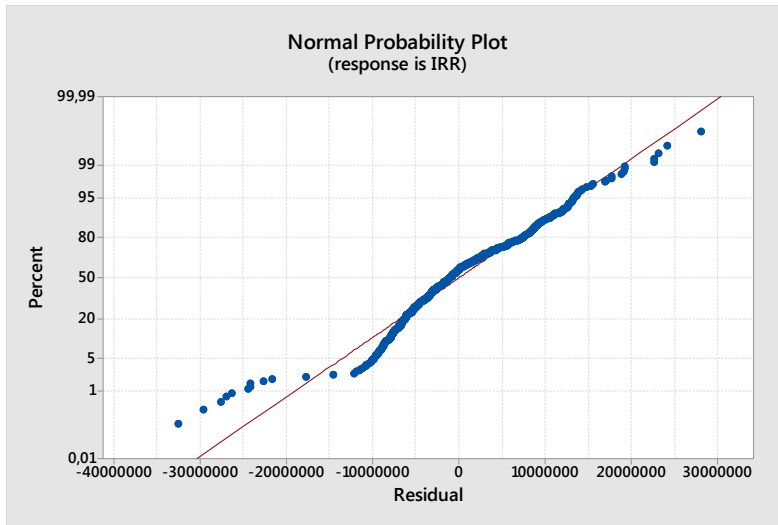
Figure 42. Normal Probability Plot.

The horizontal axis represents the value of the residuals whereas the vertical axis represents their corresponding percentile. The blue dots represent the design points. Normally distributed residuals would give a straight line (i.e., the residuals' distribution would align with the red line). This graph indicates that the first assumption of normality is violated. We see that the dotted line follows a non-linear pattern and it has long tails.
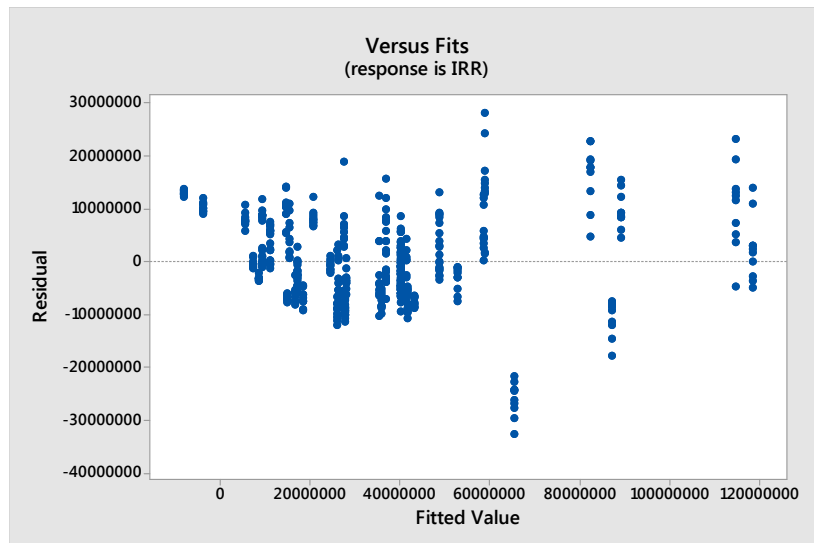

Figure 43. Versus Fits Plot.

The "versus fits" plot shows the difference that each observed value (obtained by the simulation) has from the value that the fitted mathematical model would give for the same set of factor values. The horizontal axis represents the value that the statistical model would give as a result for the corresponding parameter value combination. The vertical axis shows the difference that the actual simulation result has from the statistical model result. This graph shows that the error variance increases as we go at higher fitted values, indicating that the constant variance assumption is also violated.

Since we failed to fulfill both model assumptions, we cannot trust this model for further analysis. Instead, we use a response transformation to see if that results in a better fit. Several transformations were tested and the logarithmic one appears to be the best. As shown in Figure 44, the design points now follow an almost straight line, which makes us more confident that we achieved normally distributed residuals. Note that the horizontal axis scale has now changed, since we are using the natural log of the peak irradiance value.
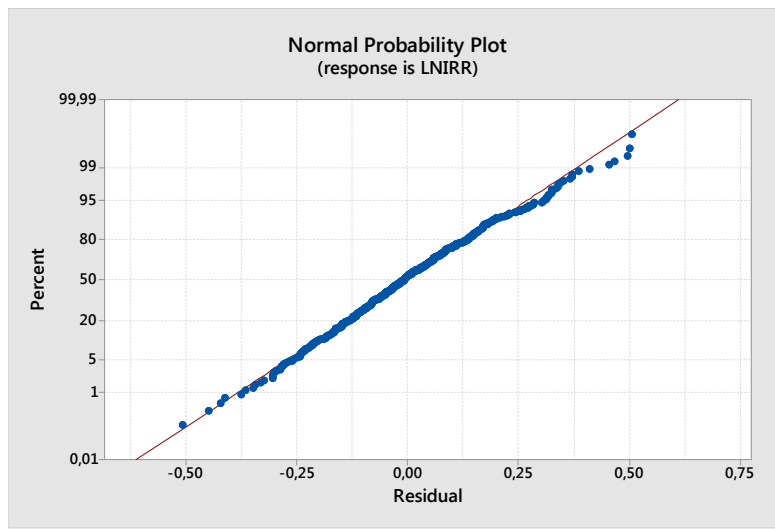

Figure 44. Normal Probability Plot.

The "versus fits" plot, shown in Figure 45, is also improved and shows that residuals are randomly distributed all along the response's value range. Again, both axes scales have changed to their natural log. Two indicators support the model's validity. The overall F-ratio of the mathematical model, which is found to be 529.1, means that the

model explains the response variability 529 times more than the error does. This indicates that our model seems to capture the important trends. Finally, the model yields an R^2=95.5 percent, which describes the amount of variation in the observed response values that is explained by the predictors.
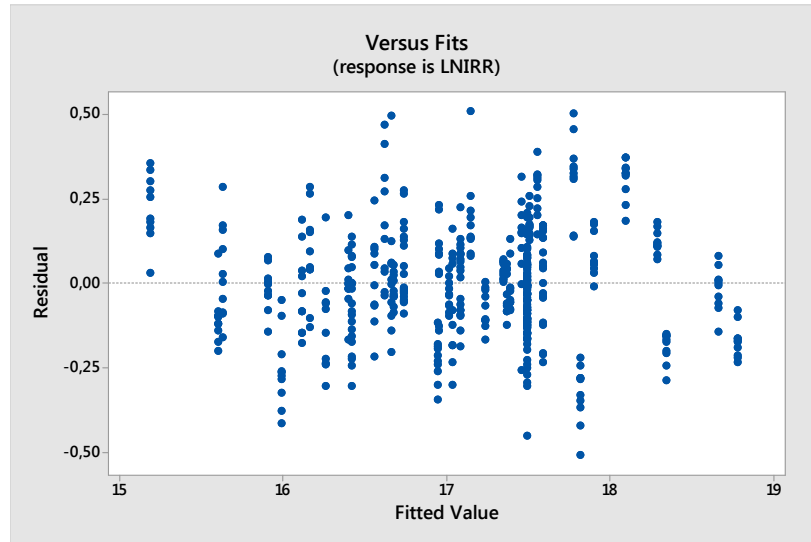

Figure 45. Versus Fits Plot.

The next plot we generate in Minitab contains the main effects of each factor, shown in Figure 46. We use this plot to examine the effect that each factor has on the mean transformed response and to compare their relative strength. The vertical axis indicates the natural logarithm of peak irradiance and the horizontal axis shows the levels used in the design. The blue line within each box shows how changing the value of each factor affects the mean peak irradiance: the steeper the line, the greater the effect. Therefore, we can see that the altitude's effect is the greatest; however, when reaching the 4000 m upper level, the line tends to become parallel to the horizontal axis, indicating that we will not gain much by operating at higher altitudes. The same phenomenon occurs with the output power values, where at the level of 150 kW, the slope is much less than at lower powers. The same is not the case for the beam director size, where we see that it keeps improving the response as it gets bigger. Note also that the main effect lines for speed and direction are almost parallel to the horizontal axis, indicating only a small

effect on the irradiance. We identify an optimum speed at around 110 m/s and an optimum direction at 0 degrees.
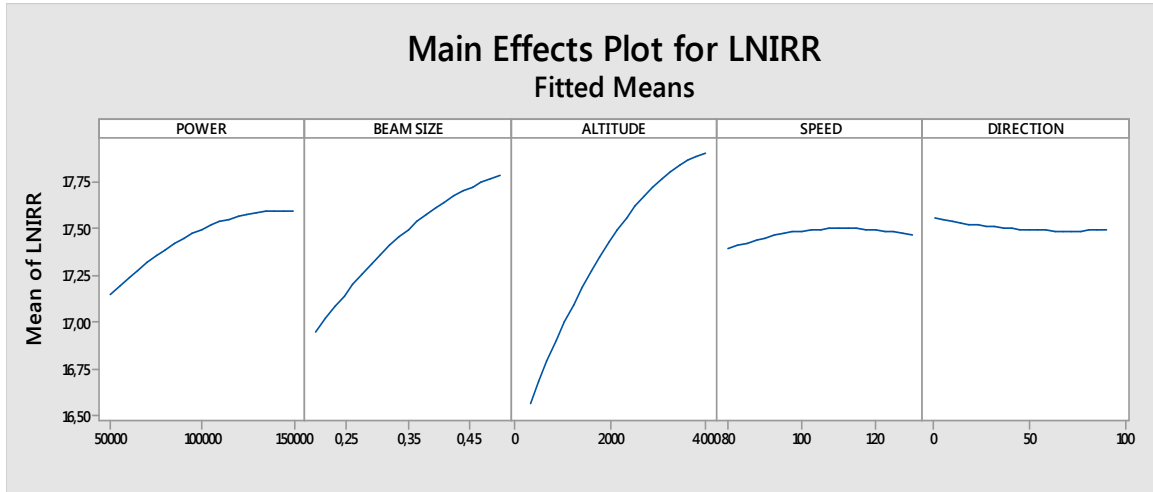

Figure 46. Main Effects Plot for Natural Logarithm of Irradiance.

Finally, to establish the relationship between the operating altitude and the output power, we generate a contour plot illustrating the performance of the HEL for different combinations of these two factors, as shown in Figure 47. These plots also give an idea of the trade space between UCAV tactics (altitude) and HEL design (power).
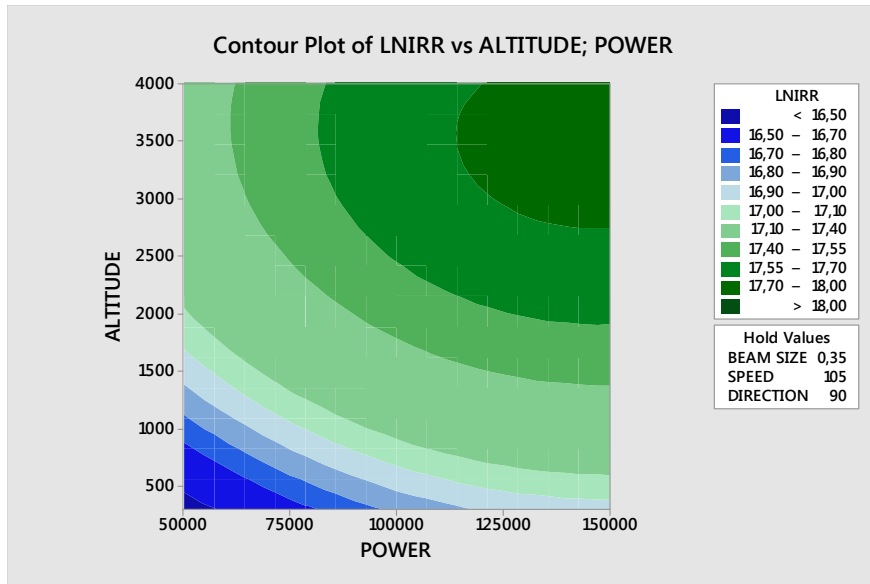
Figure 47. Contour Plot for Altitude versus Power (50 kW–150 kW).

Note that the graph is separated into ten distinct areas. Each area represents a different peak irradiance level whose range of values is indicated along the right side of Figure 48. These values are the natural logarithm of the peak irradiance, so we need to exponentiate them to convert them into watts per square meter. The values of the rest of factors are constant and are shown at the lower right side of Figure 47. In Figure 23, we estimated the required irradiance to melt a spot on the target's surface. Assuming a laser shot dwell time of no greater than 5 seconds, the required irradiance would be greater than 22 MW/m^2. This irradiance level corresponds to plotted values greater than ~16.9, which corresponds to the light blue contour. Thus, in this particular case, all combinations of power and altitude within or above the light blue contour will sufficiently damage the target within 5 seconds. Looking at the two extreme cases, we can see that a UCAV flying at 300 m with a HEL weapon of 150 kW would have the same performance as a UCAV flying at 1500 m with a HEL weapon of 50 kW. Taking into account the huge difference in terms of size, weight, and energy requirements that a lower power HEL will have, the benefit of operating at higher altitudes is apparent.

The same process is again followed for an output power range extending from 150kW to 250 kW. A natural logarithm transformation was again required to fit a more

accurate model to the simulation results. Looking at the main effects of each factor again in Figure 48, we now see that the output power has a lesser effect, probably due to the thermal blooming, indicated by the slope of the blue line above 220 kW becoming negative. On the other hand, the effect of beam size is significant; this likely indicates that laser beam director sizes lend to less thermal blooming, which is a known trend.
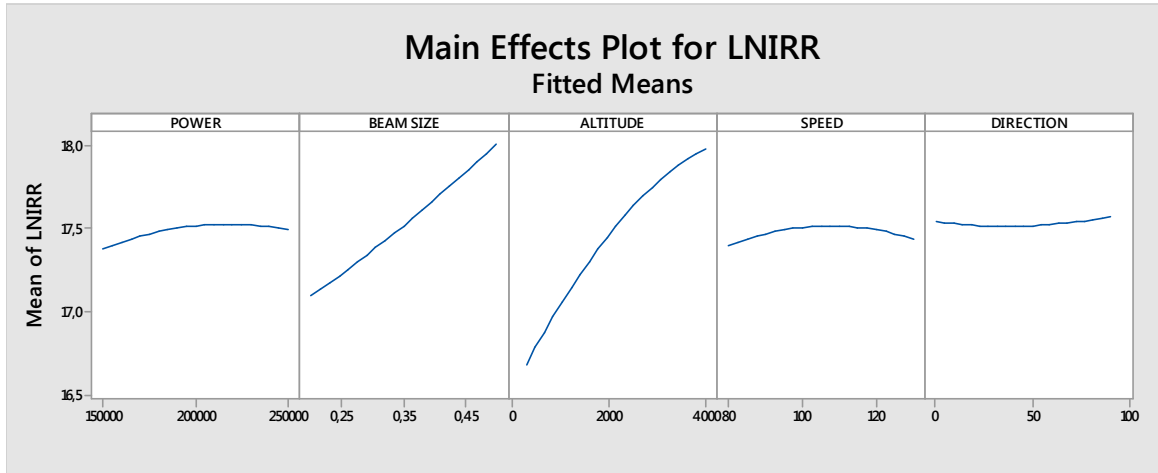

Figure 48. Main Effects Plot (Power 150 kW–250 kW).

Figure 49 is equivalent to Figure 47 and shows the relationship between operating altitude and power. As we see now the contour lines have a much smaller negative slope in the region from 150 kW to around 220 kW, and after that point, the contour starts heading upward. This pattern indicates the effect of thermal blooming on higher power laser weapons, limiting their performance with respect to peak irradiance. However, we have to stress the fact that these results do not account for the beam quality of the HEL weapon and the platform jitter. These two design parameters could not be incorporated in WaveTrain, and would definitely cause further laser beam degradation. Including non-ideal beam quality and platform jitter would likely mitigate the effect of thermal blooming (at the expense of reduced overall irradiance). Then, increasing the output power above the level mentioned before would likely offer some advantage.
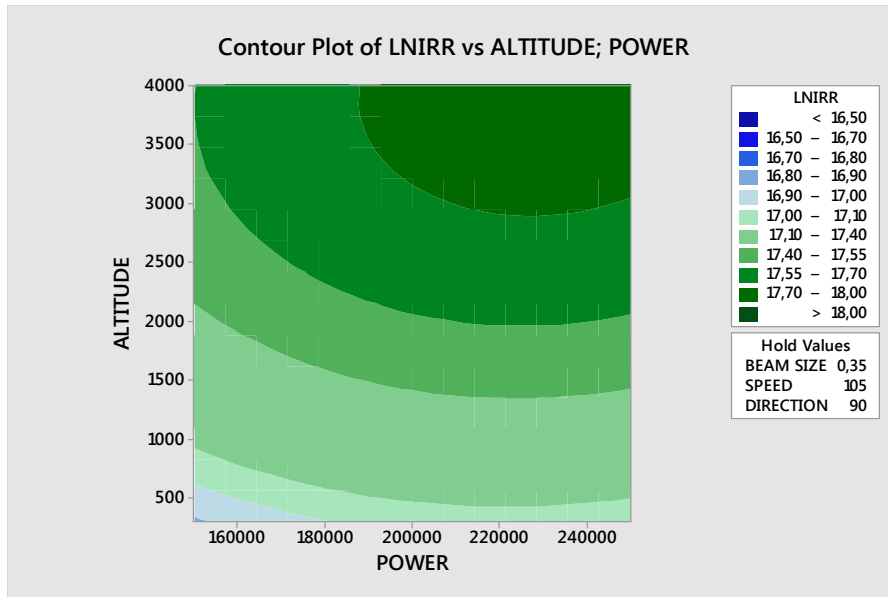
Figure 49. Contour Plot for Altitude versus Power (150 kW–250 kW).

To further validate the statistical model in terms of physics, we use WaveTrain to plot the natural logarithm of peak irradiance along the entire range of output power, as shown in Figure 50. This plot represents the "real" picture of the response. Apparently, it is not as "smooth" as the plot generated by Minitab; this is because the peak irradiance on the target is very sensitive to all the atmospheric effects that cause much variance in performance. However, the main pattern of the contour lines, which is of most interest for this study, seems to follow the same trends as the ones from Minitab. Starting from a 50 kW power, it has a negative slope that, by the level of around 150 kW, is stabilized, and in some cases it starts rising again, beyond the ~200 kW level (Figure 51).
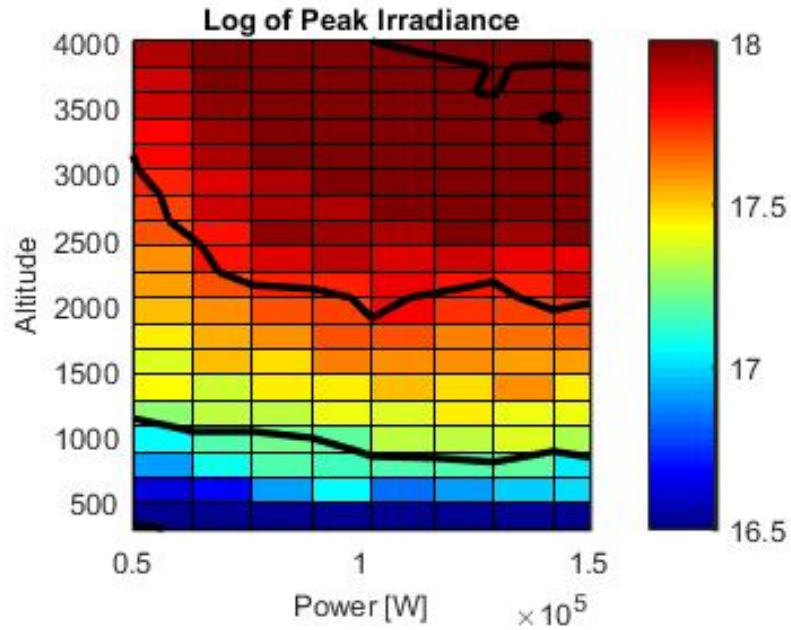
Figure 50. Contour Plot for Altitude versus Power, Generated by WaveTrain (50 kW–150 kW).
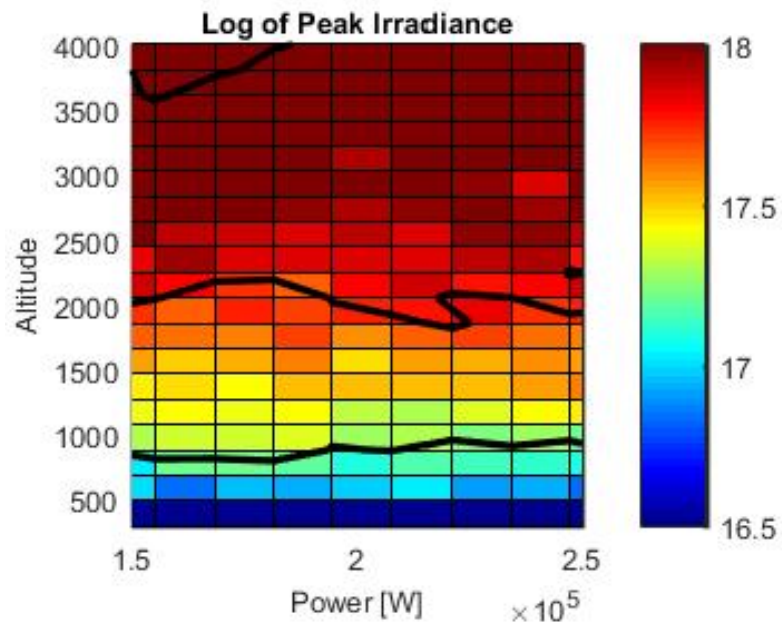

Figure 51. Contour Plot for Altitude versus Power, Generated by WaveTrain (150 kW–250 kW).

2.   Power-in-Bucket

PIB represents the actual power delivered in a pre-defined area (the "bucket") on the target within a certain radius; it is another metric of the HEL weapon's performance and more representative of the HEL weapon's lethality if the target susceptibility is known.

The statistical model we tried to fit to the PIB simulation data does not seem to be as good as the one for peak irradiance. Several response transformation methods were tested (squared, log, square root) without resulting in a very good fit, as indicated in Figures 52 and 53. However, the high F-ratio for the overall model (836) along with an R^2 value of 97 percent, allows for some practical use of the model despite the significant lack of fit.
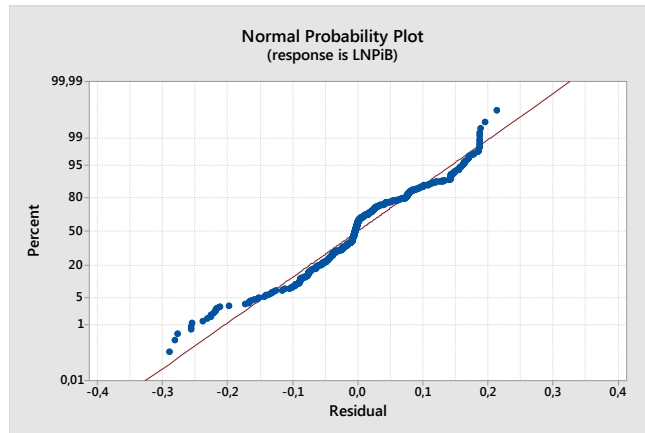

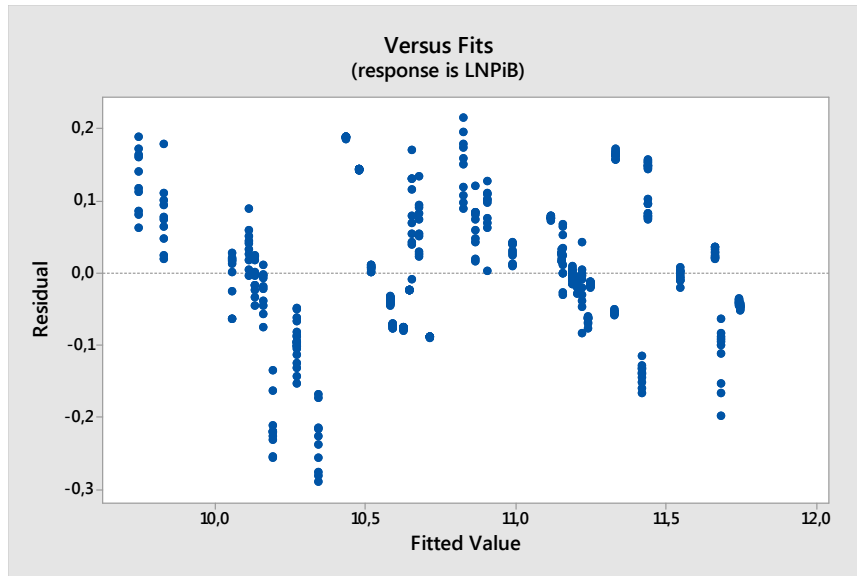Figure 52. Normal Probability Plot for PIB (Power 50 kW–150 kW).

Figure 53. Versus Fits Plot for PIB (Power 50 kW –150 kW).

However, when we compare the model contour plots generated by Minitab and WaveTrain, we see that the trends match up well. Figure 54 shows the contour plot (Minitab) for power ranging from 50 kW–150 kW. We can see a quite steep pattern on the contour lines, showing that the higher altitude advantage is not as significant as it was on the peak irradiance. Figure 55 shows a similar plot for power levels between 150 kW– 250 kW. Here we can see that for altitudes lower than 1500 m, the contour lines have a relatively parallel pattern to the horizontal axis, showing only a small increase from the power increase. On the other hand, by increasing the operating altitude of the HEL for a certain output power, the PIB is improved.
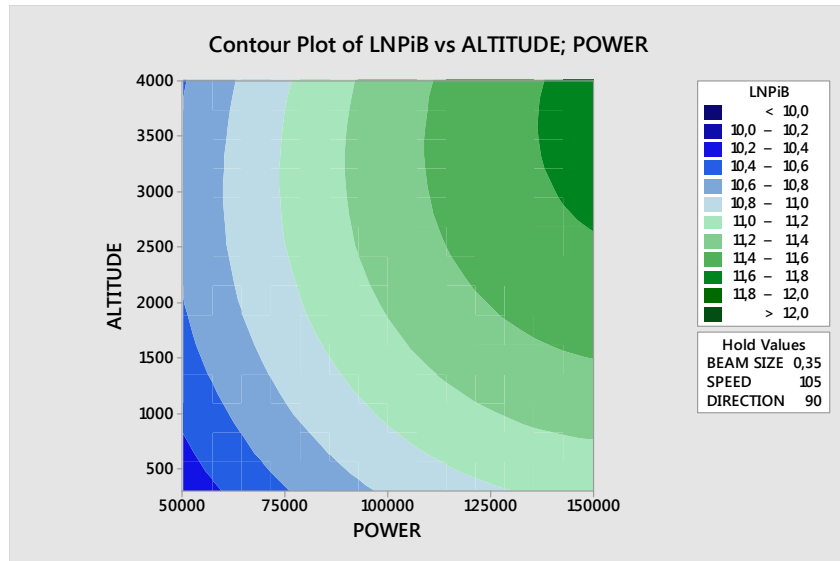
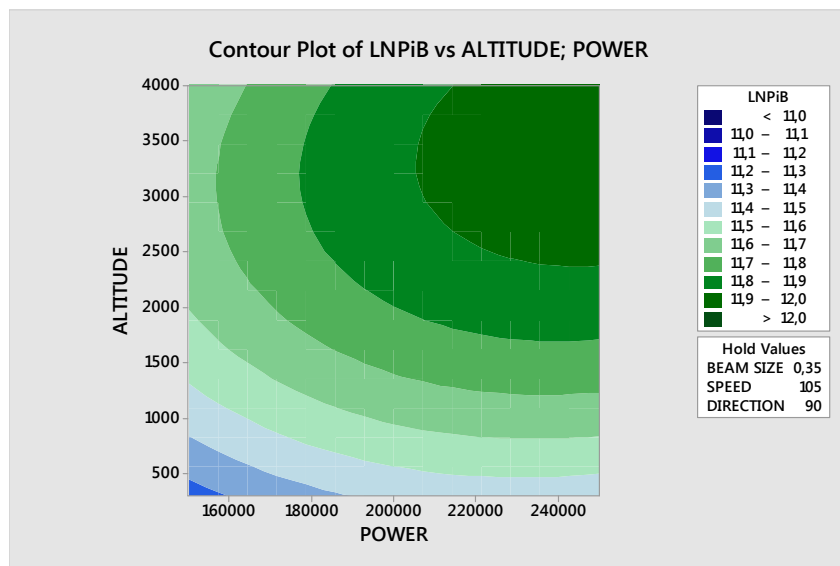Figure 54. Contour Plot for Altitude versus Power (50 kW–150 kW).

Figure 55. Contour Plot for Altitude versus Power (150 kW–250 kW).

Corresponding plots, generated by WaveTrain, are shown in Figure 56 and 57. These clearly show a similar "picture" for the relation between altitude and power against PIB. For power levels up to 150 kW, the power increase has a significant effect on PIB equal to that at low altitudes, as indicated by the almost vertical contour lines. Beyond the 150 kW power level, the contour lines become more parallel to the horizontal axis,

showing that the power increase (for the same altitude) does not offer as much increase in performance, mainly because thermal blooming effects start becoming problematic.
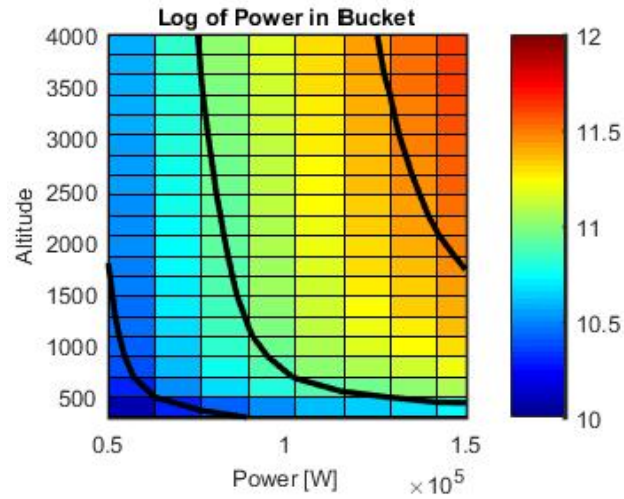

Figure 56. Contour Plot for Altitude versus Power, Generated by WaveTrain (50 kW–150 kW).
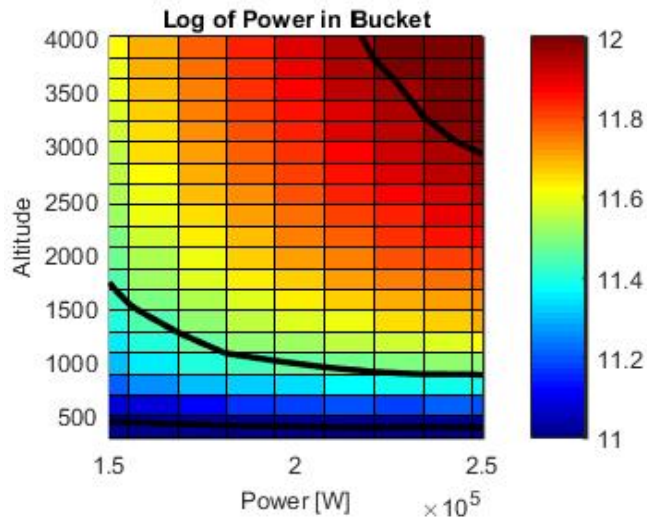

Figure 57. Contour Plot for Altitude versus Power, Generated by WaveTrain (150kW–250 kW).

E. DESIGN ANALYSIS

As we have already mentioned, the size, weight, and power requirements of a UCAV-based HEL weapon is of very high interest. Therefore, the following part of this study is devoted to making estimates about the SWaP requirements. In the first part of our analysis, we demonstrated the significant effect that the operating altitude has on the performance of the HEL. Looking at Figures 54 and 55, we can see that in the first case (50kW–150kW) there is not much to gain by flying at higher altitudes. On the other hand, in the second case, we can see that the 150 kW and 250 kW HEL under certain conditions could have the same performance. This fact leads us to further explore and compare those two designs. The comparison of those two alternatives has two parts. The first one estimates the weight and power requirements of each design, and the second one shows how a non-ideal beam quality and platform jitter will affect them.

By making some assumptions utilizing existing commercial technology as references, and based upon discussions with a subject matter expert, we estimate the weight and power requirements for several different laser configurations.

1. HEL 150 kW

The first case assumes an HEL weapon with 150 kW output power and an electrical-to-optical efficiency of 30 percent.

a. Energy Storage Requirements

The total electrical power required to fire the HEL is:

$$P_{total} = \frac{150kW}{0.3} = 500kW$$

(35)

Supposing the UCAV-HEL system has an operational requirement of a total of 60 seconds of lasing time, the total required stored energy to utilize the HEL is:

$$Energy_{stored} = 500kW * 60s = 30MJ$$

(36)

90

One likely option to store this energy is with lithium-ion batteries. With a specific energy density of 0.36 MJ/kg and by adding an additional 30 percent on to the required stored energy to account for battery losses (Motes and Berdine 2009), we end up with a total battery weight:

$$W_P = \frac{1.3 * 30 MJ}{0.36 \frac{MJ}{kg}} = 108 kg$$

(37)

b.   Weight Requirements

To estimate the total weight of the HEL weapon system, we have to add separately the weight of the beam delivery subsystem (W_{BD}), the weight of the laser module (W_L), the weight of the power supply subsystem (W_{ES}), and the weight of the cooling subsystem (W_T) (Motes and Berdine 2009):

$$W = W_{BD} + W_L + W_{ES} + W_T$$

(38)

The energy storage weight W_{ES} was estimated in the previous paragraph to be around W_{ES}=**108 kg**. General Atomics Inc., which is developing the HELLADS laser system, claims that its weight-to-power ratio of the laser module will be 5 kg/kW. That means that for every 1 kW of power, 5 kg will be added, giving a total of W_L=**750 kg** for the 150 kW HEL weapon. The thermal management subsystem weight estimation is based upon thermal energy storage (TES) technology, developed by RINI technologies. As stated in the products information sheet, the advantage of this cooling system technology is that it "rapidly stores heat during weapon use and then slowly rejects it during inactive periods which typically last 5 to 30 minutes" resulting in "dramatic SWaP reductions, enabling the deployment of these power hungry weapons systems on compact tactical platforms" (RINI Technologies 2016). The energy storage of TES is 2 MJ and the maximum power load 25 kW, with a corresponding weight of 24 kg. The waste heat for the 150 kW HEL with 30 percent electrical-optical efficiency is

$$Heat_{waste} = Power_{total} - Power_{output} = 500kW - 150kW = 350kW$$

(39)

Assuming lasing shots with a 10-second dwell time, the thermal energy storage we need is 3.5 MJ. However, since the maximum power load is only 25 kW, to handle a waste heat power of 350 kW we estimate the TES weight to be approximately W_T =590 kg. Finally, we estimate the weight of the beam delivery subsystem based upon the Othela Beam Director system developed by MZA, which provides a very lightweight and compact telescope with a diameter of 30 cm. Its corresponding weight is approximately W_{BD}=225 kg. Summing up the weights of all subsystems, we estimate the total weight of the HEL weapon to be W=1670 kg. While this is a rough estimate, it is well within the capabilities of UCAVs.

c.   *Platform Jitter and Beam Quality Effects*

The WaveTrain runs (and therefore Minitab results) did not include the effects of the beam quality and platform jitter. To have a better idea of the negative effects that these will have on HEL performance, we run a new simulation utilizing ANCHOR. Starting with a perfect laser beam quality (M2=1) and zero platform jitter (as we did previously), we now add a nominal platform jitter (6 μrads), followed by a gradually worse beam quality (M2=3 and M2=7). Table 10 summarizes the input parameters to ANCHOR.

Table 10.   Input Parameters Used in ANCHOR

Wavelength λ	1.064 μm
Target Height H_T	10 m
Beam Size D	0.35 m
Beam Shape	Uniform
Platform Direction	North
Wind Direction	90°
Target Speed V_{target}	0 m/s
Platform Speed V_{UCAV}	105 m/s
Bucket Size r_b	0.05 m
Fractional Target Absorption	0.2

(1)   Operating Altitude 300 m

The first set of runs simulates a UCAV with a 150 kW HEL flying at an altitude of 300 m. The plots produced by ANCHOR show the peak irradiance and PIB for various target ranges and altitudes. Figures 58 and 59 show how increased jitter and M^2 lead to a lower effective range of the HEL, especially at higher target altitudes where turbulence is less severe. The contour line in each plot indicates the estimated threshold of the peak irradiance and PIB, as discussed before, for a 5 cm radius, 3 mm thick aluminum target, and an assumed dwell time of 6 seconds.
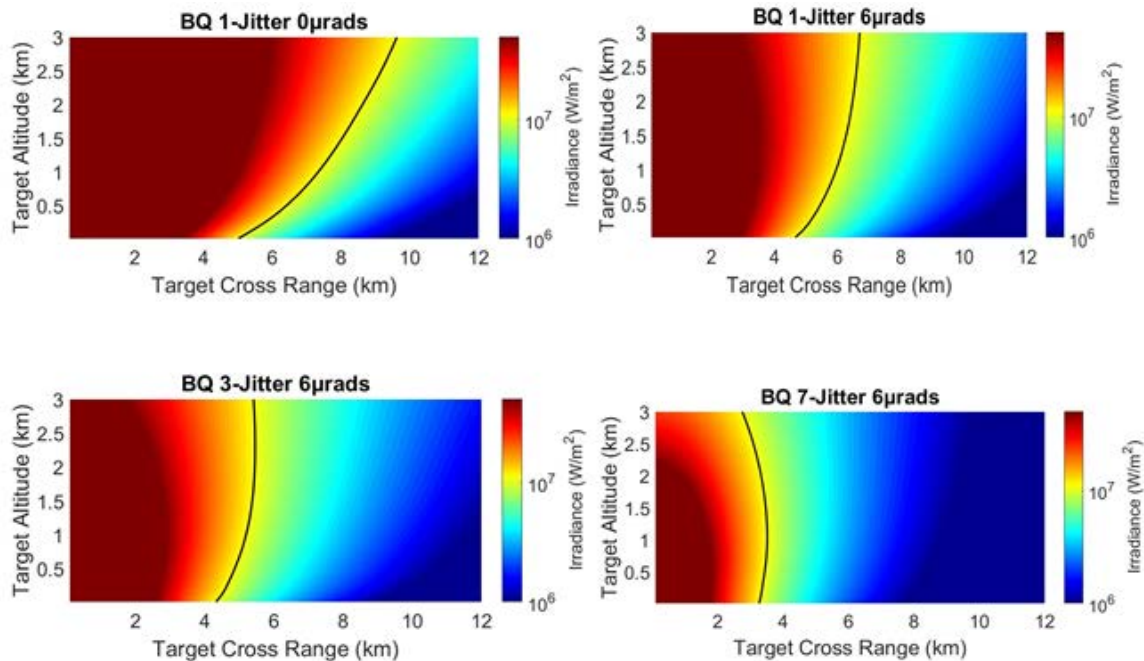

Figure 58. Peak Irradiance for a 150 kW HEL Operating from an Altitude of 300 m.
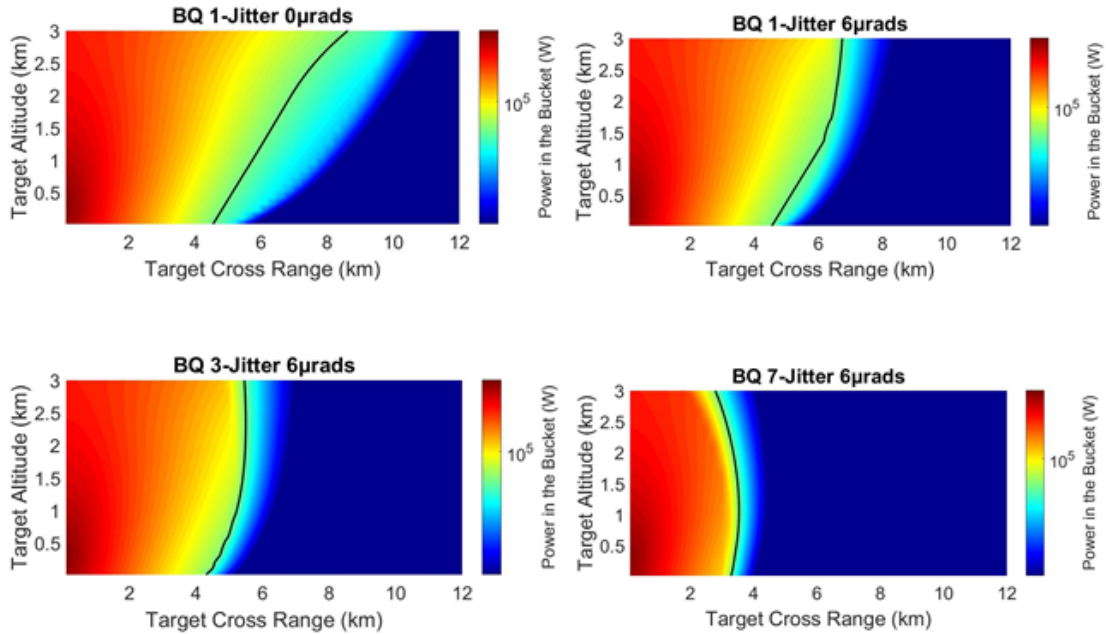
Figure 59. Power-in-the-Bucket (5 cm radius) for a 150 kW HEL Operating from an Altitude of 300 m.

(2)   Operating Altitude 3000 m

The second set of runs simulates the same HEL operating at an altitude of 3000 m. The advantage of the higher operating altitude is once more obvious in both performance measures. Comparing the plots from Figures 58 and 59 to those in Figures 60 and 61, we note the differences between the slant effective and the horizontal effective ranges. Going from an altitude of 300 m to an altitude of 3000 m may result in a lower horizontal range, but we are still more interested in the slant range for ground targets. Therefore, it is very important to notice that higher M^2 and jitter requires the UCAV to be closer to the target (and thus in lower altitude).
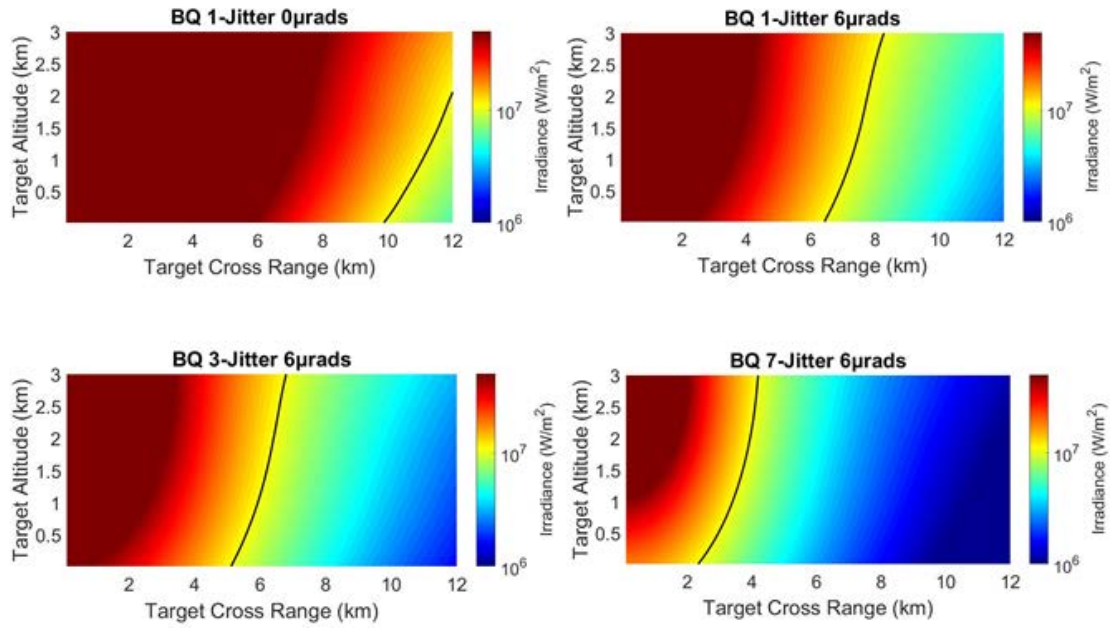
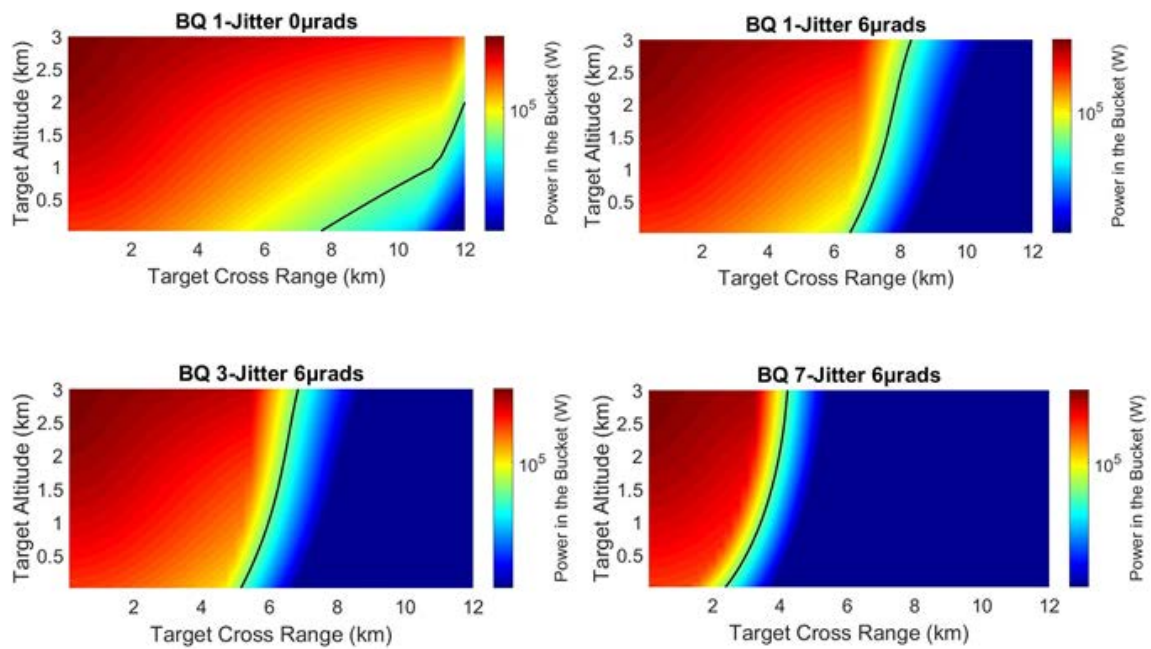Figure 60. Peak Irradiance for a 150 kW HEL Operating from an Altitude of 3000 m.

Figure 61. Power-in-the-Bucket (5 cm radius) for a 150 kW HEL Operating from an Altitude of 3000 m.

2. HEL 250 kW

The second case assumes a HEL weapon of 250 kW output power with an electrical to optical efficiency of 30 percent.

a. *Energy Storage Requirements*

The total power required to fire the HEL is:

$$Power_{total} = \frac{250kW}{0.3} = 833.3kW \tag{40}$$

Using the same operational requirement of a total of 60 seconds of lasing time, we determine the total required stored energy to utilize the HEL is:

$$Energy_{stored} = 833.3kW * 60s = 50MJ \tag{41}$$

The lithium-ion battery design configuration with a specific energy density of 0.36 MJ/kg and an additional 30 percent of required stored energy to account for battery losses (Motes and Berdine 2009) will give a total battery weight of:

$$W_P = \frac{1.3*50MJ}{0.36\dfrac{MJ}{kg}} = 180kg \tag{42}$$

b. *Weight Requirements*

W_P was estimated in the previous paragraph to be around W_P=**180 kg,** including solely the weight of the batteries. The laser module weight with the same weight-to-power ratio gives a total of W_L=**1250 kg**. The waste heat for the 250 kW HEL with 30 percent electrical-optical efficiency is:

$$Heat_{waste} = Power_{total} - Power_{output} = 833.3kW - 250kW = 583.3kW \tag{43}$$

Assuming again lasing shots with a 10-second dwell time, we need thermal energy storage of 5.8 MJ. Thus, the estimated weight of the TES will be W_T =980 kg. Finally, the weight estimation of the beam delivery subsystem does not change, so W_{BD}=225 kg. Summing up the weights of all subsystems, we estimate the total weight of the HEL weapon to be W=2635 kg.

c. Platform Jitter and Beam Quality Effects

(1) Operating Altitude 300 m

Figure 62. Peak Irradiance for a 250 kW HEL operating from an Altitude of 300 m.

Figure 63. Power-in-the-Bucket (5 cm radius) for a 250 kW HEL Operating from an Altitude of 300 m.
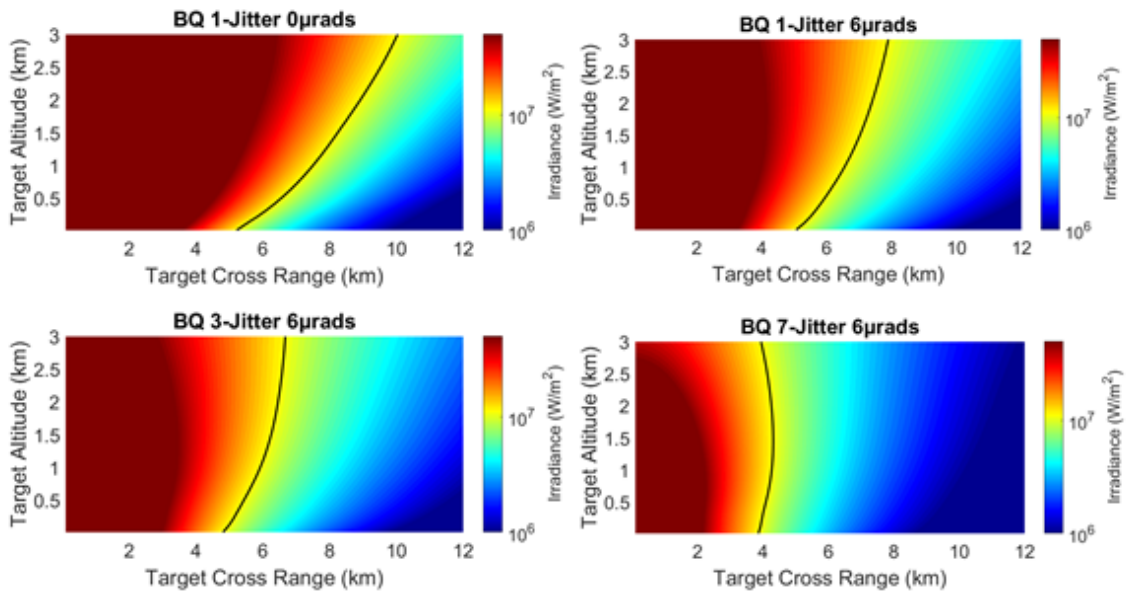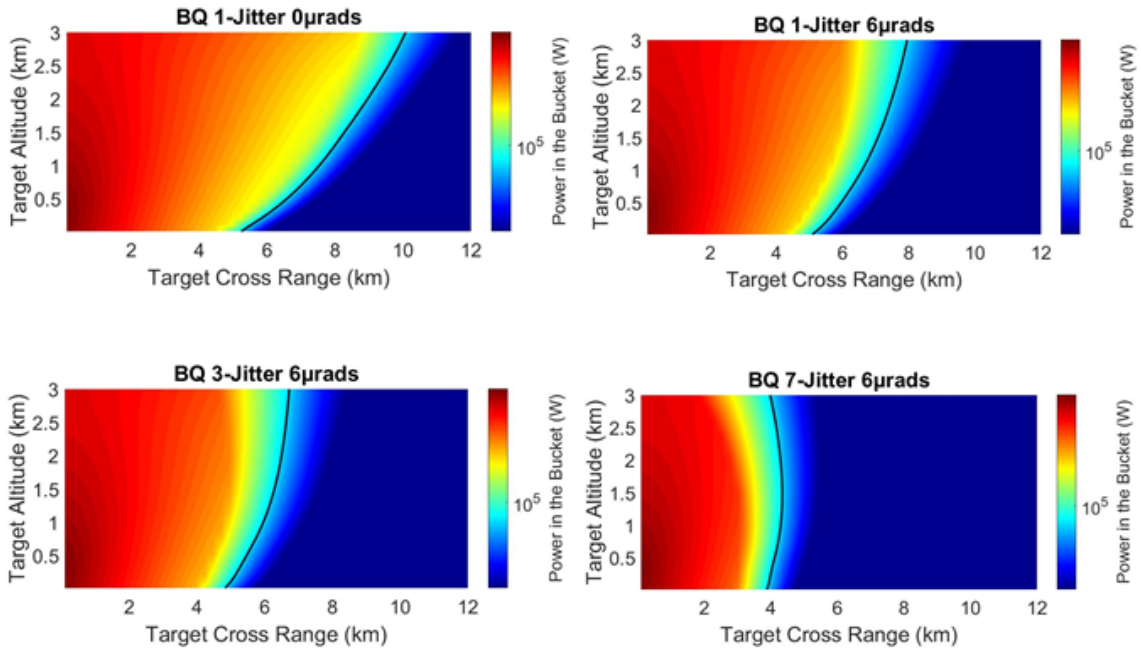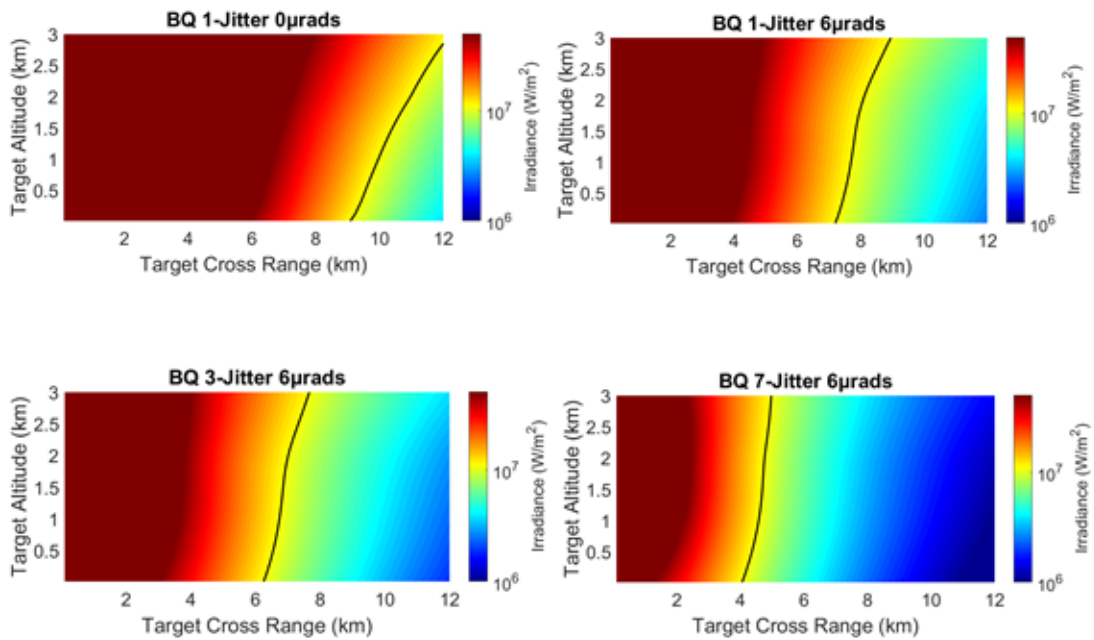
(2)   Operating Altitude 3000 m

Figure 64. Peak Irradiance for a 250 kW HEL Operating from an Altitude of 3000 m.
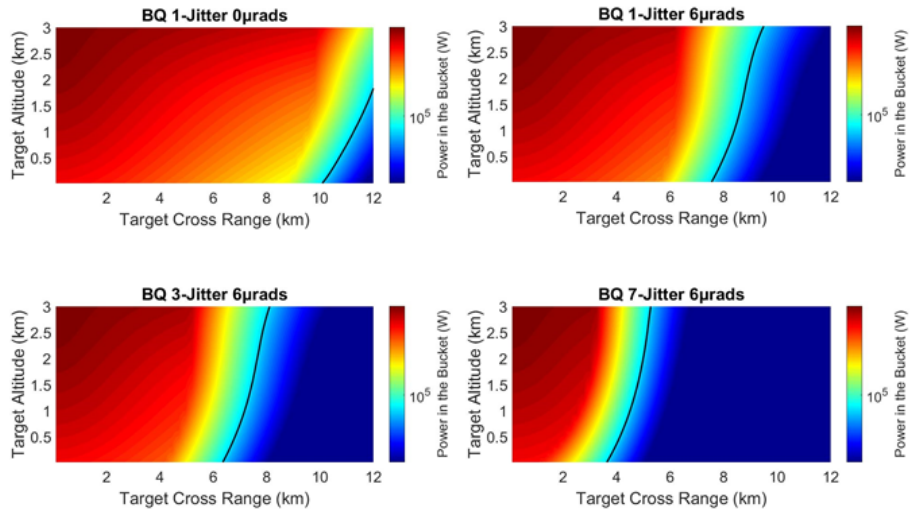
Figure 65. Power-in-the-Bucket (5 cm radius) for a 250 kW HEL Operating from an Altitude of 3000 m.

Table 11 summarizes the power and weight estimates for both alternatives.

Table 11.   Weight Estimation Comparison between a 150 kW and a 250 kW HEL.

	150 kW	250 kW
Electrical-optical efficiency	30%	30%
Total Power (kW)	500	833
Total Lasing Time (s)	60	60
Energy Storage (MJ)	30	50
Battery Energy Storage (including 30% losses) (MJ)	39	65
Lithium-ion Specific Energy Density (MJ/kg)	0.36	0.36
Power Supply Subsystem Weight (kg)	108	180
Laser Module Weight (kg)	750	1250
Beam Control Subsystem Weight (kg)	225	225
Waste Heat Power (kW)	350	583
Thermal Energy Storage (MJ)	3.5	5.83
TES Weight (kg)	590	980
Total HEL Weight (kg)	**1670**	**2635**

3. Endurance versus HEL Power

The last step of our analysis is the linkage between the total endurance of the UCAV and the power of the HEL weapon. In the previous paragraphs, we estimated the corresponding weights of two alternative HEL weapon configurations. The difference in the HEL weight will affect the total take-off weight of the UCAV; consequently, we expect its endurance to be affected, too. To be able to link the HEL power with the UCAV endurance, we first developed a simple linear mathematical relation between the payload weight of the UCAV (assuming only HEL weight) and its total endurance. This mathematical relation was developed after written communication with a subject matter expert on UAVs (the CEO of Vstar Systems Inc.), who kindly provided some estimates on how the endurance of a UAV is affected by changing its payload weight. The estimation was based upon the UAV Predator B and is tabulated in Table 12.

Table 12.   Payload versus Endurance Estimates.

Payload Weight (kg)	Total Endurance (hours)
250	30
1250	27

Utilizing these data points, we derived the following simple formula to establish the relationship between payload weight and total endurance:

$$Endurance = 30.75hr - 0.003\frac{hr}{kg}*(Weight)$$

(44)

Assuming a linear relationship between HEL power and weight, we can estimate the corresponding weight for different HEL power levels. Figure 66 shows the endurance of the UCAV for five different HEL power levels using this formula. We can see that the low power alternative (150 kW) slows for an endurance of 25.5 hours, whereas the higher power alternative (250 kW) has an endurance of approximately 23 hours.
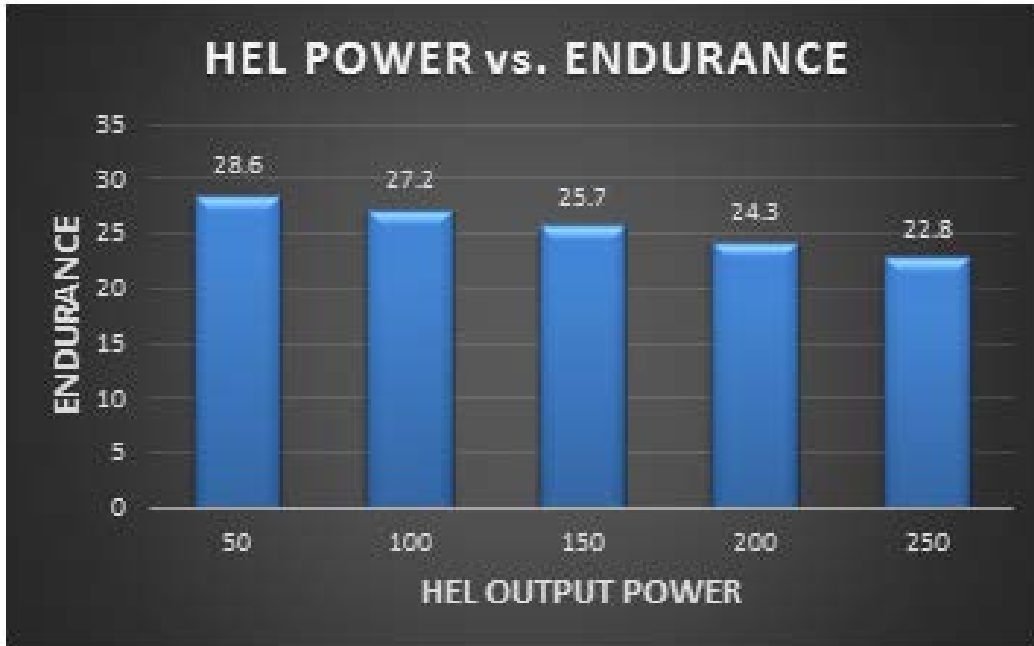
Figure 66. HEL Power versus UCAV Endurance.

THIS PAGE INTENTIONALLY LEFT BLANK

VIII. CONCLUSIONS

A. CONCLUSIONS FOR EXPERIMENTAL DESIGN RESULTS

By using the experimental design methodology, we managed to manipulate and explore an entire set of parameters at the same time in a computer experiment. It would have been impossible to obtain this amount of information using the one-factor-at-a-time approach.

The most significant result from the experimental design of the UAV-HEL system showed that the operational tactics followed by the UAV controller can affect the lethality of the HEL. Specifically, a HEL of lower power (150 kW) mounted on a UCAV flying at altitudes more than 3000 m, under certain conditions, could have the same performance as a higher power HEL (250 kW) on a UCAV flying at altitudes lower than 500m.

Additionally, we saw that increasing the power level of the HEL above 200 kW will not offer much to the end result, because of the thermal blooming effect. The beam director size, ideally, would reap the greatest benefits. Altitude plays the most significant role in the HEL's lethality, especially up to the 4000 m height level. Speed and direction of the UCAV, despite affecting the HEL's lethality, do not seem to be crucial.

B. CONCLUSIONS FOR WEIGHT AND POWER REQUIREMENTS

The weight and power requirements for a 150 kW and a 250 kW HEL showed that both alternatives could be mounted on a UCAV having a similar size and capabilities as a Predator B. With an estimated total weight of 1125 kg, the first alternative offers a much lighter option with consequent benefits to the endurance, range, and speed of the platform. On the other hand, the second alternative, with an estimated total weight of 1725 kg and despite being at the upper limits of the UCAVs' payload capacity, will mitigate the negative effects of a worse than ideal beam quality and platform jitter.

C.   CONCLUSIONS FOR UCAV ENDURANCE

To be able to link the HEL power with the UCAV's endurance, we first developed a simple linear mathematical relation between the payload weight of the UCAV (assuming only HEL weight) and its total endurance. We then saw that the low power alternative (150 kW) slows for an endurance of 27.5 hours, whereas the higher power alternative (250 kW) has an endurance of approximately 25.5 hours.

D.   CONCLUSIONS FOR BEAM QUALITY AND JITTER EFFECTS

The ideal situation in which beam quality is one and platform jitter is zero is not a realistic situation. Consequently, the second simulation set provides a more accurate idea of the HEL lethal range. The results showed that a 150 kW HEL's effective range, measured by the PIB threshold achievement, on a UCAV flying at 300 m could decrease from 4.5 km (M^2=1, Jitter=0 µrads) to 3 km (M^2=7, Jitter=6 µrads). By contrast, for the 250 kW HEL, the effective range would decrease from 5 km (M^2=1, Jitter=0 µrads) to 4 km (M^2=7, Jitter=6 µrads). For a UCAV flying at 3000 m, a 150 kW HEL effective range would decrease from 7.5 km (M^2=1, Jitter=0) to 2.5 km (M^2=7, Jitter=6 µrads), in contrast to a 250KW HEL, whose effective range would decrease from 10 km (M^2=1, Jitter=0) to 3.5 km (M^2=7, Jitter=6 µrads). The results show that a higher power HEL can compensate better for the degrading effects of beam quality and platform jitter, and can perform better.

LIST OF REFERENCES

Abarzhi, S. I., S. Gauthier, and K. R. Sreenivasan. 1982. "Turbulent Mixing and Beyond: Non-equilibrium Processes from Atomistic to Astrophysical Scales, Volume I." *Philosophical Transactions of the Royal Society of A.* 371(1982).

Alkire, Brien, Kallimani, James G., Wilson, Peter A., and Moore Louis R. 2010, *Applications for Navy Unmanned Aircraft Systems*. Santa Monica, CA: RAND.

Austin, Reg. 2010. *Unmanned Aircraft Systems. UAVs Design, Development and Deployment.* West Sussex, UK: Wiley.

Barnhart, Richard K. et al. 2012. *Introduction to Unmanned Aircraft Systems.* Boca Raton, FL: CRC Press.

Bartley, Michael. 2002. "Unmanned Combat Aerial Vehicles: A Close Air Support Alternative," Studies Paper, Air War College.

Blanchard, Benjamin S., and Wolter J. Fabrycky. 2011. *Systems Engineering and Analysis*. 5th ed. Upper Saddle River, NJ: Prentice Hall.

Blau, Joe. 2015. PH4858 Electric Ship Weapon Systems. Lecture, Naval Postgraduate School, Monterey.

Bone, Elizabeth, and Christopher Bolkcom. 2003. *Unmanned Aerial Vehicles: Background and Issues for Congress.* CRS Report No. RL31872. Washington, DC: Congressional Research Service. http://www.fas.org/irp/crs/RL31872.pdf.

Buede, Dennis M. 2009. *The Engineering Design of Systems: Models and Methods*. 2nd ed. Hoboken, NJ: Wiley.

Coy, S. 2013. WaveTrain: A User-friendly Wave Optics Propagation Code. Available: https://www.mza.com/publications/wtspiepaper.htm.

Defense One. "Drones Armed with High Energy Lasers May Arrive in 2017." September 2015. http://www.defenseone.com/technology/2015/09/drones-armed-high-energy-lasers-may-arrive-2017/121583/.

DSB Task Force on Directed Energy Weapons. 2007. Directed Energy Weapon Systems and Technology Applications. Final Report. Office of the Under Secretary of Defense for Acquisition, Technology and Logistics. Washington, DC. http://www.acq.osd.mil/dsb/reports/ADA476320.pdf

Department of Defense. 2016. "Unmanned Systems Integrated Roadmap FY2013–2038." Accessed February 16. www.defense.gov/Portals/1/Documents/pubs/DOD-USRM-2013.pdf.

Department of the Navy. 2007. "Joint and Naval Capability Terminology Lists." White paper. Washington, DC: Department of the Navy.

Fussman, Chris R. 2013. "High Energy Laser Propagation in Various Atmospheric Conditions Utilizing Accelerated Scaling Code." Master's thesis, Naval Postgraduate School.

Geer, Harlan, and Bolkcom Christopher. 2005. *Unmanned Aerial Vehicles: Background and Issues for Congress*. CRS Report No. RL31872. Washington, DC: Congressional Research Service. http://www.offiziere.ch/wp-content/uploads/RL31872_20051121.pdf.

General Atomics Aeronautical. 2016. "HELLADS." http://www.ga-asi.com/hellads.

Gertler, Jeremiah. 2012. *U.S. Unmanned Aerial Systems*. CRS Report No. RL42136. Washington, DC: Congressional Research Service. https://www.fas.org/sgp/crs/natsec/R42136.pdf.

INCOSE. 2015. *INCOSE Systems Engineering Handbook: A Guide for System Life Cycle Processes and Activities*. Hoboken, NJ: Wiley.

Koechner, W., and M. Bass. 2003. *Solid-State Laser: A Graduate Text*. New York: Springer-Verlag.

Kossiakoff, William, and N. Sweet. 2003. *Systems Engineering Principles and Practice*. 2nd ed. Hoboken, NJ: Wiley.

Law, Averill M. 2015. *Simulation Modeling and Analysis*. 5th ed. New York: McGraw-Hill Education.

Melin, Megan M. 2011. "Modeling and Analysis of High Energy Laser Weapon System Performance in Varying Atmospheric Conditions." Master's thesis, Air Force Institute of Technology.

Motes, Andrew R., and Richard W. Berdine. 2009. *Introduction to High-Power Fiber Lasers*. 1st ed. Albuquerque, NM: Directed Energy Professional Society.

O'Rourke, Ronald. 2015. *Navy Shipboard Lasers for Surface, Air, and Missile Defense: Background and Issues for Congress*. CRS Report No RL41526. Washington, DC: Congressional Research Service. https://fas.org/sgp/crs/weapons/R41526.pdf

Ozone Hole. 2016. "Atmosphere." Accessed February 16, 2016. http://www.theozonehole.com/atmosphere.htm.

Perram, G. P., S. J. Cusumano, R. L. Hengehold, and S. T. Fiorino. 2009. *Introduction to Laser Weapon Systems*, 1st ed. Albuquerque, NM: Directed Energy Professional Society.

Reierson, Joseph L. 2011. "Analysis of Atmospheric Turbulence Effects on Laser Beam Propagation Using Multi-wavelength Laser Beacons." Master's thesis, University of Dayton.

Rini Technologies. 2016. "Thermal Energy Storage (TES) Technology." http://rinitech.com/wp-content/uploads/2016/01/ThermEnergyStorage.pdf

Risen, Tom. 2015. "Weapons of the Future, Available Soon." *U.S. News and World Report*. April 21. http://www.usnews.com/news/articles/2015/04/21/us-navy-tests-laser-weapons.

Sofieva, V. F., F. Dalaudier, J. Vernin. 2013. *Using Stellar Scintillation for Studies of Turbulence in the Earth's Atmosphere.* Philosophical Transactions of the Royal Society A. 371(1982).

Sprangel, P., J. Penano, and B. Hafizi. 2007. *Propagation of High Energy Laser Beams in Various Environments.* NRL Report 6790–07-9032. Arlington, VA. Naval Research Laboratory. https://www.dtic.mil/cgi-bin/GetTRDoc?AD=ADA471880

Torun, Erdal. 1999. "UAV Requirements and Design Considerations." Paper presented at the RTO SCI Symposium on Warfare Automation: Procedures and Techniques for Unmanned Vehicles. Ankara, Turkey, April 26–28.

Tucker, Spencer C., and Priscilla M. Roberts. 2008. *The Encyclopedia of the Arab-Israeli Conflict. A Political, Social, and Military History.* Santa Barbara, CA: ABC–CLIO Inc.

Vitech Corporation. 2011. *A Primer for Model-Based Systems Engineering.* Blacksburg, VA.

Welch, Savannah G. 2011. "Investigating the Link between Combat System Capability and Ship Design." Master's thesis, Naval Postgraduate School.

Wikipedia. 2016. S.v. "Population Inversion." Last modified September 10. https://en.wikipedia.org/wiki/Population_inversion.

Wilson, J. R. 2013, June. "Stealth Sneaks into UCAVs." *America Aerospace Journal* 51(6): 28–33.

THIS PAGE INTENTIONALLY LEFT BLANK

INITIAL DISTRIBUTION LIST

1.   Defense Technical Information Center
        Ft. Belvoir, Virginia

2.   Dudley Knox Library
        Naval Postgraduate School
        Monterey, California